Universidad Pública de Navarra
Nafarroako Unibertsitate Publikoa

PUBLIC UNIVERSITY OF NAVARRE (UPNA)

Department of Engineering

DOCTORAL THESIS

Effects of Agricultural Activities on Water Quality:

Catchment-Scale Modeling of Nutrient Pollution and Management in Cultivated Lands, Case Studies of Northern Spain and Southeastern Sweden

Presented by:

BRIAN OMONDI ODUOR

Thesis Advisors:

Prof. Miguel Ángel Campo-Bescós

Prof. Javier Casalí

Prof. Noemí Lana-Renault

A dissertation submitted to the **Doctoral School of Navarre (EDONA)** in partial fulfillment of the requirements of the **doctorate degree** in **Science and Industrial Technologies (Hydrology and Structural Analysis)**

@Pamplona, 2023

https://doi.org/10.48035/Tesis/2454/47538

Dedication

This dissertation is dedicated to my late uncle, Dr. Wilfred Ongaro, whose unwavering encouragement ignited the flames of curiosity and guided me toward the path of knowledge. His belief in my potential continues to inspire and guide me as I pursue the realms of education that he so passionately advocated. Though no longer with us, his spirit lives on as a guiding light, illuminating every step of my academic journey. This work is a testament to the seeds of inspiration he nurtured within me, and I will be eternally grateful for his guidance and love.

Acknowledgment

First and foremost, I would like to express my heartfelt gratitude to my doctoral advisors, Prof. Miguel Ángel Campo-Bescós, Prof. Javier Casalí, and Prof. Noemí Lana-Renault for their unwavering commitment, profound insights, and relentless belief in my potential which have been instrumental in shaping the trajectory of this dissertation. Their mentorship transcended beyond academic supervision, inspiring not only my research but also my personal growth as a scholar. My appreciation goes to the THERRAE research group members for their invaluable support throughout my doctoral journey.

Many thanks to INTIA for opening its doors and providing me with a platform for a research-to-practice internship. The experience from this internship has been useful in bridging the gap between theory and implementation. Special thanks to Alberto Alfaro for his guidance and supervision during this apprenticeship.

My acknowledgment goes to the Swedish University of Agricultural Sciences (SLU) for hosting me on an international scientific research visit at the department of Soil and Environment in Uppsala, Sweden. Thanks to the collaboration with Katarina Kyllmar, whose hospitality, mentorship, and insightful contributions enriched my stay at SLU. Appreciation to Kristina Mårtensson, whose indispensable assistance ensured a smooth research experience at SLU. Many thanks to the Environmental Modeling and Agricultural Water Management research groups at SLU for enriching discussions and talks that added depth and breadth to my work. Special thanks to Stephan Andersson and Helena Linefur from SLU for their invaluable support in obtaining data in Sweden.

Thank you to the Government of Navarre and Spanish national agencies for facilitating data acquisition in Spain for this research. Thanks to Javier Eslava from the Soils and Climatology Department in Navarre for his indispensable support in obtaining soil data.

Finally, I would like to appreciate the administrative support from UPNA and the IberustTalent and Campus Iberus programs during the entire research period. This research was supported by funding from the European Union's H2020 research and innovation program under Marie Skłodowska-Curie grant agreement no. 801586 and from the Ministerio de Economía y Competitividad (Government of Spain) via Research Project CGL2015–64284-C2–1-R and PID2020–112908RB-I00 funded by MCIN/AEI/10.13039/501100011033/FEDER "Una manera de hacer Europa".

Abstract

The intensification of agriculture to meet the increasing food demands and changing climate dynamics necessitates sustainable land and water resource management. This doctoral thesis examines the complex interaction between agricultural activities and water quality by exploring two agricultural-dominated watersheds in northern Spain and southeastern Sweden using the Soil Water Assessment Tool (SWAT) model. The research focuses on (i) evaluating the SWAT model's applicability in the study areas, (ii) assessing the effects of changing from rainfed to irrigated agriculture, (iii) understanding the effects of climate change on water quantity and quality, and (iv) quantifying the efficacy of agricultural best management practices (BMPs) in minimizing nutrient export.

The transition from rainfed to irrigated agriculture in the Cidacos River watershed (480 km^2) in northern Spain increased annual streamflow, nitrate load, and concentration, as well as alterations in seasonal patterns due to increased irrigation and fertilization aimed at enhancing agricultural productivity. The climate change projection analysis for this watershed showed a projected decline in streamflow and nitrates load, particularly in the long-term (2071-2100) projection scenario of RCP8.5. Comparatively, the projected decline in autumn and winter was greater than in spring and summer. These changes were attributed to the projected decreasing precipitation coupled with increasing temperatures affecting streamflow and, subsequently, the nitrate load. In Catchment C6 (33 km^2) of southeastern Sweden, filter strips and sedimentation ponds emerged to be the most effective in reducing sediment and phosphorous exports, providing valuable insights for sustainable land management practices that might contribute to the preservation and revitalization of aquatic ecosystems in this region.

Overall, this dissertation emphasizes the crucial need for a comprehensive grasp of agricultural impacts on water quality. The research not only elucidates the complicated dynamics of agricultural activities and water quality by utilizing advanced hydrological modeling approaches but also provides stakeholders with practical tools to guide informed decision-making. The findings of this research provide a transformative approach toward protecting water quality, nurturing resilient ecosystems, and promoting sustainable agricultural practices in diverse geographical contexts.

Keywords: agriculture; best management practices; climate change; irrigation; nutrient pollution; SWAT model; water quality

Resumen (Abstract in Spanish)

La intensificación de la agricultura para satisfacer la creciente demanda de alimentos y la dinámica climática cambiante requiere una gestión sostenible de los recursos de la tierra y el agua. Esta tesis doctoral examina la compleja interacción entre las actividades agrícolas y la calidad del agua mediante la exploración de dos cuencas hidrográficas dominadas por la agricultura en el norte de España y el sureste de Suecia utilizando el modelo Soil Water Assessment Tool (SWAT). La investigación se centra en (i) evaluar la aplicabilidad del modelo SWAT en las áreas de estudio, (ii) evaluar los efectos del cambio de agricultura de secano a agricultura de regadío, (iii) comprender los efectos del cambio climático en la cantidad y calidad del agua, y (iv) cuantificar la eficacia de las mejores prácticas de manejo agrícola (BMP) para minimizar la exportación de nutrientes.

La transición de la agricultura de secano a la de regadío en la cuenca del río Cidacos (480 km^2), en el norte de España, dio lugar a un aumento del caudal anual, de la carga de nitratos y de su concentración, así como a alteraciones en los patrones estacionales debido al aumento del riego y de la fertilización destinados a mejorar la productividad agrícola. El análisis de proyección de cambio climático para esta cuenca indicó una disminución proyectada en el flujo de agua y la carga de nitratos, particularmente en el escenario de proyección a largo plazo (2071-2100) de RCP8.5. Comparativamente, la disminución proyectada en otoño e invierno fue mayor que en primavera y verano. Estos cambios se atribuyeron a la disminución prevista de las precipitaciones, unida al aumento de las temperaturas, que afectaron al caudal de los arroyos y, por consiguiente, a la carga de nitratos. En la cuenca C6 (33 km^2) del sudeste de Suecia, las franjas filtración y los estanques de sedimentación resultaron ser los más eficaces para reducir las exportaciones de sedimentos y fósforo, proporcionando información valiosa para las prácticas de gestión sostenible de la tierra que podrían contribuir a la preservación y revitalización de los ecosistemas acuáticos en esta región.

En general, esta tesis enfatiza la necesidad de obtener una comprensión integral de los impactos agrícolas en la calidad del agua. La investigación no solo esclarece la complicada dinámica que se establece entre las actividades agrícolas y la calidad del agua mediante el uso de modelización hidrológica avanzada, sino que también brinda a los agentes interesados herramientas prácticas para guiar la toma de decisiones informadas. Los hallazgos de esta investigación brindan un enfoque transformador hacia la protección

de la calidad del agua, el fomento de ecosistemas resilientes y la promoción de prácticas agrícolas sostenibles en diversos contextos geográficos.

Palabras clave: agricultura; mejores prácticas de gestión; cambio climático; agricultura de regadío; contaminación por nutrientes; modelo SWAT; calidad del agua

Table of Contents

List of Figures

List of Tables

List of Abbreviations

95PPU	95 Percent Prediction Uncertainty
AAT	All-At-a-Time
AEMET	State Meteorological Agency of the Government of Spain
AdapteCCa	Platform on Adaptation to Climate Change
ANLeC	Average Nutrient Leaching Calculator
AnnAGNPS	Annualized Agricultural Non-Point Source
BMP	Best Management Practice
CAP	Common Agricultural Policy
CHE	Confederación Hidrográfica del Ebro (Ebro River Basin Authority)
CIMP	Coupled Model Intercomparison Project
DDRMAAL	Departamento de Desarrollo Rural, Medio Ambiente y Administración Local (Department of Rural Development, Environment and Local Administration)
DEM	Digital Elevation Map
EU	European Union
EEA	European Environment Agency
EPRS	European Parliamentary Research Service
ETRS	European Terrestrial Reference System
FAO	Food and Agricultural Organization
GAN-NIK	Environmental Management of Navarra
GCM	Global Climate Model
GHG	Greenhouse Gas
GLUE	Generalized Likelihood Uncertainty Estimation
HELCOM	Helsinki Commission
HRU	Hydrological Response Unit
IDENA	Spatial Data Infrastructure of Navarre
INTIA	Navarre Institute of Agri-Food Technologies and Infrastructures
IPCC	Intergovernmental Panel on Climate Change
IUSS	International Union of Soil Sciences
LULC	Land Use Land Cover

MAPA	Ministerio de Agricultura, Pesca y Alimentación (Ministry of Ministry of Agriculture, Fisheries and Food)
MCMC	Markov Chain Monte Carlo
MUSLE	Modified Universal Soil Loss Equation
N	Nitrogen
ND	Nitrate Directive
NH_3	Ammonia
NLeCCS	Nutrient Leaching Coefficient Calculation System
NO_3	Nitrates
NO_x	Nitrogen oxides
NSE	Nash-Sutcliffe Efficiency
OAT	One-At-a-Time
OECD	Organization for Economic Co-operation and Development
P	Phosphorus
ParaSol	Parameter Solution
PBIAS	Percent Bias
PSO	Particle Swarm Optimization
R^2	Coefficient of Determination
RCP	Representative Concentration Pathway
RCM	Regional Climate Models
SCS-CN	Soil Conservation Service Curve Number
SEPA	Swedish Environmental Protection Agency
SLU	Swedish University of Agricultural Sciences
SMED	Swedish Environmental Emissions Data
SMHI	Swedish Meteorological and Hydrological Institute
SNLS	Swedish National Land Survey
Soluble P	Soluble phosphorous
SUFI-2	Sequential Uncertainty Fitting, version 2
SWAT	Soil and Water Assessment Tool
SWAT-CUP	Soil Water Assessment Tool Calibration and Uncertainty Procedures
SWEDAC	Swedish Board for Accreditation and Conformity Assessment

SWEREF99	Swedish Reference Frame 1999
THERRAE	Teledetección, Hidrología, Erosión, Riegos y Análisis Estructural (Remote Sensing, Hydrology, Erosion, Irrigation and Structural Analysis)
TN	Total nitrogen
Total P	Total phosphorous
UNEP	United Nations Environment Programme
USDA-ARS	United States Department of Agriculture's Agricultural Research Service
USLE	Universal Soil Loss Equation
UTM	Universal Transverse Mercator
WFD	Water Framework Directive
WHO	World Health Organization
WRB	World Reference Base for Soil Resources

Chapter 1:

1 General Introduction and Objectives

1.1 Background information

1.1.1 Introduction

The current agricultural practices globally have been intensified to boost crop yields and livestock production to meet increasing food demand. Unfortunately, this intensification has resulted in widespread water quality challenges. Agricultural activities significantly impact water quality, adversely affecting the environment (Sutton *et al.*, 2011) and, in some cases, human health (WHO, 2017). The transport of fertilizers, pesticides, agrochemicals, animal waste, and soil erosion from these activities contribute substantially to pollution in surface and groundwater sources. When excess nutrients such as nitrogen (N) and phosphorus (P) enter water bodies, they cause eutrophication. Eutrophication is a process through which excessive plant and algae growth occurs. It disrupts aquatic ecosystems by depleting oxygen levels and causing harmful algal blooms (Dodds and Smith, 2016; Le Moal *et al*., 2019). These changes reverberate through the food chain, endangering aquatic biodiversity and ecosystem stability (Carpenter *et al.*, 1998).

The water quality challenges from agricultural activities in Europe mirror those experienced globally, with elevated nutrient pollution potential due to agricultural intensification. The European Environment Agency (EEA) (2021) reports that agriculture is the primary source of nitrogen and phosphorus inputs to Europe's surface waters. This has resulted in Europe's water bodies facing eutrophication threats with negative ecological consequences. The persistent water quality challenge across several European Union (EU) member states has resulted in the search for sustainable agricultural practices under the Common Agricultural Policy (CAP) (Boezeman *et al.*, 2020). Integrating agricultural practices that minimize nutrient export and optimize their use is critical for protecting water resources and ecosystem health.

At the regional level, countries face contrasting nutrient pollution challenges. In Spain, for instance, water quality issues from agricultural practices are exacerbated by the Mediterranean climate, characterized by water scarcity. Irrigation remains an integral aspect of crop production in this region; however, it has been reported to increase nutrient leaching and pollution in water bodies (Merchán *et al.*, 2020). The Ebro River basin is an important agricultural area grappling with high nutrient levels, threatening the aquatic ecosystems and water supply (Isidoro and Aragüés, 2007; Ladrera *et al*., 2019). In more

humid countries such as Sweden, excessive nutrient enrichment has resulted in widespread hypoxia, endangering biodiversity and commercial fishing in the Baltic Sea (Conley *et al.*, 2011). Therefore, to develop effective mitigation strategies, it's imperative to understand the dynamics of nutrient pollution in the different regions and their associated challenges.

Similarly, climate change presents a serious challenge to water resources, necessitating the development of sustainable adaptation, mitigation, and policy intervention strategies (Krysanova *et al.*, 2017). However, the specific impacts of climate change on water quality and its interactions with agricultural activities vary across geographical regions. Therefore, understanding the complex interplay between agricultural activities, climate change, and water quality is essential in achieving the standards outlined by regulations such as the European Water Framework Directive (European Communities, 2000). The Mediterranean region, for instance, faces a unique confluence of vulnerabilities, including geographical, climatic, and socio-economic factors, making it a focal point for climate change case studies (Vargas-Amelin and Pindado, 2014).

Agricultural best management practices (BMPs) play a pivotal role in tackling the water quality challenges associated with intensified agricultural activities. BMPs are a set of conservation practices and techniques designed to minimize the negative impacts of agriculture on water quality and the environment (Jain and Singh, 2019). They are an important component of a comprehensive strategy to protect water resources and sustain ecosystem wellbeing in the face of increasing food demand and changing environmental conditions. The adoption of BMPs not only helps protect surface and groundwater sources but also promotes sustainable agricultural practices, which are in line with Europe's agricultural policy goals (Boezeman *et al.*, 2020).

Moreover, mathematical and hydrological models serve as valuable tools to comprehend, evaluate, and predict the impacts of agricultural activities on water quality. These models offer a quantitative framework for understanding the complex interactions between various factors affecting water quality, such as land use, soil, climate, and hydrology. Mathematical models aid in simulating and predicting nutrient transport and management within ecosystems, which would otherwise be challenging if done experimentally due to time and resource constraints (Moges *et al.*, 2021; Yu, 2015).

One such model used extensively in this research to assess the effects of agricultural activities on water quality is the Soil and Water Assessment Tool (SWAT) model. The SWAT model is a widely recognized hydrological model developed to simulate the impact of land management practices on water quality (Neitsch *et al.*, 2011). The model takes into account various factors, such as soil properties, land use, climate data, agricultural management, and hydrological processes, to predict nutrient and sediment transport in watersheds. SWAT has been successfully applied in diverse geographical regions and has proven to be a valuable tool for quantifying streamflow, sediment, and nutrient export, studying climate change impacts, analyzing BMPs, and identifying vulnerable areas (Arnold *et al.,* 2012; Neitsch *et al.,* 2011). The SWAT model was chosen for this study due to its robustness in integrating hydrological cycle and water quality components, high spatial-temporal resolution, and ability to analyze different scenarios of interest. By integrating the insights gained from applying the SWAT model with on-the-ground agricultural practices, this research aims to provide a comprehensive understanding of the challenges posed by agricultural activities to water quality, focusing on the unique circumstances in cultivated areas of Spain and Sweden.

1.1.2 Nutrient pollution from agricultural areas

The intensification of agriculture has enhanced food production for the ever-increasing global population by utilizing modern technologies such as irrigation, farm machinery, and increased agricultural inputs, such as fertilizer and pesticides (Mateo-Sagasta *et al.*, 2017; OECD, 2012). However, the inefficiency of these inputs, coupled with the continued expansion of agricultural areas, has resulted in increased pollutant export, soil degradation, deforestation, and many other environmental changes. According to Leip *et al.* (2011), only 60% of the nitrogen applied to agricultural lands is taken up by plants, with the rest being exported to water as nitrates (NO_3) or emitted to the air as nitrogen oxides (NO_x) or ammonia (NH_3). These nutrient pollutants, particularly nitrogen and phosphorus, can cause eutrophication, thereby deteriorating water quality when conveyed into water bodies through runoff. Table 1.1 provides an overview of the key agricultural pollutants, their sources, and their challenges to the receiving water bodies.

Table 1.1: Sources of agricultural water pollution (Source: Adapted from OECD (2012))

Pollutant	Agricultural activities that contribute to the pollutant	Main pollutant-related water quality issues
Nutrients (N and P)	– Agricultural production (runoff of excess nutrients, e.g., N and P from fertilizers into water bodies)	– Causes eutrophication, which is harmful to aquatic life and human health
Sediments	– Ineffective soil conservation practices	– Harmful to aquatic life and water transport system due to turbidity of water
Organic matter	– Manure application	– Harmful to aquatic life through deoxygenation of water
Toxic contaminants (heavy metals, pesticides, etc.)	– Application of sewage sludge on agricultural lands (heavy metals) and plant protection (pesticides)	– Harmful to aquatic life and human health
Acid substances	– Livestock production (ammonia volatilization)	– Harmful to aquatic life through the acidification of water
Biological contaminants	– Fecal sludge discharge from livestock into water	– Pathogens, bacteria, and viruses contaminate water
Mineral salts	– Ineffective land use practices (clearing of perennial vegetation and irrigation practices)	– Results of salinization through activities such as irrigation

While agriculture is a primary contributor to the deterioration of water quality, other sources, such as natural, urban, and industrial pollution, also significantly contribute to water pollution (Farzin and Grogan, 2008; Wittmer *et al*., 2011). Achieving zero pollution from agricultural areas is technically impossible; however, the main challenge lies in improving production while minimizing nutrient export from cultivated lands, which can affect water quality (Galloway *et al.*, 2008). The naturally-induced nitrogen and phosphorus loss (background/natural loss) is typically minimal compared to human-induced losses, and it's estimated at 1-2 kg ha^{-1} for nitrogen and about 0.1 kg ha^{-1} for phosphorus (Dubrovsky *et al.*, 2010; EEA, 2005). These losses vary depending on underlying geological conditions and potential atmospheric depositions.

1.1.3 Trends of agricultural impacts on water quality

According to the European Environment Agency (EEA, 2022), nutrient concentration levels in the European environment have considerably declined over the past three decades, following a peak in the 1980s. This decline could be attributed to a drop in excessive mineral fertilization (Oger, 2022; Vigiak *et al.*, 2023). However, these developments are insufficient to fully protect European aquatic and terrestrial ecosystems, as there are substantial regional disparities among the EU member states. Agriculture continues to be the primary source of pollution in surface and groundwater across most EU countries. About 25% of surface and groundwater stations across Europe have reported an increase in nitrate concentration between 2016 and 2019 (EEA, 2021). Some countries have reported over 50% of total nitrogen (TN) discharged into surface waters despite a general declining trend within the region. The European Environment Agency (EEA, 2020) has recommended reducing European nutrient runoff by at least 50% to address the existing challenge.

Agriculture consumes approximately 80% of the freshwater resources in the Mediterranean region, with irrigation being the primary consumer (Crovella *et al.*, 2022; FAO, 2022). This intensive irrigation water use results in large nutrient export from agricultural areas into rivers, aquifers, and coastal zones. According to the Mediterranean Action Plan (UNEP, 2019), land-based activities such as agriculture contribute 80% of pollution to the Mediterranean Sea, creating eutrophication and endangering marine ecosystems. The agricultural water consumption in the region increased by 20% between 2000 and 2020, resulting in the over-extraction of groundwater, causing aquifers to be depleted faster than they can replenish (Duarte *et al.*, 2021). Widespread soil erosion has been reported in the Mediterranean region, affecting an estimated 70% of agricultural land (EEA, 2021).

Over the last century, eutrophication has transformed the Baltic Sea from an oligotrophic clear-water sea into an eutrophic marine environment in the Baltic region. Approximately 75% of N load and 95% of P load is discharged into the sea directly from rivers and streams from the bordering countries (OECD, 2012). Agriculture contributes about 80% of the total diffuse load in Finland and Sweden (Helsinki Commission (HELCOM), 2009; Malmaeus and Karlsson, 2010). In Norway, agriculture contributes up to 60% of N and 45% of P loadings released in the coastal areas of the North Sea (OECD, 2012).

1.2 Problem Statement

The dynamic relationship between agricultural activities and water quality has been at the forefront of the environmental discourse, underscoring the complex interplay between human sustenance and ecosystem sustainability. In the nexus of this intricate balance, nutrient pollution from agricultural activities emerges as a formidable challenge, a subtle yet potent force that threatens the equilibrium in catchments and the vitality of ecosystems. Caught within this intricate web are not only the ecosystems that rely on clean and healthy water but also the communities that depend on these ecosystems for their livelihoods and well-being. The traditional approach of separating agricultural development and environmental conservation no longer works well to tackle these evolving challenges. In this context, catchment-scale modeling emerges as a beacon of insight, involving a multidisciplinary endeavor that combines science, technology, and policy to unravel the complexities of nutrient pollution, project its effects, and chart a path toward sustainable land use and water resource management.

This research attempts to analyze these complex interactions between agricultural activities and water resources to obtain sustainable solutions. An in-depth assessment of the environmental consequences of agricultural activities and their resultant pollution is imperative to formulating effective strategies and interventions to control and manage the pollutants. However, investigating the effects of agriculture on water quality is a complex phenomenon due to the diversity and extent of the processes and factors involved, as well as the lack of proper know-how of their relevance and measures of controlling such processes. Non-point source pollution exhibits extensive spatial and temporal variations in their occurrence, and thus, it is quite challenging to identify their sources. These pollutants are highly unpredictable due to variations in climate, land use, soil types, and other environmental factors. The complexity of the non-point source pollution pathways and contamination is not well known as it extends far beyond its sources into the ecosystem, impacting social and economic livelihoods. Central to addressing this challenge is the ability to identify the effects of these pollutions and then translate these insights into appropriate actions for mitigation. This thesis is a compilation of the research findings from exploring some of these challenges, and it proposes solutions to mitigate environmental degradation and foster a harmonious coexistence between human endeavors and the ecosystems of the Mediterranean and Baltic regions. The research

transcends the domains of data assimilation, predictive modeling, and scenario analysis to craft a narrative resulting in sustainable agricultural and water resources development.

1.3 Justification

This research aimed to contribute and lay the foundations for sustainable agricultural activities, resulting in positive social and economic impacts. It provided valuable insights into the potential impacts of nutrient pollution and proposed control measures. It contributed to a better understanding of the intensity and reality of the problems and challenges of nutrient pollution by associating them with the different land uses, management practices, climatic conditions, and edaphic factors. The research identified tools for evaluating nutrient pollution and its control measures by generating management scenarios that minimize export. This information is valuable for policy and decision-makers in planning for the future and developing effective agricultural policies and strategies. The findings from this research could provide crucial information that would contribute to the implementation of the European Communities' Nitrate Directive (ND, Directive 91/676/EEC) and the Water Framework Directive (WFD, Directive 2000/60/EC), both of which are primarily concerned with protecting water bodies from agricultural nutrient pollution. The outcomes from this research could influence the development of robust policies that benefit farmers by enhancing crop yields while mitigating the adverse effects of nutrient pollution. These findings could also be beneficial in guiding the promotion and adoption of sustainable agricultural practices.

1.4 Objectives

1.4.1 General objective

The general objective of this research was to analyze the effects of agricultural activities on water quality through modeling nutrient pollution and management in selected agricultural-dominated catchments in northern Spain and southeastern Sweden.

1.4.2 Specific objectives

The following specific objectives were formulated to address the general objective:

i) Assessing the SWAT model's applicability for simulating streamflow and nitrate load in the Cidacos River watershed in northern Spain (Papers 1 and 2)
ii) Evaluating the impact of changing from rainfed to irrigated agriculture in the Cidacos River watershed in northern Spain (Paper 1)

iii) Analyzing the effects of climate change on streamflow and nitrate pollution in the Cidacos River watershed in northern Spain (Paper 2)
iv) Examining the SWAT model's applicability for simulating streamflow, sediment load, and phosphorous load in a small agricultural catchment in southeastern Sweden (Paper 3)
v) Quantifying agricultural best management practices' impacts on sediment and phosphorous export in a small catchment in southeastern Sweden (Paper 3)

1.5 Research Questions

To comprehensively address the specific objectives of this research, the following research questions were explored:

i) How does the SWAT model perform in simulating streamflow and nitrate load in an agricultural watershed under rainfed conditions in the Mediterranean region, and what parameters greatly influence the model performance in this region?
ii) How has the transition from rainfed to irrigated agriculture affected the streamflow, nitrate load, and nitrate concentration in an agricultural watershed in the Mediterranean region?
iii) What are the projected streamflow and nitrate export changes in a Mediterranean agricultural watershed under different climate change scenarios?
iv) How well does the SWAT model simulate streamflow, sediment load, and phosphorus load in an agricultural catchment in southeastern Sweden, and what parameters influence the model performance in this region?
v) How do different agricultural best management practices (BMPs) affect sediment and phosphorus export in the southeastern Sweden catchment, and what are the most effective BMPs for reducing these pollutants?

1.6 Scope and limitations of the research

This research focused on analyzing nutrient export and management from agricultural areas within the Mediterranean environment of northern Spain (Cidacos River watershed) and the Baltic environment of southeastern Sweden (Catchment C6). These two watersheds were chosen because they represent the predominant agricultural activities in their respective regions and have comprehensive, long-term hydrological and water quality data suitable for model analysis. The SWAT model version 2012 was employed as the sole hydrological modeling tool to simulate and assess the impact of agricultural

activities on water quality. The SWAT model was evaluated to ensure its suitability for each watershed through calibration and validation before its application.

This research was limited to hydrological modeling of nutrient export and management, specifically nitrate and phosphorous loads, with no field experiments. Instead, it analyzed the long-term time series data obtained from the various agencies that collect and store them. Only nitrate export was studied in the Spanish watershed, whereas sediment and phosphorus export were studied in the Swedish catchment. All model simulations were run under rain-fed conditions. For instance, analyses were done in the Cidacos River watershed until Olite station, which was unaffected by irrigation. The data from the irrigated region was only utilized to compare the transformation from rainfed to irrigated agriculture.

For the climate change application, the focus was on the moderate (RCP4.5) and extreme (RCP8.5) climate change scenarios, despite the Intergovernmental Panel on Climate Change (IPCC) having numerous climate change scenarios and projections. Due to the complexity of the climate simulation modeling and time constraints, only an ensemble of six climate models from the Coupled Model Intercomparison Project phase 5 (CMIP5) was utilized. The availability of downscaled climate change projections data for Spain and the Navarre region influenced the CMIP5 selection. Similarly, only four most pertinent agricultural best management practices (BMPs) were analyzed in the Swedish catchment, even though numerous BMPs exist. The criteria for their selection have been elaborated in Chapter 6, section 6.2.5.

1.7 Thesis structure

This doctoral thesis followed the following structure:

The **first chapter** introduces the thesis by outlining the research background and presenting the state-of-the-art on how agriculture affects water quality. This chapter also articulates the central research problem, elucidating the necessity for this research, enumerating the objectives, and specifying the scope and limitations of the research.

The **second chapter** provides an overview of the SWAT model, including a detailed explanation of its hydrology, sediment and nutrient simulation processes, and related equations. The chapter also expounds on using SWAT-CUP for sensitivity and uncertainty analyses, calibration and validation, and model performance evaluation.

The **third chapter** describes the two study areas in Spain and Sweden. This includes a detailed description of the catchment factors such as climate, soil type, land use, and agricultural practices. This chapter further delves into the data acquisition and processing for model integration.

The **fourth chapter** evaluates the application of the SWAT model to simulate the impact of changing from rainfed to irrigated agriculture in the Cidacos River watershed on streamflow, nitrate load, and concentration. This chapter examines the SWAT model's applicability for estimating streamflow and nitrate load in this watershed. The analysis of the change from rainfed to irrigated agriculture is based on simulating the rainfed conditions (pre-irrigation) within the irrigated zone and comparing them to the measured observations during the irrigated period (post-irrigation).

The **fifth chapter** utilizes the SWAT model to investigate the long-term effects of climate change on streamflow and nitrate export in the Cidacos River watershed under rainfed conditions.

The **sixth chapter** applies the SWAT model to quantify the impacts of four agricultural best management practices on sediment and phosphorous export from a small catchment in southeastern Sweden. The SWAT model evaluation for streamflow, sediment, and phosphorous in the study area is presented in this chapter, followed by the BMP assessment.

The **seventh chapter** draws together the conclusions derived from each objective, culminating in an overall conclusion. The chapter also offers the thesis's final remarks and recommends prospective research endeavors.

Chapter 2:

2 Description of the SWAT Model and SWAT-CUP

2.1 Overview of the SWAT model

The Soil and Water Assessment Tool (SWAT) model is a freely available open-source software developed by the United States Department of Agriculture's Agricultural Research Service (USDA-ARS). It assists water resources managers, policy experts, and decision-makers in predicting and quantifying the impact of land use management on water and diffuse pollution. The model can be applied to small watersheds (catchment scale) and large basins (regional, continental, or global scale) with varying soil types, land use, and management practices (Lévesque *et al.*, 2008).

SWAT is a data-driven, semi-distributed, continuous timescale, physical, and process-based hydrological model that simulates water, sediment, and agricultural chemicals/pollutant yields. The model simulates various watershed processes, including but not limited to surface runoff, streamflow, percolation, erosion, nutrient and pesticide load/yield and transportation, irrigation, groundwater flow, reservoir storage, channel routing, field drainage, and plant water use. (Rostamian *et al.*, 2008). The model consists of multiple components such as weather, hydrology, erosion/sediments, soil temperature and properties, plant growth, nutrients, pesticides, land management, and channel and reservoir routing. Collectively, these components represent the various aspects of the hydrologic cycle and the processes that influence water balance in the watershed.

The SWAT model operates on a daily time step and divides the watershed's hydrology into two phases: the land phase and the routing phase. The land phase controls the amount of water, sediments, pesticides, and nutrient loadings that enter the main channel in each sub-basin, whereas the routing phase controls the movement of water and sediment through the channel network of the watershed to the outlet (Arnold *et al.,* 2012).

SWAT adopts a two-level disaggregation scheme in which a preliminary sub-basin identification is carried out based on topographic data (Digital Elevation Map, DEM), followed by further discretization by overlaying the DEM with the land use and soil maps to form the Hydrological Response Units (HRUs). The HRU refers to a unique homogeneous combination of similar land use/land cover, soil type, and topography (elevation/slope) characteristics (Neitsch *et al.*, 2011). The model uses the HRUs to describe the spatial heterogeneity in the watershed and represent its basic computational unit, which is assumed to be homogeneous in hydrologic response to land cover changes. Figure 2.1 summarizes the SWAT model's input and output datasets.

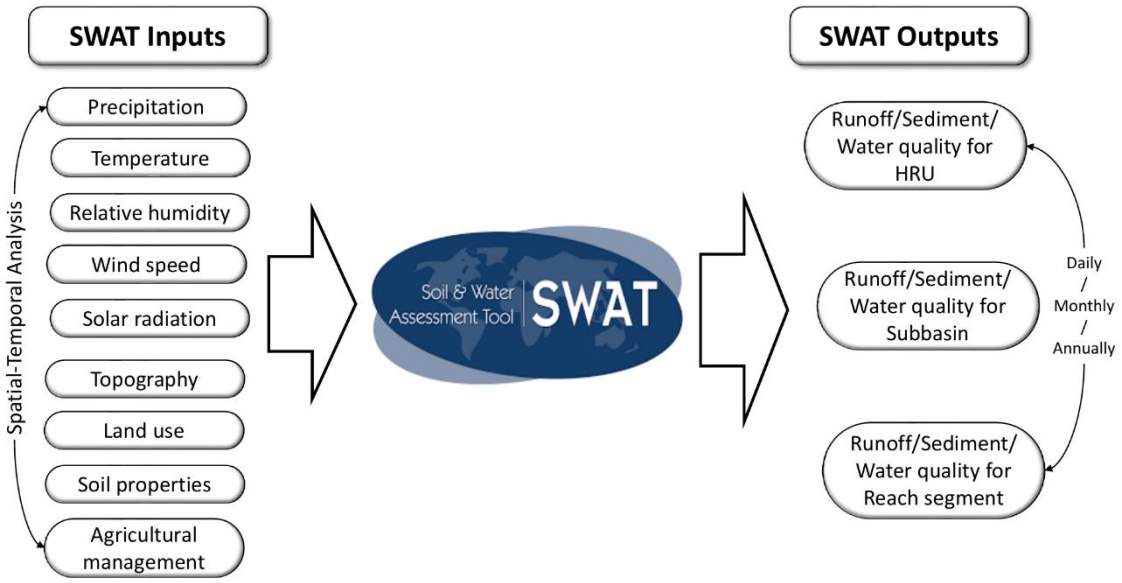

Figure 2.1: Overview of the SWAT model's input and output data

2.2 Hydrology simulation in the SWAT model

The hydrologic balance in the SWAT model is simulated for each HRU using the water balance equation, as shown in Equation (2.1) (Neitsch *et al.*, 2011).

$$SW_t = SW_o + \sum_{i+1}^{t}\{R_{day} - Q_{surf} - ET_a - W_{seep} - Q_{gw}\} \quad (2.1)$$

Where, SW_t represents the final soil water content (mm of H_2O), SW_o represents the initial soil water content on day i (mm H_2O), t represents the time (days), R_{day} represents the amount of precipitation on day i (mm H_2O), Q_{surf} represents the amount of surface runoff on day i (mm H_2O), ET_a represents the amount of evapotranspiration on day i (mm), W_{seep} represents the amount of water entering the vadose zone on day i (mm H_2O), and Q_{gw} represents the amount of return flow on day i (mm H_2O).

The model calculates the daily soil and water temperatures in the watershed using the maximum and minimum temperature inputs. Percolation in the model is computed using a layered storage routing technique paired with a crack flow model (Chaubey *et al.*, 2006). Potential evapotranspiration is estimated using either the Food Agricultural Organization's (FAO) Penman-Monteith method, the Hargreaves method, or the Priestly-Taylor method (Neitsch *et al.*, 2011). The Penman-Monteith method requires air temperature, wind speed, solar radiation, and relative humidity, the Priestly-Taylor method requires air temperature and solar radiation, while the Hargreaves method requires only air temperature. The Penman-Monteith method was adopted for this

research since it has been widely used and proven to be very effective when using daily data (Allen, 2005). Each HRU in the watershed maintains a water balance that encompasses four storage volumes: snow, soil profile (from 0-20 m), shallow aquifer (from 2-20 m), and deep aquifer (>20 m) (Chaubey *et al.*, 2006).

Surface runoff is the portion of precipitation that flows overland on the Earth's surface. It occurs when the amount of water on the ground exceeds the infiltration rate. The SWAT model uses the Muskingum routing method (Gill, 1978) to estimate the runoff routing through the stream channel. In the model, surface runoff can be estimated using either the Green and Ampt infiltration method (Green and Ampt, 1911) or the modified Soil Conservation Service Curve Number (SCS-CN) method (USDA, 2004). The Green and Ampt infiltration method requires sub-daily precipitation data to calculate infiltration as a function of the wetting front metric potential and effective hydraulic conductivity, whereas the SCS-CN requires daily precipitation data to calculate runoff as a function of soil permeability, antecedent moisture condition, and land use. Due to the readily available daily precipitation data, this study adopted the SCS-CN method for the surface runoff simulation, as presented in Equation (2.2).

$$Q_{surf} = \frac{(R_{day} - I_a)^2}{(R_{day} - I_a) + S} \quad (2.2)$$

Where, Q_{surf} represents the accumulated surface runoff or excess rainfall (mm), R_{day} represents the precipitation depth for the day (mm), I_a represents the initial abstractions (mm), including surface storage, interception, and infiltration before the runoff, and S represents the retention parameter (mm). The retention parameter (S) varies spatially due to changes in slope, land use, soil type, and management, and temporally due to changes in soil water content, and is inversely proportional to the surface runoff; that is, the higher the S value, the smaller the surface runoff and vice versa. Equation (2.3) calculates S based on the curve number (CN).

$$S = 25.4\left(\frac{100}{CN} - 10\right) \quad (2.3)$$

Generally, the initial abstraction, I_a is commonly approximated as 0.2S for small agricultural watersheds, and thus Equation (2.2) can be simplified into Equation (2.4) as follows:

$$Q_{surf} = \frac{(R_{day} - 0.2S)^2}{(R_{day} + 0.8S)} \quad (2.4)$$

Thus, runoff only occurs when the rainfall depth for the day is less than the initial abstraction, that is, $R_{day} > I_a$

2.3 Sediment simulation in the SWAT model

The Modified Universal Soil Loss Equation (MUSLE) (Williams, 1975) is used to estimate soil loss in the model. MUSLE estimates sediment yield using the runoff factor rather than the rainfall energy factor used by the Universal Soil Loss Equation (USLE) (Neitsch *et al.*, 2011). MUSLE, as a result, accounts for antecedent soil moisture and estimates of sediment from a single storm event. This improves the sediment yield prediction and eliminates the need for delivery ratios because the runoff factor represents the energy utilized in the detachment and transport of sediments. Equation (2.5) shows the model's sediment yield calculation.

$$Sed = 11.8 \times (Q_{surf} \times q_s \times A_{hru})^{0.56} \times K \times C \times P \times LS \times CFRG \quad (2.5)$$

Where Sed represents the sediment yield or soil erosion (metric tons), q_s represents the peak runoff rate ($m^3\ s^{-1}$), A_{hru} represents the area of the HRU (ha), K represents the USLE soil erodibility factor, C represents the USLE land use/cover and management factor, P represents the USLE support practice factor, LS represents the USLE topographic factor, and CFRG represents the USLE coarse fragment factor. CFRG is calculated as a function of the percentage of rock (%Rock) in the first soil layer and can be estimated using Equation (2.6). CFRG = 1 when no rock is present in the first soil layer.

$$CFRG = \exp(-0.053 \times \%Rock) \quad (2.6)$$

When routing, SWAT uses Manning's Equation to calculate the rate and velocity of flow. Sediment routing occurs in stream channel networks and on the land surface. The model tracks the particle size distribution of eroded sediments on the land surface and routes them through ponds, channels, and surface waterbodies (Neitsch *et al.*, 2011). The sediment transport through the channel is controlled by both deposition and degradation operating simultaneously (Setegn *et al.*, 2008). The maximum amount of sediment transported from a reach segment is simulated as a function of the peak channel flow rate and is calculated using Equation (2.7).

$$conc_{sed,max} = C_{sp} \left(\frac{q_s}{A_{ch}}\right)^{sp} \quad (2.7)$$

Where, $conc_{sed,max}$ represents the maximum sediment concentration transported or the channel carrying capacity (ton m^{-3} or kg L^{-1}), C_{sp} is an empirical coefficient defined by the user that needs to be calibrated, q_s represents the peak flow rate (m^3 s^{-1}), A_{ch} represents the cross-sectional flow area in the channel, and sp is an exponent defined by the user, typically ranging from 1.0 to 2.0, with 1.5 being the common value.

Sediment routing in streams involves comparing the available sediment load with the estimated transport capacity of the particular stream segment (Cho *et al.*, 2010). The sediment yield in each HRU is routed to the corresponding sub-basin channel. When the sediment load exceeds the stream transportation capacity, that is, $conc_{sed,i} > conc_{sed,max}$, then deposition occurs within the channel, and the net amount of sediment deposited can be calculated using Equation (2.8).

$$sed_{dep} = (conc_{sed,i} - conc_{sed,max}) \times V_{ch} \quad (2.8)$$

However, when the stream transportation capacity exceeds the sediment load, that is, $conc_{sed,max} > conc_{sed,i}$, then degradation will occur, and the net amount of sediment re-entrained can be calculated by Equation (2.9).

$$sed_{deg} = (conc_{sed,max} - conc_{sed,i}) \times V_{ch} \times K_{ch} \times C_{ch} \quad (2.9)$$

Where, sed_{dep} and sed_{deg} represents the amount of sediment deposited and re-entrained in the channel segment respectively (metric tons), $conc_{sed,i}$ represents the initial sediment concentration in the reach (ton m^{-3} or kg L^{-1}), $conc_{sed,max}$ represents the maximum sediment concentration transported by the water (ton m^{-3} or kg L^{-1}), V_{ch}, represents the volume of water in the reach segment (m^3 of H_2O), K_{ch} represents the channel erodibility factor and C_{ch} represents the channel cover factor.

Once the deposition and degradation calculations are complete, the final amount of sediment in the channel segment is determined using Equation (2.10).

$$sed_{ch} = sed_i - sed_{dep} + sed_{deg} \quad (2.10)$$

Where, sed_{ch} represents the amount of sediment in the channel segment or reach (metric tons), sed_i represents the initial amount of sediment in the reach at the beginning of the time period (metric tons), sed_{dep}represents the amount of sediment deposited in the reach

segment (metric tons), sed_{deg} represents the amount of sediment re-entrained in the reach segment (metric tons).

The sediment transported out of the reach is calculated using Equation (2.11).

$$sed_{out} = sed_{ch} \times \frac{V_{out}}{V_{ch}} \quad (2.11)$$

Where, sed_{out} represents the amount of sediment transported out of the reach (metric tons), sed_{ch} represents the amount of sediment in the reach (metric tons), V_{out} represents the volume of outflow during the time step (m^3 of H_2O), and V_{ch}represents the volume of water in the reach segment (m^3 of H_2O).

This method assumes that erosion is limited by the transportation capacity, thereby limiting the sediment supply from the channel erosion (Neitsch *et al.*, 2011). In cases where sediment data is limited or continuous daily sediment data is unavailable, a sediment rating curve could be established to estimate the daily sediment concentrations and loads calibration and validation of the SWAT model (Lu and Chiang, 2019).

2.4 Nutrient simulation in the SWAT model

The SWAT model tracks nutrients dissolved in the stream and adsorbed to the sediment. The dissolved nutrients are carried with the water, while those adsorbed to sediment are deposited along the channel bed with the sediment. Excessive nutrient loading into streams and waterbodies accelerates eutrophication, polluting the water and rendering it unsuitable for human consumption. Organic and inorganic nitrogen cycles, as well as phosphorous fractions, are simulated in SWAT by dividing the nutrients in the soil into organic and inorganic parts and component pools (Figure 2.2), which can increase or decrease depending on the transformation and additions or losses occurring within each pool (Green and van Griensven, 2008).

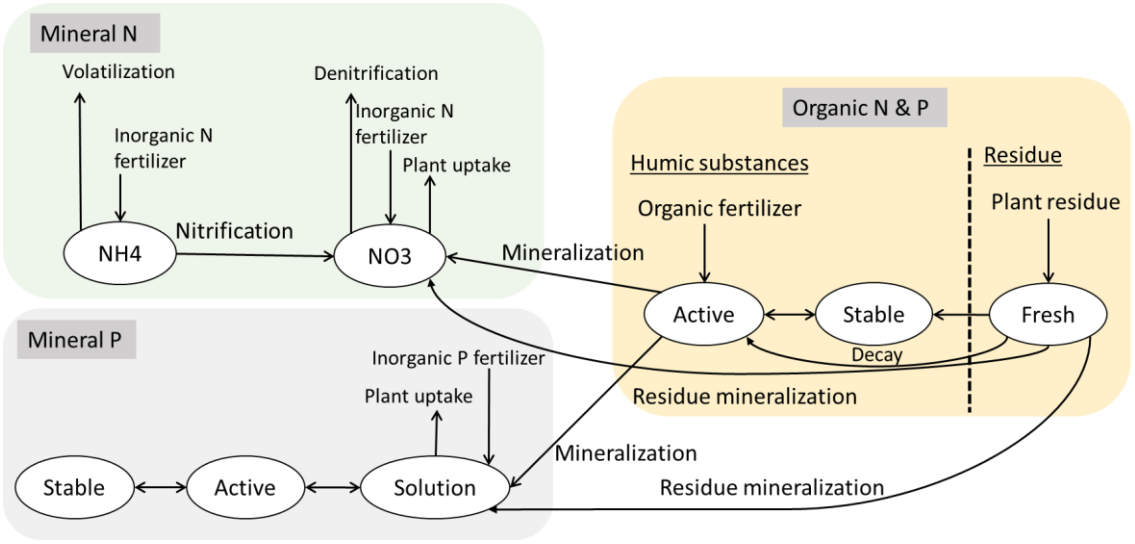

Figure 2.2: Nitrogen and phosphorous pools and transformation processes simulated in the SWAT model (adapted from Neitsch *et al.* (2011)).

2.4.1 Nitrate transportation in the SWAT model

Nitrate and nitrogen movement and transformation are simulated in the model through denitrification, nitrification, mineralization, plant uptake, decay, fertilization, and volatilization processes. SWAT distinguishes three pools of organic nitrogen (active, stable, and fresh) and two pools of mineral nitrogen (ammonia and nitrates), as shown in Figure 2.2. The movement and transformation of several forms of nitrogen within the watershed are introduced into the main channel through surface runoff, lateral flow, or percolation and transported downstream with the flow (Arabi *et al.*, 2008). The nitrate transported by water is calculated using the nitrate concentration in mobile water, as shown in Equation (2.12). This helps to obtain the mass of nitrate lost from each soil layer.

$$\mathrm{conc}_{\mathrm{NO3,mobile}} = \frac{\mathrm{NO3}_{\mathrm{ly}} \times \left\{1 - \exp\left[\frac{-w_{\mathrm{mobile}}}{(1-\theta_e)\times \mathrm{SAT}_{\mathrm{ly}}}\right]\right\}}{w_{\mathrm{mobile}}} \qquad (2.12)$$

Where $\mathrm{conc}_{\mathrm{NO3,mobile}}$ represents the nitrate concentration in mobile water for a given soil layer (kg N mm^{-1} H_2O), $\mathrm{NO3}_{\mathrm{ly}}$ represents the nitrate amount in the soil layer (kg N ha^{-1}), w_{mobile} represents the amount of mobile water in the soil layer (mm H_2O), θ_e represents the fraction of porosity from which anions are excluded, and $\mathrm{SAT}_{\mathrm{ly}}$ represents the saturated water content of the soil layer (mm H_2O). The amount of mobile water in the soil layer is the total amount of water lost by surface runoff, lateral flow, and percolation and is calculated using Equations (2.13) and (2.14).

$$w_{mobile} = Q_{surf} + Q_{lat,ly} + w_{perc,ly}$$ for the top 10 mm soil layer (2.13)

$$w_{mobile} = Q_{lat,ly} + w_{perc,ly}$$ for the lower soil layers (2.14)

Where Q_{surf}, $Q_{lat,ly}$, and $w_{perc,ly}$ are the surface runoff generated in a given day (mm H_2O), the water discharged from the soil layer by lateral flow (mm H_2O), and water percolating the underlying soil layers (mm H_2O).

The nitrate removed in surface runoff ($NO3_{surf}$), lateral flow ($NO3_{lat,ly}$), and percolation ($NO3_{perc,ly}$) are based on the following Equations:

$$NO3_{surf} = \beta_{NO3} \times conc_{NO3,mobile} \times Q_{surf}$$ for surface runoff (2.15)

$$NO3_{lat,ly} = \beta_{NO3} \times conc_{NO3,mobile} \times Q_{lat,ly}$$ for lateral flow in the top 10 mm layer (2.16)

$$NO3_{lat,ly} = conc_{NO3,mobile} \times Q_{lat,ly}$$ for lateral flow in the lower soil layers (2.17)

$$NO3_{perc,ly} = conc_{NO3,mobile} \times w_{perc,ly}$$ for percolation (2.18)

Where $\beta_{NO3}$is the nitrate percolation coefficient, and the nitrate removal units are kg N ha^{-1}.

The modeling of nitrates in agricultural lands using SWAT is mainly concerned with the anthropogenic pollution resulting from nonpoint and point sources of pollutant loads, such as the excessive use of pesticides and fertilizers. The impacts of nitrates and nitrogen pollutants from agricultural watersheds on the environment are based on various factors, among them the type and amount of fertilizer applied, fixation, type of crops being cultivated, crop management practices, soil characteristics, and hydro-meteorological conditions like hydrogeology and climate (Jégo *et al.*, 2008).

2.4.2 Phosphorous transportation in the SWAT model

Phosphorous (P) movement in the model is tracked at the HRU level across six pools: three organic (active, stable, and fresh) and three inorganic (stable, active, and solution), as shown in Figure 2.2. The soluble inorganic (mineral) P is readily taken up by plants and is in rapid equilibrium with the active inorganic pool. However, the active inorganic pool is in slow equilibrium with the stable inorganic pool, which is relatively unavailable. On the other hand, fresh organic P is associated with crop residue and microbial mass and

can sometimes be transformed into inorganic solution or soil humus pools. The active organic pool is associated with soil humus and easily mineralizes into the inorganic pool. However, it maintains a slow equilibrium with the stable organic pool, which does not mineralize as quickly as the active pool despite also being associated with the soil humus. At the subbasin and HRU levels, the model outputs include sediment P, which is attached to the eroded sediment particles; organic P, which is found in organic matter transported from the fields; soluble P, which is the portion of phosphorus that is dissolved in the overland flow, and tile P, which is the soluble P exported through tile drains. However, when these HRU and subbasin-based P outputs are exported to the stream, they are aggregated into mineral (soluble and tile) and organic (sediment and organic) phosphorus, which sums up to the total phosphorous, as shown in Figure 2.3 (Chaubey *et al.*, 2006).

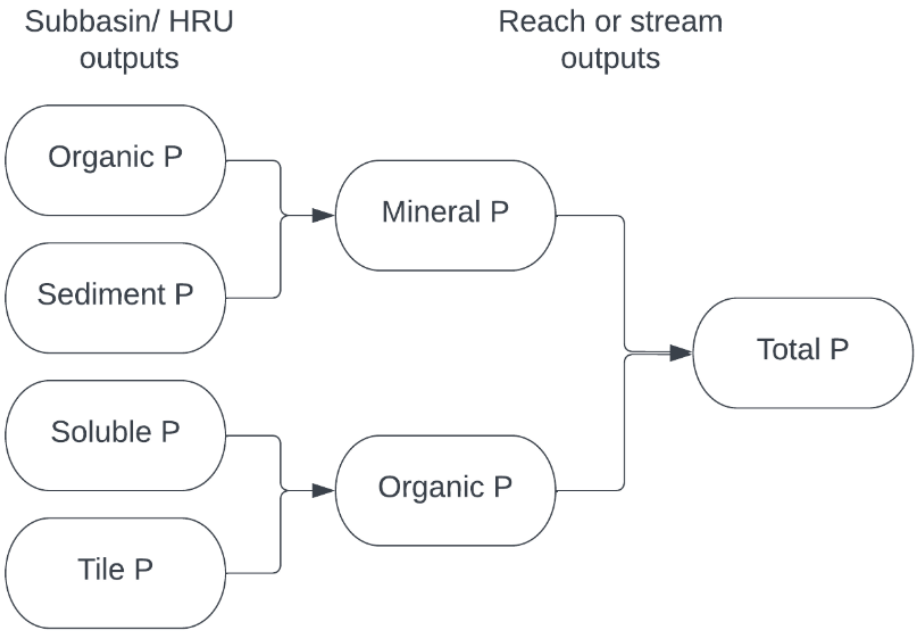

Figure 2.3: Schematic diagram of phosphorus output pools aggregation at the subbasin and HRU levels and at the reach and stream levels

The movement of phosphorous in the soil is primarily through diffusion. Diffusion is the movement of ions in a soil solution over a small distance (1-2 mm) in response to a concentration gradient. The surface runoff will only partially interact with the solution P stored within the top 10 mm of the soil due to its low mobility. The amount of solution P transported in surface runoff is given by Equation (2.19).

$$P_{surf} = \frac{P_{sol,surf} \times Q_{surf}}{\rho_b \times depth_{surf} \times k_{d,surf}} \quad (2.19)$$

Where P_{surf} represents the amount of soluble P lost in surface runoff (kg P ha^{-1}), $P_{sol,surf}$ represents the amount of P in solution in the top 10 mm soil layer (kg P ha^{-1}), ρ_b represents the bulk density of the top 10 mm soil layer Mg m^{-3}), $depth_{surf}$ represents the depth of the surface layer (10 mm), $k_{d,surf}$ represents the P soil portioning coefficient (m^3 Mg^{-1})

The organic and mineral P attached to soil particles are transported into the main channel through surface runoff. The model estimates the amount of P transported with sediment to the stream using a loading function developed by McElroy *et al.* (1976) and Williams and Hann (1978), as shown in Equation (2.20).

$$sedP_{surf} = 0.001 \times conc_{sedP} \times \frac{sed}{area_{hru}} \times \varepsilon_{P:\,Sed} \quad (2.20)$$

Where $sedP_{surf}$ represents the amount of P transported with sediment to the main channel in surface runoff (kg P ha^{-1}), $conc_{sedP}$ represents the concentration of P attached to sediment in the top 10 mm soil layer (g P (metric ton soil)$^{-1}$), Sed represents the sediment yield on a given day (metric tons), $area_{hru}$ represents the area of the HRU (ha), and $\varepsilon_{P:\,Sed}$ represents the P enrichment ratio. The $conc_{sedP}$ is computed using Equation (2.21).

$$conc_{sedP} = 100 \times \frac{(minP_{active,surf} + minP_{stable,surf} + orgP_{humic,surf} + orgP_{fresh,surf})}{\rho_b \times depth_{surf}} \quad (2.21)$$

Where $minP_{active,surf}$, $minP_{stable,surf}$, $orgP_{humic,surf}$, $orgP_{fresh,surf}$ represents the amount of P in the active mineral pool, stable mineral pool, humic organic pool, and fresh organic pool in the top 10 mm soil layer (kg P ha^{-1}).

The enrichment ratio is the ratio of the P concentration transported with sediment to the concentration of P in the soil layer and is calculated for each storm event using Equation (2.22).

$$\varepsilon_{P:\,Sed} = 0.78 \times \left(conc_{sed,surq}\right)^{-0.2468} \quad (2.22)$$

Where $conc_{sed,surq}$ represents the concentration of sediment in surface runoff (Mg sed m^{-3} H_2O) and is calculated using Equation (2.23).

$$conc_{sed,surq} = \frac{sed}{10 \times area_{hru} \times Q_{surf}} \quad (2.23)$$

2.5 SWAT Calibration and Uncertainty Procedures (SWAT-CUP)

The SWAT-CUP (Soil Water Assessment Tool Calibration and Uncertainty Procedures) is a standalone software that provides an integrated framework for parameterization, sensitivity and uncertainty analysis, calibration, and validation of the SWAT models (Abbaspour, 2015). It comprises five calibration routines that could be used to optimize the SWAT model output files, namely: Sequential Uncertainty Fitting, version 2 (SUFI-2), Particle Swarm Optimization (PSO), Generalized Likelihood Uncertainty Estimation (GLUE), Parameter Solution (ParaSol), and Markov Chain Monte Carlo (MCMC) procedures. Figure 2.4 illustrates the linkage between the SWAT model and SWAT-CUP. The multi-site SUFI-2, a semi-automated inverse modeling routine procedure of SWATCUP, was adopted in this study since it is the most extensively used routine for the SWAT model calibration. The SUFI-2 procedure is an iterative optimization algorithm that combines parameter calibration and stochastic analysis of model outputs (Faramarzi *et al.*, 2009). The SUFI-2 algorithm consists of several crucial steps in achieving effective model calibration, sensitivity, and uncertainty estimation.

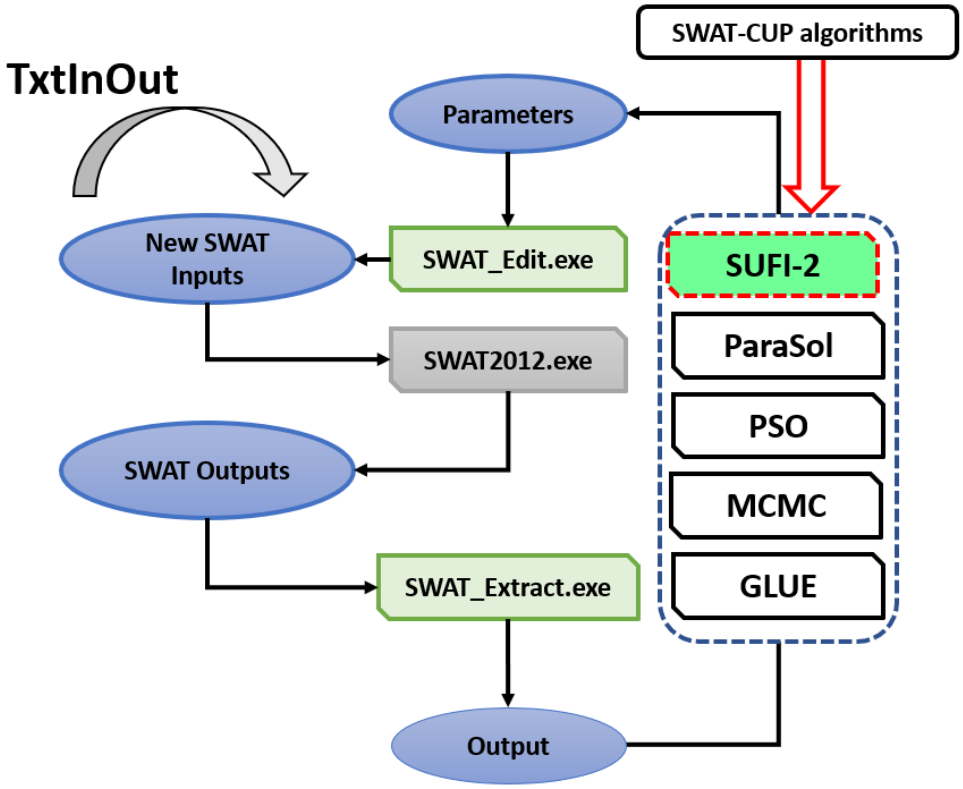

Figure 2.4: Schematic linkage between the SWAT model and SWAT-CUP's five optimization algorithms (adapted from Abbaspour, (2015)).

2.5.1 Sensitivity analysis in SWAT-CUP

The sensitivity analysis identifies the parameters that have the most influence on the model outputs. It streamlines the calibration process by eliminating those deemed as not sensitive, allowing prioritization of efforts and resources toward calibrating the most influential parameters, thereby improving the model performance. The SUFI-2 algorithm offers two types of sensitivity analysis: one-at-a-time (OAT) or local sensitivity analysis and the all-at-a-time (AAT) or global sensitivity analysis. In the local sensitivity analysis, one parameter is changed while keeping all others constant and observing its effect on the model outputs and objective function. This method requires only a few iterations (3-5), therefore straightforward and quick; however, the parameter sensitivity depends on the accuracy of the other fixed parameters. In contrast, the global sensitivity analysis involves simultaneous changes in all the parameters, necessitating a larger number of runs (usually 500 to 1000 or more) to observe the influence of each parameter on the model outputs and objective function. This method is known to produce more reliable results, although the selection of parameter ranges and the number of runs could affect the relative sensitivity of the parameters.

The global sensitivity in SWAT-CUP uses multiple regression, as illustrated in Equation (2.24(to quantify the sensitivity of each parameter (Abbaspour *et al*., 2018).

$$g = \alpha + \sum_{i=1}^{n} \beta_i b_i \qquad (2.24)$$

Where g represents the objective function value, α represents the regression constant, β_i represents the co-efficient of the parameter, and b_i represents the relative significance of each parameter determined using a t-test and assessed by t-stat and p-value. The smaller the p-value, the more sensitive the parameter was, and vice versa. The best combination for the most sensitive parameter is a very small p-value and a large t-stat value (absolute). Parameters with p-values less than 0.05 (p-value < 0.05) are considered to be highly sensitive.

The sensitivity analysis in SWAT-CUP is based on the Latin Hypercube sampling for parameter space exploration (Zhao *et al.*, 2018). Latin Hypercube sampling is preferable to random sampling since it allows for more efficient and effective sampling. It maximizes the diversity of parameter combinations while ensuring adequate parameter space coverage. The Latin Hypercube sampling procedure divides the parameter ranges into multiple intervals (usually 100) to generate equally probable parameter values within

each interval in a process known as stratification. The algorithm then randomly selects a single parameter value from each interval to form a Latin Hypercube sample set. The selected set of parameter values represents one combination of the parameters for executing the SWAT model. This process is repeated iteratively to generate numerous Latin Hypercube sample sets. The generated parameter sets are used to run the SWAT model multiple times, and the SUFI-2 algorithm calculates the objective function for each model run.

2.5.2 Uncertainty analysis in SWAT-CUP

The propagation of all model parameter input uncertainties to the model output is quantified using the 95 percent prediction uncertainty (95PPU). The 95PPU is a statistical indicator derived from Latin Hypercube sampling that provides a measure of confidence in the SWAT model's predictions at the 2.5% and 97.5% levels of the cumulative distribution of output variables (Abbaspour, 2015; Abbaspour *et al*., 2015, 2018). The 95PPU accounts for various uncertainties in the model, including conceptual model simplifications, unaccounted processes, unknown parameter effects and interactions, input data quality, etc., and is quantified using the p-factor and r-factor. The p-factor represents the percentage of observed data bracketed within the 95PPU band, whereas the r-factor is the thickness of the 95PPU band calculated using Equation (2.25) as the ratio of the average distance between the 95PPU band and the standard deviation of the observed data (Abbaspour *et al*., 2004; Abbaspour *et al*., 2018). Satisfactory calibration was achieved when at least 50% of the observed data fell within the 95PPU band (p-factor > 0.5).

$$\mathrm{r-factor_j} = \frac{\frac{1}{n_j}\sum_{t_{i=1}}^{n_j}\left(x_{sim}^{t_i,97.5\%} - x_{sim}^{t_i,2.5\%}\right)}{\sigma_{obs_j}} \qquad (2.25)$$

Where $x_{sim}^{t_i,97.5\%}$ and $x_{sim}^{t_i,2.5\%}$ represents upper and lower bounds of the 95PPU at t time-step and i simulations; n_j represents the number of data points, and σ_{obs_j} represents the standard deviation of the jth observed variable.

2.5.3 Calibration and validation in SWAT-CUP

Calibration aims to minimize the difference between model simulations and observations through the optimization (minimization or maximization) of an objective function, as shown in Equations 2.26 and 2.27:

$$\text{Min:} \quad g(\theta) = \sum_{j=1}^{v}\left[w_j \sum_{i=1}^{n_j}(x_{obs} - x_{sim})_i^2\right] \tag{2.26}$$

or,

$$\text{Max:} \quad g(\theta) = \sum_{j}^{v}\left[w_j\left(1 - \frac{\sum_{i=1}^{n_j}(x_{obs} - x_{sim})_i^2}{\sum_{i=1}^{n_j}(x_{obs} - \bar{x}_{sim})_i^2}\right)\right] \tag{2.27}$$

Where g represents the objective function, θ represents a vector of the model parameters, x_{obs} represents an observed variable, x_{sim} represents the corresponding simulated variable, $\bar{x}_{sim}$ represent the mean of the simulated variable, v represents the number of measured variables used to calibrate the model, w_j represents the weight of the jth variable, and n_j represents the number of measured observations in the jth variable.

The objective function assesses the goodness of fit between the simulated model outputs and the observed data. SWAT-CUP facilitates understanding model performance and identifies optimal parameter values by comparing the model outputs against the observed data using different parameter sets, leading to better model calibration. SWAT-CUP achieves this by applying statistical and optimization techniques to rank and optimize the parameter sets based on objective function values. The algorithm updates parameter distributions during the iterative process using Bayesian concepts and feedback techniques (Abbaspour, 2015). This updating process helps improve the parameter distributions' precision, thus reducing the uncertainty associated with the model predictions.

Validation is used to build confidence in the calibrated parameters. It involves applying the calibrated parameter ranges to an independent set of measured observations without any alterations. In the validation process, a single iteration with the same number of simulation runs as in the last calibration is performed, and the results are quantified using the p-factor, r-factor, and objective function values. The data used in the validation period must adhere to physical conditions similar to the calibration period, such as climate and land use. Furthermore, the average variance in data during calibration and validation periods should be more or less the same.

2.6 SWAT model performance evaluation

The model performance was evaluated using various widely recognized statistical techniques. Moriasi *et al.* (2007) recommend the following quantitative statistical

techniques for evaluating the SWAT model performance: Coefficient of Determination (R^2), Nash-Sutcliffe efficiency (NSE), and percent bias (PBIAS).

The *coefficient of determination (R^2)* is the correlation between the observed and simulated values. It calculates the probability of the simulated values matching the observed data. It estimates the number of data points that fall within the results of the best-fit line created by the regression equation. The higher the coefficient of determination, the greater the proportion of points the line passes through when the data points and line are plotted, with a value of 1 indicating perfect correlation. Values of 1 or 0 would indicate that the regression line represents all or none of the data. A greater coefficient indicates better goodness of fit for the observations. However, it's important to note that R^2 is oversensitive to high extreme values (Krause *et al.*, 2005) and insensitive to additive and proportional differences between model predictions and measured data (Legates and McCabe, 1999). R^2 is calculated using Equation (2.28), using the same symbols as the previous equations.

$$R^2 = \frac{\left[\sum_{i=1}^{n}(x_{obs}-\bar{x}_{obs})\times(x_{sim}-\bar{x}_{sim})\right]^2}{\sum(x_{obs}-\bar{x}_{sim})^2\times\sum(x_{sim}-\bar{x}_{sim})^2} \quad (2.28)$$

The *Nash-Sutcliffe Efficiency (NSE)* (Nash and Sutcliffe, 1970) is a normalized statistic that determines the relative magnitude of the residual variance compared to the observed or measured data variance. It measures how well a model predicts observed data compared to the average observed value. The NSE value ranges from -∞ to 1, with 1 indicating a perfect match between the model's predictions and the observed data. Values closer to 1 signify better model performance, while negative values suggest the model performs worse than a simple average. NSE is good for continuous long-term simulations and can be used to determine how effectively the model simulates trends for a given output response (Moriasi *et al.*, 2015). However, it does not indicate whether the model underestimates or overestimates the observations; therefore, it cannot be utilized for single-event simulations. Due to the squared differences, NSE is sensitive to extreme values (Krause *et al.*, 2005). NSE is calculated using Equation (2.29), using the same symbols as the previous equations.

$$NSE = 1 - \left(\frac{\sum_{i=1}^{n}(x_{obs}-x_{sim})^2}{\sum_{i=1}^{n}(x_{obs}-\bar{x}_{obs})^2}\right) \quad (2.29)$$

Percent Bias (PBIAS) is the deviation of the results from the observations expressed as a percentage. It measures the average tendency of the simulated data to be larger or smaller than the observed data. An ideal model should have a PBIAS of 0. However, models tend to have either a positive or negative PBIAS, implying either an underestimation or an overestimation of the observations. However, PBIAS cannot be utilized for single-event simulations to identify variations in magnitude and timing for the output response because it only provides the average magnitudes. Additionally, it does not indicate how well a model simulates residual variations and trends for a given output response. PBIAS is calculated using Equation (2.30), using the same symbols as the previous equations.

$$\text{PBIAS} = \left[\frac{\sum_{i=1}^{n}(x_{obs}-x_{sim})\times 100}{\sum_{i=1}^{n} x_{obs}}\right] \quad (2.30)$$

Table 2.1 summaries the model performance evaluation criteria for the selected statistical performance techniques based on Moriasi *et al.* (2015). These indices served as the benchmark for evaluating the model's accuracy and reliability in replicating the observed data.

Table 2.1: The SWAT model performance evaluation criteria for recommended statistical performance measures at the catchment scale.

Performance metrics	Range	Optimal value	Output variable	Performance evaluation criteria			
				Minimum threshold	Very Good	Good	Satisfactory
R^2	0 – 1	1	Streamflow	≥ 0.60	> 0.85	0.75 – 0.85	0.60 – 0.75
			Sediment	≥ 0.40	> 0.80	0.65 – 0.80	0.40 – 0.65
			Nitrate	≥ 0.30	> 0.70	0.60 – 0.70	0.30 – 0.60
			Phosphorous	≥ 0.40	> 0.80	0.65 – 0.80	0.40 – 0.65
NSE	-∞ – 1	1	Streamflow	≥ 0.50	> 0.80	0.70 – 0.80	0.50 – 0.70
			Sediment	≥ 0.45	> 0.80	0.70 – 0.80	0.45 – 0.70
			Nitrate	≥ 0.35	> 0.65	0.50 – 0.65	0.35 – 0.50
			Phosphorous	≥ 0.35	> 0.65	0.50 – 0.65	0.35 – 0.50
PBIAS	-∞ – ∞	0	Streamflow	≤ ±25%	±5%	±5% – ±15%	±15% – ±25%
			Sediment	≤ ±55%	±10%	±10% – ±25%	±25% – ±55%
			Nitrate	≤ ±70%	±15%	±15% – ±35%	±35% – ±70%
			Phosphorous	≤ ±70%	±15%	±15% – ±35%	±35% – ±70%

Chapter 3:

3 Description of the Study Areas and Data Acquisition

3.1 Introduction

The dissertation focused on two agricultural-dominated watersheds, namely the Cidacos River watershed in northern Spain and the Swedish Environmental Monitoring Program's Catchment C6 in southeastern Sweden. These watersheds were carefully selected because of their contrasting geographical, climatic, agricultural, and water quality challenges in Europe. They represent the prevalent agricultural practices in their regions, providing valuable insights into the complexities and challenges of water management and ecological sustainability in such contexts. The two study areas exemplify agricultural landscapes with unique climatic, geographical, and socioeconomic characteristics. This chapter aims to provide detailed descriptions of these two study areas, contextualizing their geographical locations, climatic conditions, land uses, soil characteristics, and hydrological and ecological attributes. The chapter further elucidates the primary data used in the studies and their acquisition techniques.

3.2 Description of the Cidacos River watershed (Spain)

The Cidacos River is one of the tributaries of the Aragón River, a tributary of the Ebro River. It is located approximately 15 km south of Pamplona, the capital of the Chartered Community of Navarre in Spain, at latitudes 42˚ 69' and 42˚ 34' north and longitudes 1˚ 72' and 1˚ 47' west. The Cidacos River drains a watershed area of 477 km^2 and runs north-south, with an approximate length of 44 km and width of 15 km in its widest section (Figure 3.1). The watershed's headwater is somewhat mountainous in the north, with high altitudes of slightly over 1000 m above sea level, but then crosses down to slightly uneven to low terrain of approximately 300 m above sea level in the south at the river's mouth in Traibuenas, where it joins the Aragón River. The watershed's climate is humid to dry, temperate, mild Mediterranean, with cold winters (monthly average: 4.7 ºC to 5.4 ºC in January) and warm summers (monthly average: 21.2 ºC to 23.7 ºC in August) that vary spatially from North to South. The annual average temperature ranges from 12.2 ºC to 14.2 ºC (north to south). The watershed receives annual precipitation from 800 mm in the north to 400 mm in the south, characterized by strong inter-annual variability and high summer aridity. The wettest months are April and May (Merchán *et al.*, 2020). The annual evapotranspiration rate is approximately 1150 mm $year^{-1}$, with nearly 76% occurring between April and September (Merchán *et al.*, 2020).

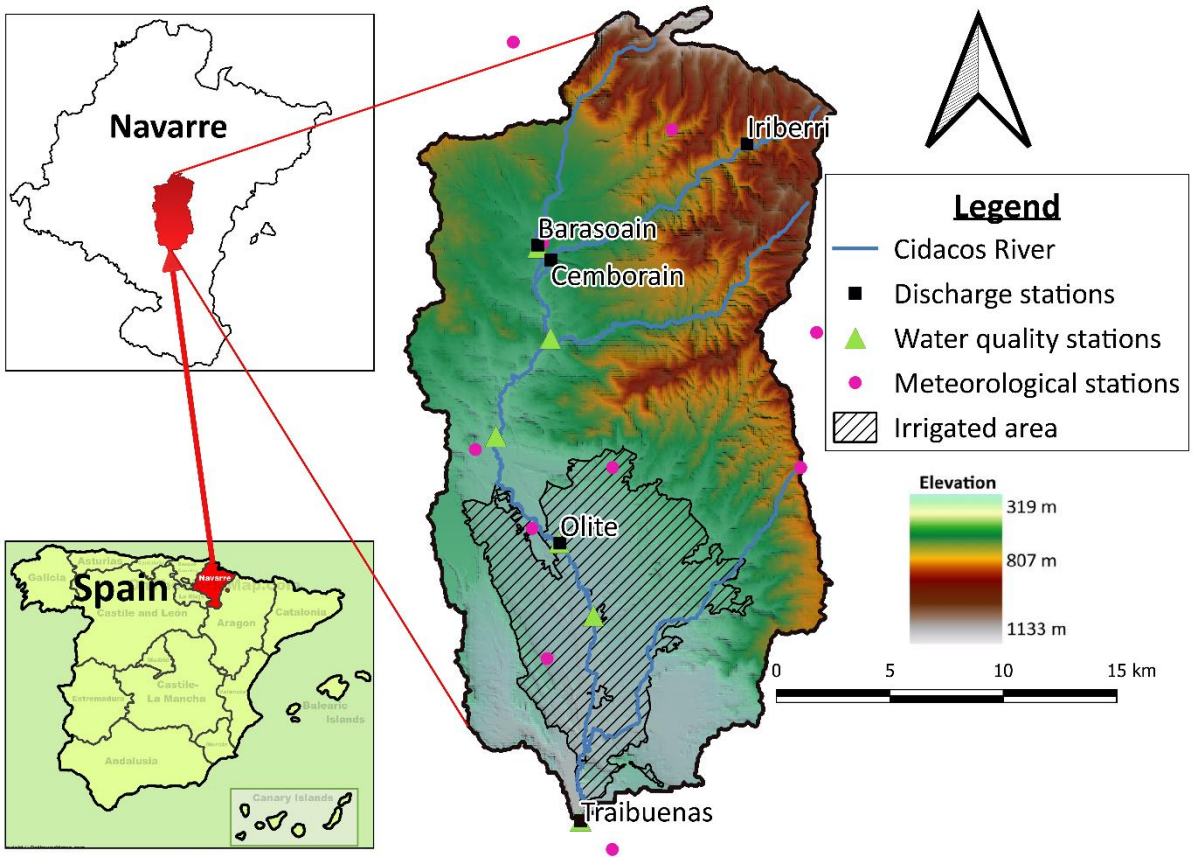

Figure 3.1: The Cidacos River watershed location, elevation map, and measuring stations.

Agriculture is the watershed's predominant land use (Table 3.1, Figure 3.2a), accounting for 53% of the total area. Other major land uses in the watershed include forests (25%) and pasture and bushlands (17%). The remaining 5% comprises urban, residential areas, built-up land, bare land, and water bodies. Rainfed agriculture covers 176 km^2 (37% of the total area and 70% of cultivated land) and is primarily in the watershed's upper reaches until Olite town. Irrigated land, on the other hand, covers 77 km^2 (16% of the total area and 30% of the cultivated land) and is mainly in the watershed's lower reaches. Table 3.1 shows the proportions of the land use land cover (LULC) classes in the watershed.

Table 3.1: Land use land cover (LULC) classes and their proportions in the Cidacos River watershed

Land Use	Land Use Class	SWAT Code	Area covered (km^2)	Percentage of watershed
Agriculture*	Corn	CORN	67.88	14.23
(53.15%)	Wheat	WWHT	77.30	16.20
	Winter Barley	WBAR	51.30	10.75
	Tomatoes	TOMA	20.53	4.30
	Potatoes	POTA	9.58	2.01
	Orchard and Vineyards	ORCD	26.21	5.49
	Asparagus	ASPR	0.71	0.15
	Apple	APPL	0.03	0.01
Forest	Deciduous Forest	FRSD	3.53	0.74
(25.06%)	Evergreen Forest	FRSE	10.09	2.11
	Mixed Forest	FRST	20.51	4.30
	Oak Tree	OAK	50.97	10.69
	Pine Tree	PINE	34.46	7.22
Pasture/Bushes	Pasture	PAST	6.67	1.40
(16.92%)	Shrubland/brushes	RNGB	73.03	15.31
	Grassland/Herbaceous	RNGE	0.99	0.21
Urban, Residentials	Urban Transportation	UTRN	6.32	1.32
and built-up land	Urban Commercial	UCOM	0.74	0.16
(2.55%)	Urban Medium Density	URML	2.39	0.50
	Urban Industrial	UIDU	1.90	0.40
	Urban Institutional	UINS	0.82	0.17
Bare land (1.50%)	Bare land	BARR	7.16	1.50
Water	Water	WATR	2.41	0.51
(0.83%)	Non-forested Wetland	WETN	1.04	0.22
	Herbaceous Wetlands	WETF	0.46	0.10
TOTAL			477.03	100

*Agriculture land use encompasses rainfed (37%) and irrigated (16%) croplands.

The irrigated area gets its water from the Navarre Canal, which flows from the Itoiz Reservoir on the Irati River, about 70 km north of the study area (INTIA, 2021). The conversion from rainfed cultivation to irrigation within the study area has been gradual, with most changes occurring between 2009 and 2012 (Figure 3.3). By 2013, approximately 90% of the current irrigated area had been converted from rainfed to irrigation. The main irrigation method used in the study area is pressurized (sprinkler)

(71%) with buried fixed sprinkler systems. Drip irrigation (20.3%) and pivot/canon irrigation (8.5%) are two other types of irrigation used in the area (INTIA, 2021).

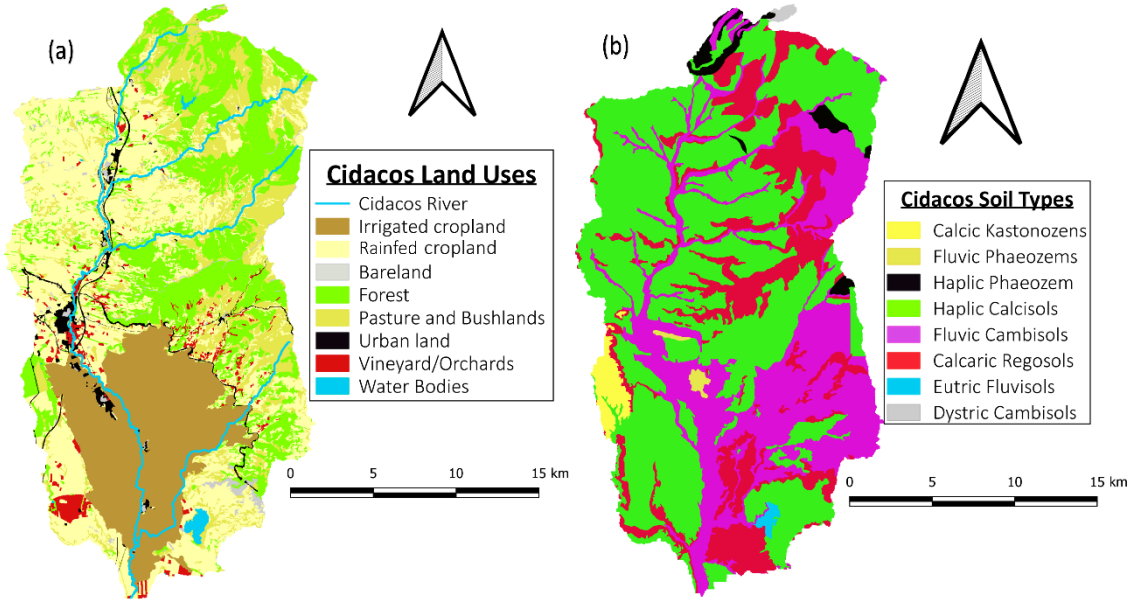

Figure 3.2: The Cidacos River watershed (a) land use land cover map and (b) soil type map (FAO-WRB classification).

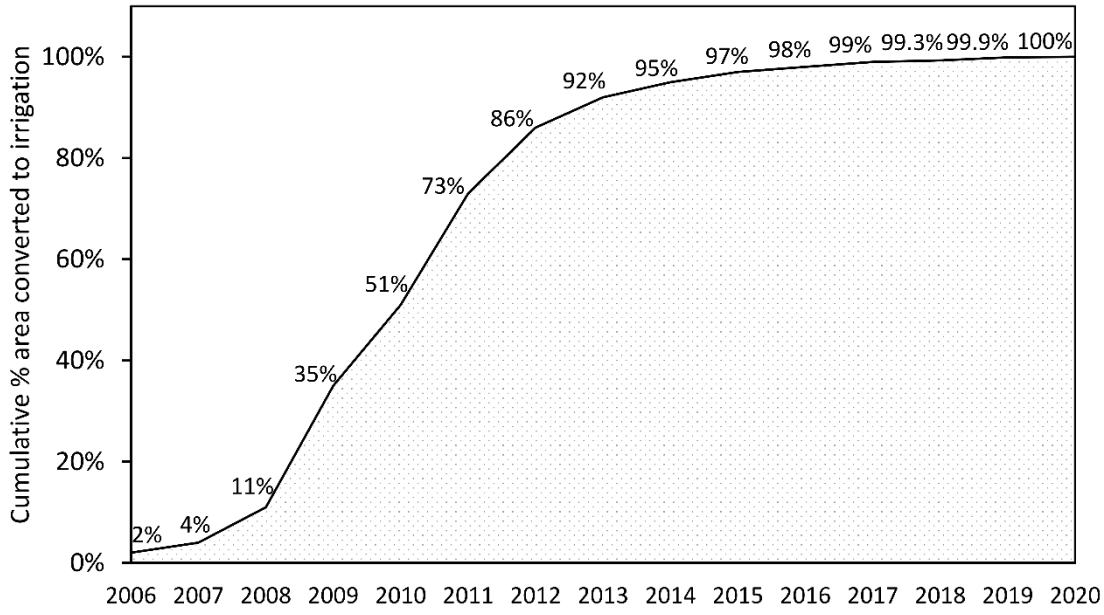

Figure 3.3: Cumulative annual percentage of the irrigated area converted from rainfed agriculture in the Cidacos River watershed from 2006 to 2020.

The main crops grown in the watershed are rainfed winter cereals (wheat and barley) and vineyards (orchards). Corn, tomatoes, and potatoes are among the crops grown in the irrigated area. The average annual fertilizer application rates range from 80 to 130 kg N

ha^{-1} for winter cereals and 40 to 50 kg N ha^{-1} for vineyards. Crop diversity is greater in the irrigated area than in the rain-fed zone. Consequently, fertilizer applications have increased to meet the increased production expectations. The annual average fertilization rates in the irrigated region are 260 to 300 kg N ha^{-1} for corn and 120 to 200 kg N ha^{-1} for tomatoes and potatoes. Table 3.2 summarizes the annual agricultural management practices in the Cidacos River watershed, including cropping cycles, tillage, fertilization, irrigation water consumption, and crop yield for the most common crops.

Table 3.2: Average annual agricultural practices and yield in the Cidacos River watershed

Crop type	Cropping cycle	Tillage date	Fertilization date	Fertilization (N kg ha^{-1} yr^{-1})	Type of fertilizer applied*	Irrig. water consumption (mm ha^{-1} yr^{-1})	Annual crop yield (100 kg ha^{-1} yr^{-1})
Wheat	01 Nov - 01 Jul	01 Oct	01 Oct 01 Jan	40 60	9-23-30 Urea + Ammonium sulfate	Rainfed	> 50
Winter barley	01 Nov - 01 Jul	01 Oct	01 Oct 1 Jan	40 60	9-23-30 Urea + Ammonium sulfate	Rainfed	> 50
Corn	01 May - 01 Nov	01 Apr	15 Apr 15 Jun	40 260	9-23-30 Urea	700 – 800	90 – 110
Tomato	10 May - 15 Sept	01 Apr	15 Apr 15 Jun	60 120	9-23-30 8-4-10	550 – 650	500 – 550
Potato	01 May - 15 Sept	01 Apr	15 Apr 15 Jun	60 120	9-23-30 NAC 27%	500 – 600	250 – 400

*9-23-30 contains 9% nitrogen (N), 23% phosphorous (P), and 30% potassium (K) (typically used for plants with high P and K requirements); Urea + ammonium sulfate fertilizer has a nitrogen content of 38% and a sulfate content of 18.75%; urea has a nitrogen content of 46%; 8-4-10 is composed of 8% nitrogen, 4% phosphorous, and 10% potassium (commonly used as a top dressing in crops that require an additional boost of N and K, and in soils with minor P deficiencies); NAC 27% is composed of calcium ammonium nitrate, which contains 27% nitrogen.

The most abundant soil textures in the watershed are loam and clay-loam, which are found in most agricultural areas, while loamy-sand and sandy-loam soils are found on eroded hillslopes. Red clay soils dominate the watershed with sandstone and mudstones. According to the FAO classification system (IUSS Working Group WRB, 2015), the

watershed's predominant soil types (Table 3.3, Figure 3.2b) are Haplic Calciols soils (51.6%), Fluvic Camisols soils (26.1%) which are mostly found along the river network path, and Alaric Regosols (18%). Haplic Phaeozem (1.7%), Calcic Castanea's (1.6%), Fluvic Phaeozem (0.4%), Eutric Fluvisols (0.3%), and Dystric Cambisols (0.2%) are among the other soils found in the watershed.

Table 3.3: Soil distribution in the Cidacos River watershed

USDA soil name	FAO soil name	FAO symbol	Area (km^2)	Percent (%)	Soil texture
Typic Calcixerepts	Haplic Calcisols	CLh	246.31	51.63	Loam
Typic/ Fluventic Haploxerepts	Fluvic Cambisols	CMf	124.49	26.10	Clay-Loam
Typic/Lithic Xerorthents, Udorthent	Calcaric Regosols	RGc	85.98	18.02	Loamy-Sand
Lithic-Ruptic Haplustolls	Haplic Phaeozem	PHh	8.19	1.72	Clay-Loam
Typic calcixeroll	Calcic Kastanozems	KSk	7.47	1.56	Loam
Fluventic Haploxerolls	Fluvic Phaeozem	PHf	1.93	0.41	Loam
Typic Xerofluvent	Eutric Fluvisols	FLe	1.58	0.33	Clay-Loam
Typic Dystrudepts	Dystric Cambisols	CMd	1.08	0.23	Sandy-Loam

3.3 Description of Catchment C6 (Sweden)

The study area, Catchment C6 (Figure 3.4), is an agricultural catchment in southeastern Sweden within the Lake Malaren basin of Uppsala County. It is one of the small Swedish agricultural monitoring catchments located in leaching region 6. Leaching regions (Figure 3.4a) are sub-divisions of agricultural production areas in Sweden that are relatively homogeneous in terms of climate and farming (Kyllmar *et al.*, 2006). These agricultural monitoring catchments have been designated as the main agricultural areas for intensive water quality monitoring since 1990 under the Swedish Environmental Monitoring Program (Kyllmar *et al.*, 2014).

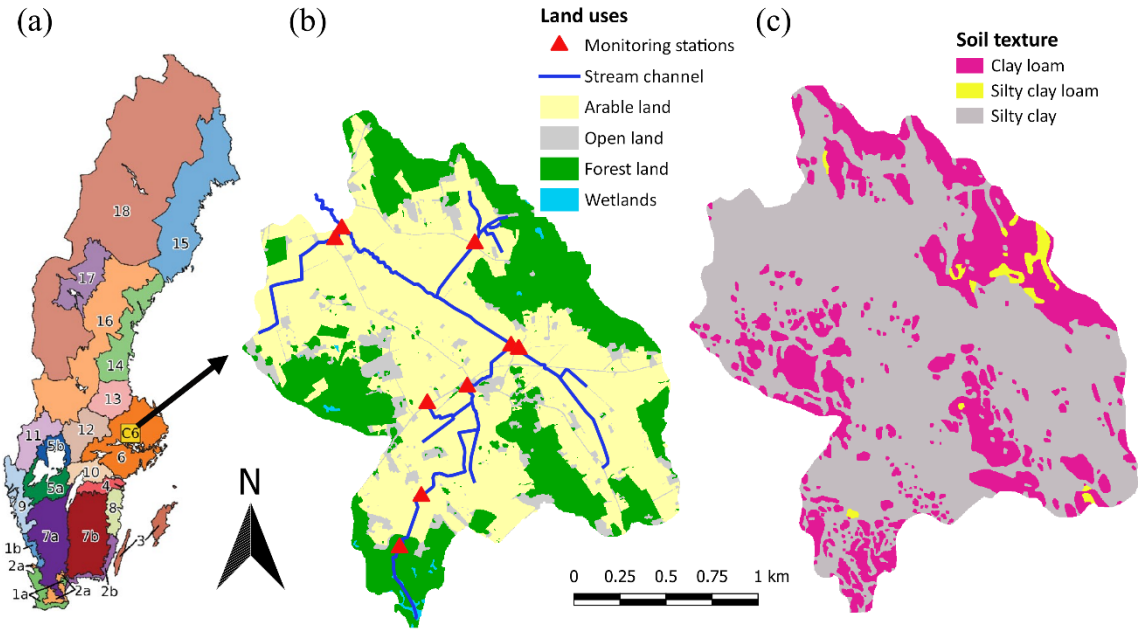

Figure 3.4: (a) Location of the catchment C6 within Sweden and in the leaching region 6, (b) land use, and (c) soil maps of the catchment C6.

Crop production within the monitored catchments is generally more intensive than in the wider region. Catchment C6 covers 3298 ha (33 km^2) and is characterized by high levels of phosphorous load and sediment (suspended solids) exportation in comparison to the other catchments (Kyllmar *et al.*, 2014). The long-term average total phosphorous export from the study area (0.50 kg P ha^{-1} yr^{-1}) is higher than the average of all agricultural monitoring areas combined (0.43 kg P ha^{-1} yr^{-1}), with the agricultural calendar year of 2021/2022 recording the highest total phosphorous load (0.65 kg P ha^{-1} yr^{-1}) among the monitored catchments (Linefur *et al.*, 2022). On the contrary, nitrogen losses from the catchment (6.3 kg N ha^{-1} yr^{-1}) are very low, ranking among the least in the monitored catchments (Linefur *et al.*, 2022). Table 3.4 details the total nitrogen and total phosphorous exported from the various agricultural monitoring catchments in Sweden.

Table 3.4: The average annual total nitrate (Total N) load and total phosphorous (Total P) load in different agricultural monitoring catchments in Sweden from 2005-2020 (source: Linefur *et al.*, 2022).

Catchment ID	Area (km^2)	Long-term averages (kg ha^{-1} yr^{-1})		Values for 2020/2021 (kg ha^{-1} yr^{-1})	
		Tot-N load	Tot-P load	Tot-N load	Tot-P load
C6	**33**	**6.3**	**0.50**	**5.3**	**0.65**
E21	16.3	15.2	0.08	17.6	0.03
E23	7.4	7.4	0.39	9.7	0.21
E24	6.3	6.6	0.55	8.2	0.36
F26	1.8	15.8	0.52	15.7	0.13
H29	7.2	11.9	0.15	7.5	0.04
I28	4.8	16.3	0.33	19.0	0.44
K31	7.7	7.0	0.16	8.2	0.09
K32	8.6	15.2	0.28	-	-
M36	7.9	16.9	0.58	20.7	0.42
M39	6.8	33.1	0.41	55.1	0.61
M42	8.2	26.6	0.43	21.9	0.25
N34	13.9	32.7	0.41	24.9	0.16
O14	10.2	13.1	0.56	27.8	0.65
O17	9.7	12.8	0.20	17.5	0.29
O18	7.7	15.1	1.64	15.7	0.51
S13	35.2	8.5	0.32	-	-
U8	5.7	6.7	0.54	4.1	0.35
X2	32.8	4.1	0.20	2.5	0.24

The catchment receives an average of 550 mm of precipitation annually, has an annual average temperature of 5.5 ºC (ranging from -21ºC to 28ºC), and a potential evapotranspiration rate of 400 to 500 mm. Most of the arable land is artificially drained through subsurface tile drains at an average depth of 1 meter. Runoff on the soil occasionally occurs during snowmelt or intensive rainfall events. The average annual flow at the stream outlet is estimated to be 220 mm.

Agriculture is the predominant land use in the catchment, accounting for nearly 60% of the total area, while forest land accounts for slightly more than 30% (Figure 3.4b). The main crops cultivated in the arable land are cereals (winter wheat and spring barley). Other crops commonly cultivated in the catchment are oilseed rape, oats, rye, and some leguminous plants (beans and peas). The catchment has a heavy soil texture primarily

composed of postglacial clay soils with silty clay soil, mainly the arable land surface, while clay loam and silty clay loam soils dominate the forested areas (Figure 3.4c).

The catchment receives nitrogen and phosphorous primarily from mineral fertilizers, with an average annual supply of 120 kg N ha^{-1} (ranging from 100 to 150 kg N ha^{-1}) and 12 kg P ha^{-1} (ranging from 7 to 21 kg P ha^{-1}), respectively (Swedish Environmental Emissions Data (SMED), 2019). Only a tiny portion of the cultivated land (≤5%) is organically farmed with stable manure. The annual average mineral phosphorous fertilization rates for the dominant crops are 21 kg P ha^{-1} yr^{-1} for winter wheat and 14 kg P ha^{-1} yr^{-1} for spring barley. The Swedish authorities have set a phosphorous threshold of a maximum of 22 kg P ha^{-1} yr^{-1} on average over five years. The annual average nitrogen fixation by leguminous crops is 100 kg N ha^{-1} yr^{-1}. Table 3.5 summarizes the average mineral fertilization rates and crop yields for the commonly cultivated crops in the catchment.

Table 3.5: Average annual agricultural practices and yield in Catchment C6

Crop type	Cropping cycle	Date of Tillage	Annual mineral fertilization		Annual Crop yield (100 kg ha^{-1})
			N (kg ha^{-1})	P (kg ha^{-1})	
Spring Barley	30 Apr – 20 Aug	14 Oct	95	14	52.1
Winter Wheat	11 Sep – 27 Aug	03 Sep	153	21	73.6
Oats	30 Apr – 20 Aug	06 Oct	75	13	44.9
Spring Wheat	30 Apr – 30 Aug	06 Oct	114	14	46.4
Grain Legumes	13 May – 30 Aug	06 Oct	-	20	34.5
Rape	05 Sep – 06 Aug	02 Sep	162	17	34.3
Rye	11 Sep – 16 Aug	02 Sep	98	17	66.6

3.4 Data acquisition in the Cidacos River watershed

The data used for the research in the Cidacos River watershed were primarily obtained from the Government of Navarre agencies and websites, as shown in Table 3.6. The climate data were obtained at a daily time-step from 25 weather stations (both manual and automatic) located within and near the watershed from 1990 to 2020 (Figure 3.5). The selected stations represented the spatial heterogeneity of the watershed's climate. The meteorological data included daily data of precipitation (mm), maximum and minimum daily temperatures (˚C), solar radiation (MJ m^{-2} s^{-2}), wind speed (m s^{-1}), and relative humidity (%) data. The agricultural management information (Table 3.1), which included planting and harvesting dates, the average annual fertilizer application rates, and the main crops cultivated in the watershed, were obtained from INTIA's technical team and

extension advisors who conduct field interviews in consultation with key informants such as farmers within the watershed. The monthly observed streamflow data and nitrate loads from 2000-2020 were used for the model evaluation. The data used were obtained from the Olite gauging station since it was the only station in the watershed with consistent and extensive long-term data of observed discharge and nitrate concentration data. This station has been operational since 1988 and covers the watershed area under rainfed agriculture. The contribution of nitrate pollution from point sources in the study area is negligible, accounting for only about 1.5% of the nitrate loads (Merchán *et al.*, 2020); thus, it was not considered in the modeling.

Table 3.6: The SWAT model input data requirement and their sources

Dataset	Resolution*	Source**
Topography map	25m, ETRS89 UTM Zone 30N projection	IDENA portal for Digital Elevation Map (DEM) data
Land use map	25m, 2019 LULC map	IDENA portal for Land Use/Cover data
Soil type map	1:25000	IDENA portal, Soil type data
Meteorological	Daily (1990-2020)	Meteorology and climatology portal
Streamflow	Daily (2000-2020)	Water in Navarra portal
Water quality	Monthly (2000-2020)	GAN-NIK and INTIA
Agricultural management	Annual	Consultation with the farmers and key stakeholders (INTIA)
Irrigation	Monthly (2017-2020)	INTIA and Aguacanal reports
Climate change	Daily (1961-2100)	Spanish climate change portals of AdapteCCa and AEMET

*ETRS89 UTM Zone 30N projection refers to a coordinate reference system of the Universal Transverse Mercator (UTM) projection based on the European Terrestrial Reference System 1989 (ETRS89) datum.

**IDENA is the government portal for spatial data and infrastructure in Navarre; meteorology portal is the government website with data from all the weather stations in Navarre; Water in Navarre portal is the government website for all river discharge data in Navarre; INTIA is the government agency for agri-food technologies and infrastructure in charge of agriculture and irrigation in Navarre; GAN-NIK is the government agency in charge of environmental management in Navarre; Aguacanal is the company in charge of the Navarre Canal's irrigable zone first phase; AdapteCCa refers to the Platform on Adaptation to Climate Change in Spain that contains statistically downscaled climate data for the whole of Spain; AEMET is the Spanish government national meteorological agency.

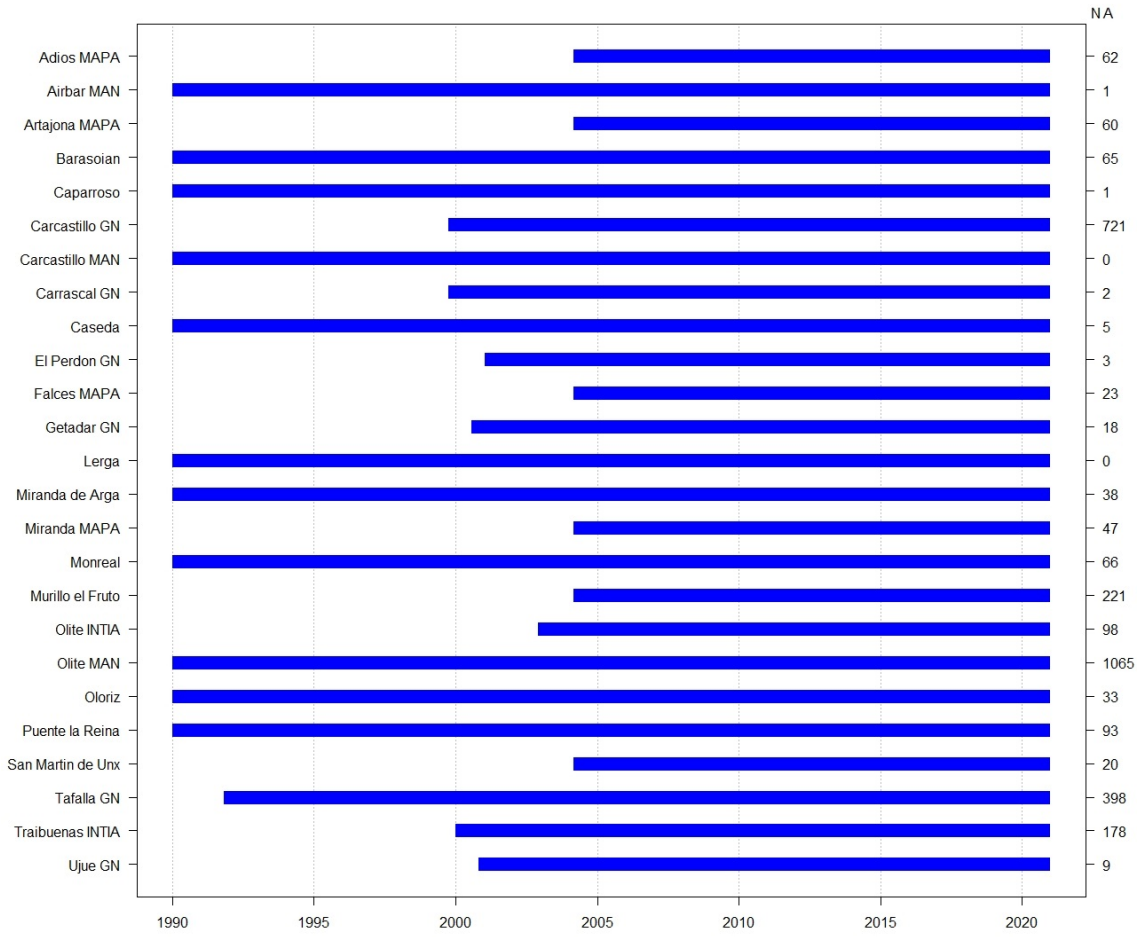

Figure 3.5: Meteorological data stations (left side) in the Cidacos River watershed, with their data length (start to end dates) between 1990 to 2020, and missing data count for each station (right side)

3.5 Data acquisition in the Catchment C6

The data used in the analysis of Catchment C6 were sourced from various Swedish government agencies' websites and portals, as shown in Table 3.7. The geospatial data, such as topography, land use (Figure 3.4b), and soil texture (Figure 3.4c) maps, were obtained from the Swedish National Land Survey portal. These data were initially preprocessed in QGIS to reclassify into the appropriate SWAT format prior to utilization in the model. The meteorological data (1990-2020), which includes precipitation, temperature (maximum and minimum), relative humidity, wind velocity, and solar radiation, was obtained at a daily time-step from the Swedish Meteorological and Hydrological Institute (SMHI) website. The data were obtained from a weather station located in Enkoping, which is about 2 km away from the catchment in the southwest. The agricultural management information (Table 3.3) from leaching region 6 obtained through

annual interviews with the farmers was used for the study. The observations (2005-2020) for streamflow, sediments, and phosphorous load were obtained from the water quality database of the Swedish environmental monitoring program. This program has been at the forefront of collecting water quality data in the catchment and other agricultural monitoring areas since the 1990s.

Table 3.7: The resolution and sources of the data used in this study.

Data type	Temporal resolution	Spatial resolution	Period	Source*
Topography map	-	5m × 5m, SWEREF99 TM**	-	SNLS
Land use map	-	5m × 5m	2021	SNLS
Soil map	-	1:50000	-	SNLS
Meteorological	Daily	Enköping station	1990-2020	SMHI
Streamflow	Daily	C6 outlet	2000-2020	SEPA
Sediment	Biweekly	C6 outlet	2004-2020	SEPA
Phosphorous	Biweekly	C6 outlet	2004-2020	SEPA
Agricultural management	Annual	Leaching region 6	2016-2020	SEPA

* SNLS is the Swedish National Land Survey; SMHI is the Swedish Meteorological and Hydrological Institute; and SEPA is the Swedish Environmental Protection Agency

** SWEREF99 TM refers to the Swedish Reference Frame 1999, the coordinate reference system used in Sweden for mapping and surveying purposes.

The streamflow at the catchment's outlet is continuously measured using a standard V-notch weir. A weight gauge, displacement body, and data logger are used to measure the water level. Heating equipment is used to prevent the measuring section from freezing during winter. The data loggers automatically retrieve data, which can be collected daily through a cellular phone network or manually by visiting the station regularly. The data is checked for any errors, such as interrupted recording and abnormal changes in water levels, which must be corrected before entering the information into the database. Weather data, expert knowledge, and data from nearby stations are used for the correction.

Water quality at the catchment outlet has been monitored since 1993. The water quality data used in this study were collected using flow-proportional (automatic) sampling techniques. In this method, water samples are collected and stored in 10-liter glass bottles, from which a composite sample is taken after shaking biweekly, and the bottle is emptied. The sampling intensity is flow-dependent, with more sub-samples collected during high

flows. Time-proportional sampling is used during low flows, with two sub-samples per day. The comprehensive sampling protocol is described in Kyllmar *et al.* (2014).

The water samples were analyzed according to the Swedish Standard methods in a water laboratory accredited by the Swedish Board for Accreditation and Conformity Assessment (SWEDAC) (Kyllmar *et al.*, 2014). Several water quality parameters were tested in the lab, but only those related to sediment and phosphorous were of interest to this study. The total phosphorous (Total P) was measured directly from unfiltered water samples, while the soluble phosphorous (Soluble P) was measured after filtration at 0.2µm to avoid the influence of particle-bound phosphorus. The nutrient loads were computed as the product of the daily streamflow and corresponding concentrations, then summarized into monthly averages for the model evaluation.

Chapter 4:

4 Evaluation of the Impact of Changing from Rainfed to Irrigated Agriculture in the Cidacos River Watershed

This Chapter is based on: **Oduor, B. O**., Campo-Bescós, M. Á., Echarri, A. A., and Casalí, J. (2023). Evaluation of the impact of changing from rainfed to irrigated agriculture in a Mediterranean watershed in Spain. *Agriculture*, *13*(1), 106. https://doi.org/10.3390/agriculture13010106

(Publisher: **MDPI**; Journal Ranking (JCR): **Q1** in Agronomy, Impact Factor (IF): **3.6**)

4.1 Introduction

Agricultural intensification and increased demand for high-value food production because of market liberalization and population growth have put a lot of pressure on the available water resources and the environment. Agriculture is the largest global freshwater consumer, accounting for more than 70% of the global freshwater resources withdrawals (FAO, 2017b; World Bank, 2020) and nearly 90% consumptive water use (Siebert *et al.*, 2010). Irrigation accounts for more than 70% of the agricultural water demand (Zeng and Cai, 2014). In the 50 years from 1965 to 2015, the global area under irrigation farming more than doubled (Mateo-Sagasta *et al.*, 2018). The need for more agricultural production, combined with the effects of climate change, pollution, population growth, and water conflicts, is expected to drive up the demand for irrigation even further (World Bank, 2020). On average, irrigated agricultural productivity per unit of land is more than double that of rainfed cultivation, resulting in increased production intensity and crop diversification (World Bank, 2020). In Spain, irrigation, which covers only 16% of the agricultural land, contributes more than 50% of total agricultural output, six times more than rainfed areas (MAPA, 2021). Over the ten years between 2003 and 2013, the irrigated area in Europe increased by 13.4%. In Spain, the increase was approximately 16% between 2007 and 2017 (MAPA, 2021). Most of the irrigable areas in Europe are mainly found within the Mediterranean region, with Italy and Spain having the largest share of irrigated agricultural lands (EPRS, 2019).

Spain's agricultural activities have relied on rainfed and irrigated cultivation, focusing more on irrigation in recent years. According to the Heinrich Böll Foundation (2019), rainfed agricultural lands in Spain's dry Mediterranean areas have decreased by 23% over the last 30 years, mainly due to low productivity and inadequate support from the Common Agricultural Policy (CAP). However, the Spanish Ministry of Agriculture reported an increase in irrigated acreage of more than 400,000 ha (which accounted for 16.2% of the irrigated land) over the past decade as of 2018 (MAPA, 2021). Navarre, located in Northern Spain and mainly in the Mediterranean region, has experienced a relatively rapid expansion of irrigated lands. The irrigated area in Navarre increased by around 25% between 2000 and 2020, with more pressurized irrigation systems installed in recent years (DDRMAAL, 2021). Irrigation expansion in the Navarre region was accelerated by establishing the “Canal de Navarra” project to convert 59,160 ha into irrigation. Approximately 40% (22,363 ha) of the proposed land has been converted into

irrigation within the project's first phase, with the remainder being transformed in the second phase (Government of Navarre, 2022). The lower reaches of our study area, the Cidacos River watershed, is part of the area converted from rainfed cultivation to irrigation under the project's first phase, with approximately 7,700 ha of its total cultivated area converted to irrigation.

Previous studies have shown that the conversion from rainfed to irrigated agriculture affects water quality by increasing its salinity (Duncan *et al.*, 2008; Pulido-Bosch *et al.*, 2018) and nitrate pollution (Merchán *et al.*, 2020; Muñoz-Carpena *et al.*, 2002; Stamatis *et al.*, 2011). Nitrate pollution leads to eutrophication, which endangers water quality for human consumption and the environment (Sutton *et al.*, 2011; WHO, 2017). Although factors such as cultivation, livestock farming, aquaculture, and so on may contribute to an increase in nitrate pollution in agricultural areas (Casalí *et al.*, 2008; Mateo-Sagasta *et al.*, 2018; Menció *et al.*, 2016), the introduction of irrigation through agricultural intensification would result in higher nitrate loads and yields in such areas. In Spain, for example, flood-irrigated areas have reported nitrate yield values exceeding 100 N kg ha^{-1} yr^{-1} (Barros *et al.*, 2012; García-Garizábal *et al.*, 2012); pressurized irrigation systems have reported values ranging from 20 to 70 N kg ha^{-1} yr^{-1} (Andrés and Cuchí, 2014a; Cavero *et al.*, 2003; Merchán *et al.*, 2015, 2018, 2020); and rainfed agricultural areas tend to report lower nitrate levels with values ranging from 16 to 37 N kg ha^{-1} yr^{-1} (Casalí *et al.*, 2008; Merchán *et al.*, 2018, 2020). Other European countries, such as Sweden and Estonia, have also recorded lower nitrate yields in rainfed areas, ranging from 6 to 32 N kg ha^{-1} yr^{-1} and 10 to 40 N kg ha^{-1} yr^{-1}, respectively (Iital *et al.*, 2014; Kyllmar *et al.*, 2014). Irrigation is generally implemented in arid and semi-arid environments where the nitrate load under rain-fed agriculture is usually lower. Hence, a change from rainfed to irrigated agriculture in these areas is likely to increase the nitrate load export from a watershed; thus, estimating their quantities is essential to determine the potential impacts. The introduction of irrigation also affects the hydrology of the irrigated areas. This includes the surface and groundwater by increasing the flows and recharging the groundwater aquifer, particularly when irrigation water is obtained outside the watershed (Zeng and Cai, 2014).

There has been limited research comparing the hydrological behavior and quality of return flows in agricultural areas before and after irrigation implementation. However, such information is important because shifting from rainfed to irrigated agriculture can

change the water regime and increase the concentrations and exports of agrochemicals, which are very harmful to the environment. This study expands on the baseline study by Merchán *et al.* (2020), which found an increase in the salt and nitrate concentrations in the Cidacos River's lower reaches, where irrigation has been implemented for the past decade. However, no information was provided about the impact of irrigation on streamflow and nitrate exportation. This was primarily due to the lack of observed streamflow data before the irrigation period (streamflow measurement in the irrigated section began in June 2017), making it impossible to understand the streamflow patterns before this period and calculate the nitrate export. This analysis is essential in the current context of the increasing scarcity of water resources and growing concern about the contamination of aquifers and surface waters with nitrates and other substances, mainly from agriculture. Furthermore, even when there are relatively long data series of the behavior before and after irrigation, the comparison is not entirely accurate because the response of the rainfed period is not compared to that of the same period and climatic conditions in irrigation. The latter can only be possible by simulating the rainfed scenario and comparing it with the same period after irrigation.

Therefore, this study aimed to use the Soil Water Assessment Tool (SWAT) model to simulate and understand the behavior of the Cidacos River in the irrigated area from mid-2017 to 2020 before irrigation implementation and then compare those simulated results (rainfed condition) with the measured values (post-irrigation). The findings from this study contribute critical information to the implementation of the European Communities' Nitrate Directive (ND, Directive 91/676/EEC) and the Water Framework Directive (WFD, Directive 2000/60/EC), both of which are concerned with protecting water bodies against nitrate pollution from agricultural areas (European Communities, 1991, 2000).

4.2 Materials and methods

4.2.1 Study area description

The study was carried out in the Cidacos River watershed in Navarre, located in northern Spain. Refer to Chapter 3, section 3.1. for the detailed description of the study area.

4.2.2 Data acquisition

Refer to Chapter 3, section 3.3. for the Cidacos River watershed's data collection and processing information.

4.2.3 Model description

Refer to Chapter 2 for a detailed overview of the SWAT model, including hydrology and nitrate load simulation, and model evaluation criteria.

4.2.4 The model setup and run

The model set-up was preceded by preparing and processing the necessary spatial datasets such as DEM, soil and land use grid maps, and discharge outlet points on the QGIS 3.18 interphase. The model was set up in the QSWAT3 1.1.1 interphase by performing watershed delineation, HRU creation, input editing, and running the SWAT model. The watershed was delineated using the DEM and the Cidacos River shapefile until the outlet at Traibuenas. Discretization was done using a minimum area threshold of 10 km^2 required to create streams, resulting in a watershed area of 477.02 km^2 with 23 sub-watersheds. A slope elevation band of 0-5%, 5-10%, and 10% and above was provided to the model. The watershed's overall elevation ranged from 315 m to 1150 m, with an average elevation of 560 m. By overlaying the LULC and soil grid maps and using a 5% threshold for land uses, soil type, and slope values, 1404 HRUs were generated. This threshold was chosen to eliminate minor land uses, soils, and slopes in each sub-watershed, facilitating model processing by improving its performance, speed, and efficiency. Using the SWAT editor, the weather data and agricultural management information were added to the model. Figure 4.1 shows the flow diagram for the SWAT model simulation of changing from rainfed to irrigated agriculture in this study.

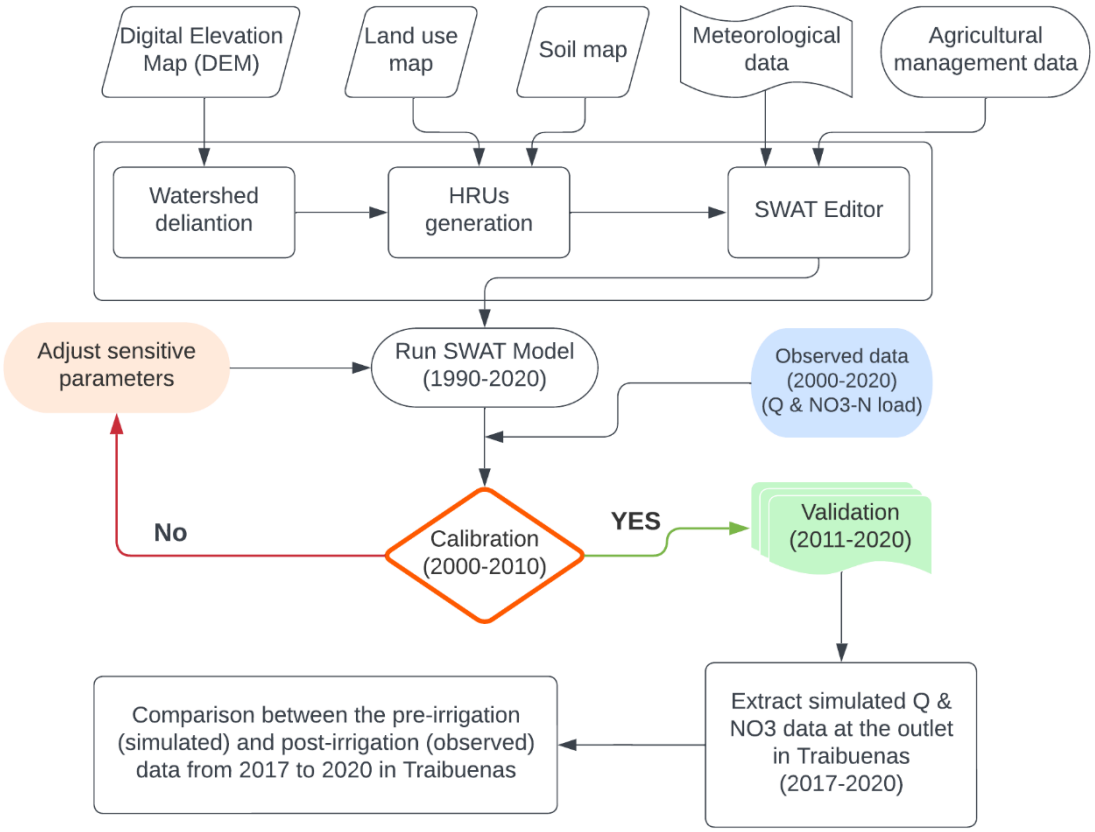

Figure 4.1: Flow diagram for the SWAT model simulation of changing from rainfed to irrigated agriculture in the lower reaches of the Cidacos River watershed

4.2.5 Sensitivity analysis, calibration, and validation

The SWAT Calibration and Uncertainty Procedures (SWATCUP) version 5.1.6, a standalone software, was used to perform sensitivity analysis, calibration, and validation of the model. The multi-site Sequential Uncertainty Fitting, version 2 (SUFI-2), a semi-automated inverse modeling routine procedure of SWATCUP, was used in this study. The model was run 500 times for each iteration, and the parameter sensitivity was determined by performing a global sensitivity analysis in which all parameters changed simultaneously. Multiple regression computations were used to identify the most sensitive parameters. The Latin hypercube-generated parameters are regressed against the objective function values in this system (Abbaspour, 2015). The t-test was used to determine the relative significance of each parameter.

The p-values and t-stat indices were used to assess the sensitivity of the parameters. The parameter was more sensitive when the p-value was lower, and vice versa. The best combination for obtaining the most sensitive parameter is a very small p-value and a large

t-value (absolute). Parameters that had p-values less than 0.05 were deemed highly sensitive. The parameter sensitivity was ranked using the t-stat index and the p-value to identify the most sensitive parameters that had the greatest impact on the model outputs (Arnold *et al.,* 2012). Larger parameter uncertainties were initially assumed to ensure that most observed data fell within the 95 Percent Prediction Uncertainty (95PPU) band (Abbaspour *et al*., 2018). 95PPU accounts for all the uncertainties within the model combined. The parameter ranges were adjusted after every iteration run during the calibration phase until most of the observed data were bracketed in the 95PPU band. The model was deemed satisfactory when more than 50% of the observed flow data were bracketed within the 95PPU.

The model was run from 1990 to 2020, with the first ten years (1990-1999) serving as the warm-up period to allow the model to reach an optimal state before reading the outputs. The model was then evaluated over the remaining period (2000-2020), which was divided into calibration (2000-2010) and validation (2011-2020) phases. The streamflow parameters were first satisfactorily calibrated and fixed before calibrating the nitrate parameters. The calibration parameters were chosen from the abundant existing literature on streamflow and nitrate calibration using the SWAT model in the Mediterranean region (Abbaspour, 2015; Abbaspour *et al*., 2015, 2018; Kamali *et al*., 2017; Kouchi *et al*., 2017; Rouholahnejad *et al*., 2014). To change the parameter values in SWAT, three methods (parameter qualifiers) are used: "R" which refers to a relative change of the specified parameter that increases or decreases the existing SWAT parameter value by multiplying it by (1 + fitted value) to obtain the new parameter value; "V" which refers to value change or replacement which means that the initial SWAT parameter value is to be directly replaced by the fitted value; and "A" which refers to addition and means that the fitted value is added to the initial SWAT parameter value. After the sensitivity analysis, the final streamflow and nitrate load calibration parameters were chosen.

The model results were presented graphically on the hydrograph plots for the simulated and observed values during the calibration and validation periods. The model's performance was evaluated using the statistical performance indicator techniques discussed in Chapter 2, section 2.6

4.2.6 Irrigation impact assessment

The impact of the change from rainfed to irrigated agriculture for the watershed was assessed at the outlet in Traibuenas using an irrigation impact index (Equation 4.1) that was established by calculating the ratio of the change (in streamflow, nitrate load, and nitrate concentration) in the post-irrigation (observed/irrigated) and pre-irrigation (simulated/rainfed) for the downstream and upstream sections located at Traibuenas and Olite, respectively to the area converted to irrigation as follows:

$$III_i = \frac{\Delta Post_{(ds-us)i} - \Delta Pre_{(ds-us)i}}{\Delta IA} \quad (4.1)$$

Where III_i represents the irrigation impact indices for streamflow ($m^3\ ha^{-1}$), nitrate load ($kg\ ha^{-1}$), and nitrate concentration ($mg\ L^{-1}\ ha^{-1}$) for the period considered; $\Delta Post_{(ds-us)i}$ represents the change in the post-irrigation values between downstream (Traibuenas) and upstream (Olite) sections for each of the variables; $\Delta Pre_{(ds-us)i}$ represents the change in the pre-irrigation values between downstream (Traibuenas) and upstream (Olite) sections for each variable; ΔIA is the change in the irrigated area in hectares.

These indices helped calculate the annual rate of change per unit area, which could be used to estimate similar changes in the watershed as well as compare different watersheds. The variation was computed as the percentage of the average annual change for each variable at the watershed outlet.

4.3 Results and discussion

4.3.1 Model evaluation

4.3.1.1 Parameterization and sensitivity analysis

The most influential parameters for the model's calibration and validation were identified using a global sensitivity analysis. The curve number, soil evaporation factor, and groundwater delay time were the most sensitive streamflow calibration parameters, while the denitrification factor and nitrate percolation coefficient were the most sensitive nitrate calibration parameters. Table 4.1 shows the ranges of selected sensitive parameters during streamflow and nitrate load calibration. All other parameters used for the model simulation in this study area are listed in Table A 1 in Appendix II. The curve number is an important parameter for the watershed's hydrology because it directly influences the surface runoff and infiltration rate. Since the initial model underestimated the baseflow

and overestimated runoff, the default curve number parameter values in each HRU were reduced by 12%, resulting in slightly reduced surface runoff and increased infiltration. The evaporation factor was sensitive because agricultural areas in the Mediterranean regions have high evapotranspiration rates. The model's evaporation generation capacity increased by lowering the default parameter value, thus appropriately representing the watershed's evaporative demand (Niraula *et al.*, 2015). Similar sensitivity analysis findings have been obtained by other researchers in the Mediterranean catchments (Ficklin *et al*., 2012; Molina-Navarro *et al*., 2014, 2016; Niraula *et al*., 2015).

Table 4.1: Selected sensitive streamflow and nitrate load parameters used for the SWAT model simulation in the Cidacos River watershed.

Parameter	Description	Change Method*	Parameter adjustment values		
			Min. value	Max. value	Fitted value
CN2.mgt	Initial SCS runoff CN number for moisture condition II	R	-0.2	0.20	-0.12
ESCO.hru	Soil Evaporation compensation factor	R	-0.40	-0.28	-0.31
GW_DELAY.gw	Groundwater delays (days)	V	20	80	53.54
CDN.bsn	Denitrification exponential rate coefficient	V	0	1.62	0.04
NPERCO	Nitrate Percolation coefficient	V	0.01	1	0.17
FIXCO.bsn	Nitrogen fixation coefficient	V	0.45	1.4	1.16

*R is a relative change method that multiplies the existing value with (1+fitted value), whereas V replaces the existing value with the fitted value

The greatest influence on nitrate load was the amount of fertilizer lost to denitrification. Denitrification losses are higher in areas with high moisture content than in dry regions; thus, its parameter value was set very low due to the watershed's Mediterranean climatic conditions. The nitrate percolation parameter governs how much nitrate is removed by surface runoff relative to the amount percolated. Typically, the default value ranges from 0.01 to 1; a lower value closer to 0 means that all of the nitrate is percolated and not in the surface runoff, while a percolation coefficient of 1 indicates that the surface runoff has the same nitrate content as percolation (Arnold *et al.,* 2012). Because of the high nitrate concentration levels in the groundwater measurements, which indicate a high watershed nitrate percolation rate, this parameter was set relatively low in the model. The nitrogen fixation parameter regulates the amount of additional nitrogen provided to the plant to meet the legume demand when insufficient nitrate is in the root zone (Neitsch *et*

al., 2011). The greater the nitrogen fixation value, the more fixed the nitrogen demand, and vice versa.

4.3.1.2 Streamflow Calibration and validation

The maximum and minimum parameter values were used to account for the uncertainty for each parameter, with the fitted value providing the best simulation. The 95PPU was used to quantify model uncertainties, such as those related to parameters, input data, and structure. During the calibration and validation periods, the 95PPU results were represented by p-factor (0.56 and 0.65) and r-factor (0.70 and 0.67) values, respectively. These uncertainties may result in overestimation or underestimation by the model, often due to the model not fully capturing all the hydrologic components in the watershed because of the model's conceptual simplifications (Ficklin *et al*., 2013; Meaurio *et al*., 2015; Rostamian *et al*., 2008; Tolson and Shoemaker, 2007).

The model produced good results for streamflow prediction during calibration and validation, reproducing most of the observed discharge and its tendency over time (Figure 4.2). The NSE values (0.82 and 0.83) and R^2 (0.83 and 0.84) during calibration and validation periods indicate a strong relationship between the observed and simulated values, indicating a 'good' fit. The negative PBIAS values (-8.7% and -5.6%) showed a slight but reasonable overestimation of the average flows by the model during the simulation periods. The RSR value of 0.42 was satisfactory because it was below the recommended threshold of less than 0.7, indicating a good model performance. The results of the four statistical performance indicators deemed the model to be 'very good' and capable of simulating monthly streamflow in the study area as per the recommendations of Moriasi *et al*. (2007). The validation period resulted in better model performance compared to the calibration period. This could be due to improved input data, such as precipitation and land use during the validation period. The validation period's input data was more accurate, such as precipitation with few to no missing gaps and using the most recent land use map from 2019. However, there were a few meteorological data inconsistencies before 2004, particularly for the automatic stations, as most were only operational after March 2004.

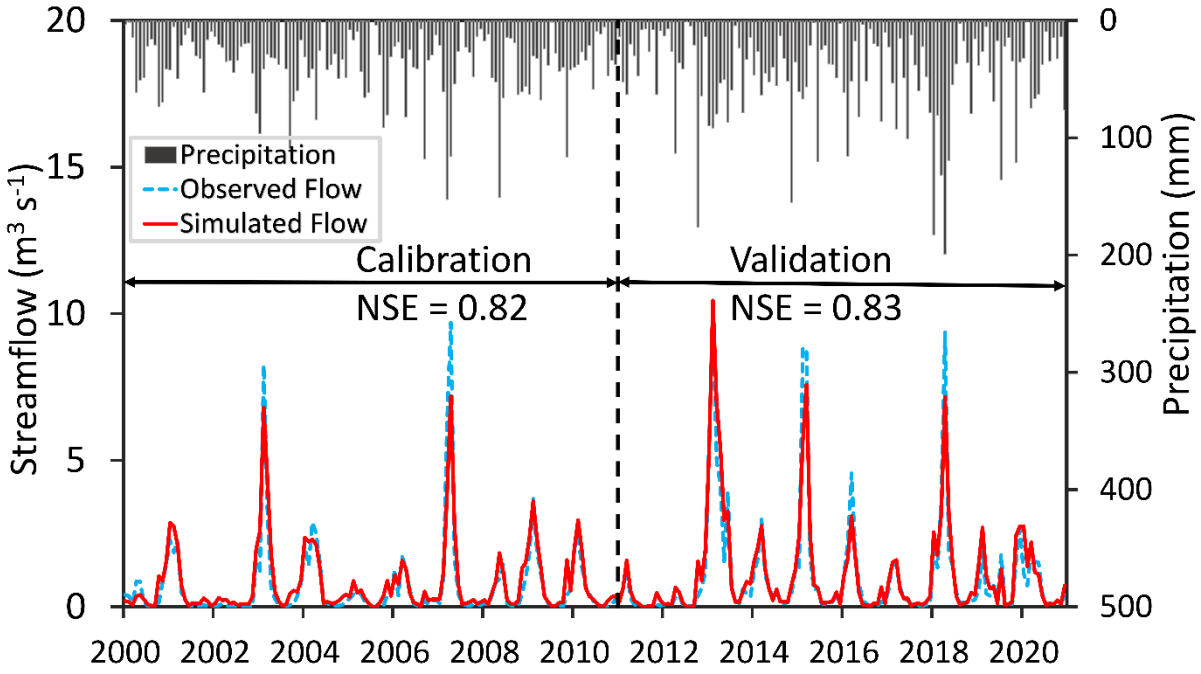

Figure 4.2: Observed (dotted blue line) and simulated (solid red line) monthly discharge hydrographs and precipitation (grey bars) during the calibration (2000-2010) and validation (2011-2020) periods at the Olite gauging station in the Cidacos River

4.3.1.3 Nitrate load calibration and validation

The nitrate load parameters were calibrated after successfully calibrating and fixing the streamflow parameters. Comparisons between the observed and simulated monthly nitrate loads hydrographs (Figure 4.3) indicated a good model performance. The uncertainties in nitrate load simulation were accounted for using the 95PPU represented by the p-factor (0.72 and 0.63) and r-factor (0.92 and 0.98) during calibration and validation periods, respectively. Some of the model weaknesses could have resulted from errors in the input data. These include estimations of missing precipitation data used to generate the discharge (Boithias *et al.*, 2014); insufficient observed nitrate load data available since the concentration data were obtained from a highly scattered sampling frequency (in most cases collected only once per month at random dates and with several months having missing data) (Epelde *et al.*, 2015); and information related to the agricultural management operations and practices such as fertilizer application or planting and harvesting dates (Zettam *et al.*, 2020). The model simulation results were in good agreement with the observed data, indicating good accountability of the model's various agricultural inputs. The model's statistical performance was adequate, with acceptable NSE values (0.71 and 0.68) and R^2 values (0.72 and 0.79) during the calibration and

validation periods, respectively. The PBIAS results show that the model underestimates the nitrate loads by -9.2% and -7% during the calibration and validation periods, respectively. These results are within the acceptable thresholds recommended by Moriasi *et al.* (2007), indicating a good model performance.

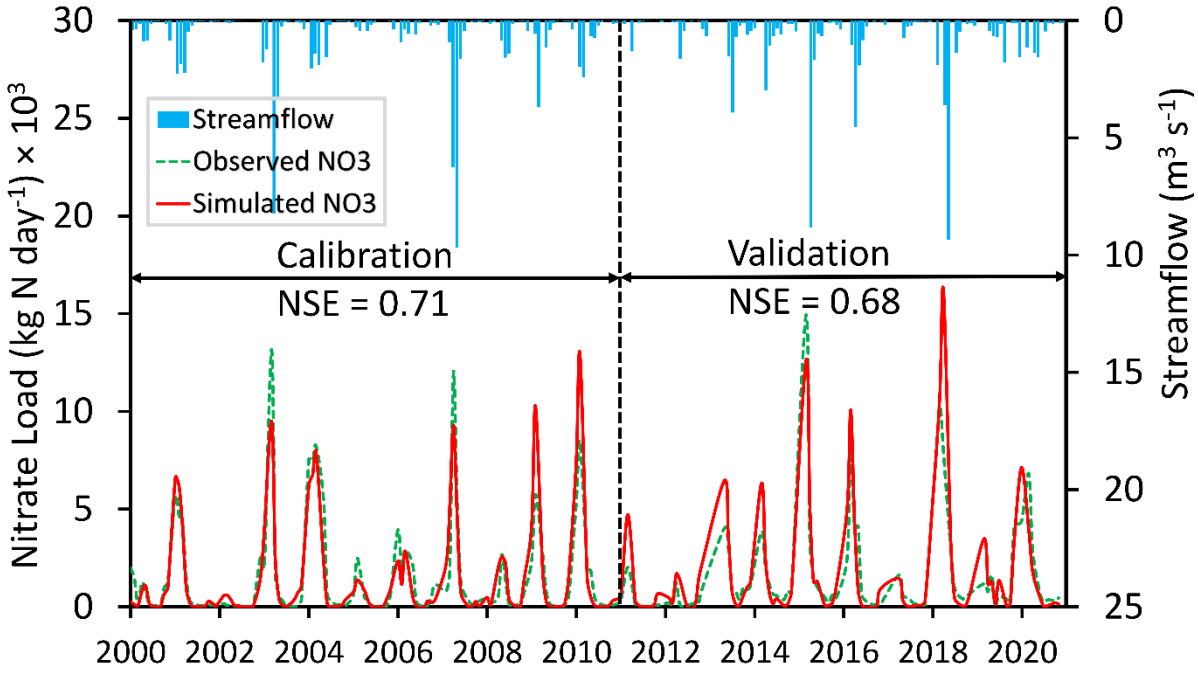

Figure 4.3: Plot of observed (dotted green line) and simulated (solid red line) monthly nitrate load and measured streamflow (blue bars) during calibration and validation periods at the Olite gauging station in the Cidacos River

The inter-annual and seasonal variability of nitrate load was very high throughout the simulation period. Loads were higher in wetter years than in dry years, and vice versa. Nitrate loads in the watershed increased from mid-autumn and peaked during winter when precipitation was abundant, and thus streamflow, but gradually decreased from spring to summer, when precipitation was scarce. This could be attributed to increased streamflow and, to some extent, the nitrogen fertilizer application on agricultural fields because the planting season begins in October/November, increasing soil nitrogen levels, nitrate concentration, and, subsequently, nitrate loads in the watershed. Because nitrate load is a function of discharge used to transport it downstream, higher precipitation in the watershed during the winter and spring months will inevitably increase nitrate load exportation in the river. However, less nitrate load is exported during the summer, when precipitation is scarce, resulting in limited streamflow; in addition, there are almost no agricultural activities in the watershed's upper reaches, which rely primarily on rain-fed

farming. These results are consistent with those obtained by Lam *et al.* (2009) when modeling agricultural catchments in Europe, where they reported that these patterns could be attributed to higher nitrogen concentrations in the winter due to nitrogen mobilization in the watershed and a lack of plant uptake, resulting in the accumulation of leachable nitrates and thus an increase in nitrogen concentration in streamflow during winter. Similar findings have also been reported by Donmez *et al.* (2020), who inferred that an increase in fertilization would lead to an increase in the amount of nitrate in the soil, which would be directly related to plant growth and agricultural production and management. According to Abbaspour *et al.* (2015), nitrate dynamics in agricultural watersheds are governed mainly by the fate and transportation of fertilizer in the soil, the rate of organic matter decomposition, and the prevailing climate.

4.3.2 Irrigation dynamics in the watershed

The conversion of agricultural land from rainfed to irrigation in the study area began in late 2006, with nearly 70% of the changes occurring between 2009 and 2012 (Figure 3.3). By 2020, at least 16% of the watershed had been converted into irrigated land. This study evaluated the conversion from rainfed to irrigation using the available data (mid-2017 to 2020). The seasonal irrigation patterns show that in winter, irrigation is minimal (only 1%), while in the summer, irrigation water applications are high (57%) (Figure 4.4). Irrigation was mostly done during periods of low precipitation, especially from July to September (Figure 4.4a). Similar seasonal irrigation patterns have been observed in other semi-arid irrigated watersheds within the Ebro basin (Andrés and Cuchí, 2014b; García-Garizábal *et al*., 2011, 2017; Merchán *et al*., 2015) and around the world (Scott *et al.*, 2011).

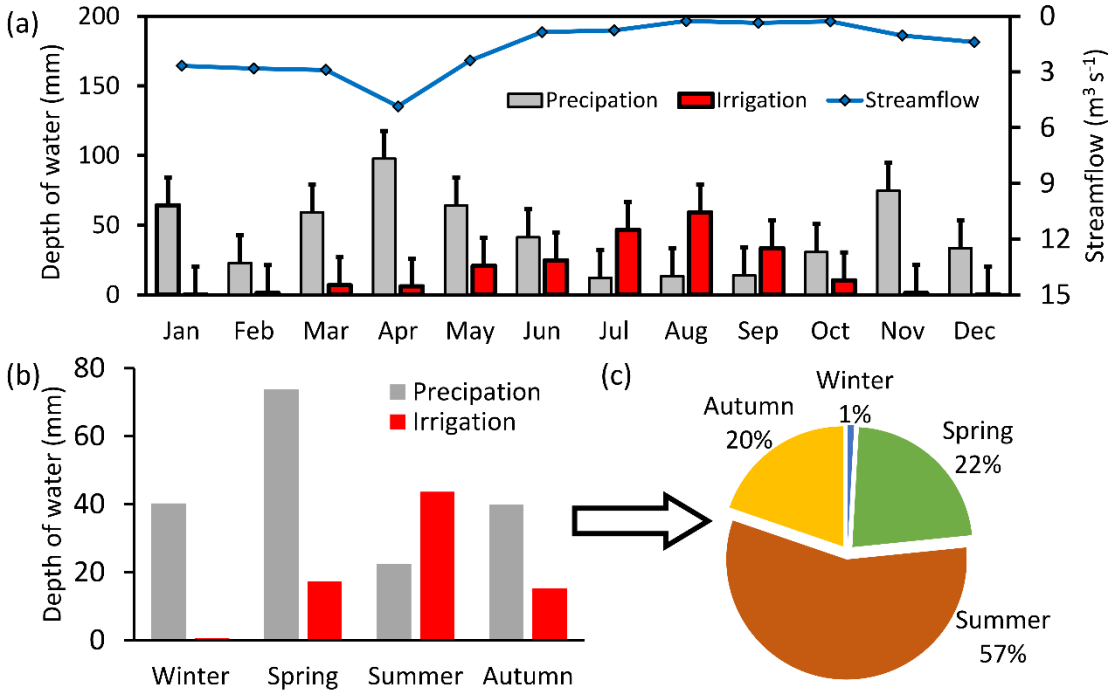

Figure 4.4: (a) Monthly average precipitation, irrigation, and streamflow distribution at the watershed outlet in Traibuenas from mid-2017 to 2020, (b) seasonal precipitation and irrigation distribution pattern, and (c) the percentage of irrigation water applied each season.

According to the INTIA reports (INTIA, 2019, 2020, 2021), the average water inflow into the irrigated section of the watershed was 51% precipitation, 31% river inflow from the Olite gauging station, and 17% irrigation water from the Navarre canal. In 2020, evapotranspiration accounted for 33.5% of output, groundwater storage accounted for 3.5%, and the outflow at the Traibuenas gauging station accounted for 42%. The irrigation performance efficiency in the study area was relatively high (84.6%), indicating a well-managed irrigation system. However, there is a spatial variation, with some irrigated plots having lower efficiencies than others, which are compensated for by the higher ones. The irrigation efficiency value was slightly higher than the figures reported by other researchers in the Ebro basin, such as 76% (Andrés and Cuchí, 2014b) and 72% (Skhiri and Dechmi, 2012) in watersheds with predominantly sprinkler irrigation.

4.3.3 Observed nitrate concentration dynamics

Nitrate concentrations at the watershed outlet in Traibuenas have been monitored since 2000. The average annual nitrate concentration distribution pattern from 2000 to 2020 is depicted in Figure 4.5. During the pre-irrigation period (2000-2008), the average nitrate

concentration at the Traibuenas gauging station was 27.72 mg L^{-1} (median value of 27.49 mg L^{-1}; interquartile range (IQR): 34.77 mg L^{-1} to 23.77 mg L^{-1}) with maximum and minimum concentrations of 57.20 mg L^{-1} and 4 mg L^{-1}, respectively. The monthly median values ranged from 45.64 mg L^{-1} in January to 11.33 mg L^{-1} in September. For the pre-irrigation period, 80 nitrate concentration samples were analyzed, with only 6.3% (5 samples) exceeding the 50 mg L^{-1} threshold recommended by Nitrate Directives and 45% (36 samples) falling below the 25 mg L^{-1} for unaffected waters. The nitrate concentration varied between the years, with the lowest value recorded in 2002 due to a severe drought, resulting in limited cultivation, and the highest in 2007 due to abundant precipitation and, thus, increased cultivation. The seasonal cycles were not consistent for all the years during the pre-irrigation period, with high nitrate concentrations in winter and spring and low concentrations in summer and autumn. The temporal fluctuation in nitrate concentration before the irrigation implementation was in tandem with the precipitation distribution pattern for each season in a specific year. These findings are consistent with those made by Orellana-Macías *et al.* (2020) in a study of nitrate vulnerable zones evolution in the north-east of Spain and Hernández-García *et al.* (2020) in a small rainfed experimental watershed in Navarre, where they both observed an increase in nitrate concentration during the years with more precipitation compared to years with less due to increased cultivation and subsequent crop fertilization. The nitrate concentration substantially declined during the transition period (2009 to 2012) because this was the period when the irrigation infrastructure was being constructed; thus, most of the agricultural land was left uncultivated except for the upstream area, which was unaffected by this development.

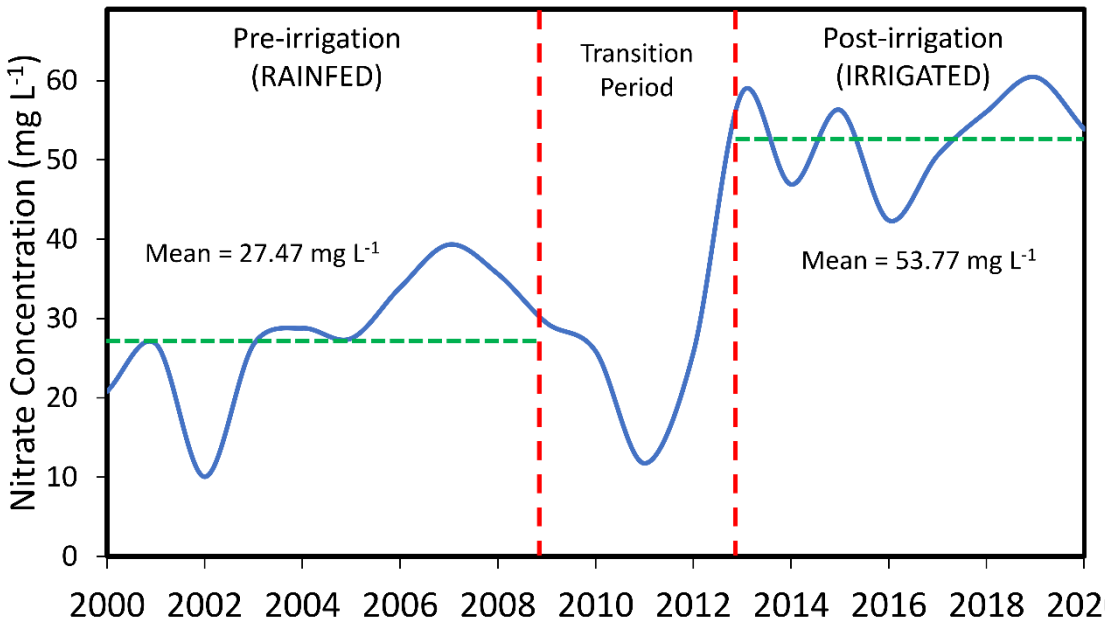

Figure 4.5: The average annual nitrate concentration distribution pattern at the watershed outlet in Traibuenas before and after irrigation implementation from 2000 to 2020

During the post-irrigation period (2013 to 2020), 71 nitrate concentration samples were analyzed. The nitrate concentration in the post-irrigation period was twice as high as in the pre-irrigation period (Figure 4.5), with a mean of 53.14 mg L^{-1} (median value of 54.99 mg L^{-1}; IQR: 57.95 mg L^{-1} to 47.83 mg L^{-1}) and maximum and minimum concentrations of 97.10 mg L^{-1} and 16.04 mg $L^{-1,}$ respectively. The monthly median concentration values ranged from 73.70 mg L^{-1} in September to 31.9 mg L^{-1} in March. Hernández-García *et al.* (2020) found similar results when comparing the nitrate concentration levels in rainfed and irrigated experimental watersheds in Navarre, with the findings indicating a threefold higher nitrate concentration in the irrigated watershed than in the rainfed one. The collected samples exceeded the recommended Nitrate Directive threshold of 50 mg L^{-1} in 56.3% (40 samples), indicating that the river was contaminated with nitrate, while only 2.8% (2 samples) fell below the 25 mg L^{-1} level (unaffected waters). The nitrate concentration was significantly higher ($p < 0.01$) during the post-irrigation period than during the pre-irrigation period from May to December. Following the irrigation implementation, the seasonal cycle of nitrate concentrations was substantially altered; the peak concentration shifted from January-February to August-September, and the lowest concentration shifted from September-October to March-April.

The nitrate concentration patterns in the watershed may be related to the cropping practices before and after irrigation. Before irrigation, the main crops grown in the

watershed were mostly rainfed winter cereals (wheat and barley), which required less nitrate fertilization. However, following the implementation of irrigation, high-value crops such as tomatoes and corn, which require more fertilization, were introduced into the watershed, increasing nitrate concentration levels, particularly during the summer and autumn. Lower nitrate concentration and export levels from rainfed cultivated areas in Navarre have also been reported by other studies (Casalí *et al.*, 2008; Hernández-García *et al.*, 2020; Lassaletta *et al.*, 2010). During the pre-irrigation period, cultivation was mostly done during the winter and spring when there was enough precipitation. However, this decreased during the summer and autumn when productivity was low due to a lack of precipitation, resulting in lower nitrate concentration. Hernández-García *et al.* (2020) obtained similar seasonal patterns during rainfed conditions in their studies of small experimental watersheds within Navarre with similar characteristics to the Cidacos River watershed. The post-irrigation phase, however, sees year-round cultivation with irrigation supporting farming during the summer and autumn, a period when productivity was previously low.

4.3.4 Variations in streamflow and nitrate (load and concentration) due to irrigation

The irrigation impact index and the average annual variation after irrigation implementation showed a positive response in streamflow, nitrate load, and nitrate concentration. The annual irrigation impact index per unit irrigated area (Equation 4.1) shows that irrigation increased the streamflow (952.33 m^3 ha^{-1}, +18.8%), nitrate load (68.17 kg ha^{-1}, +62.3%), and nitrate concentration (0.89 mg L^{-1} ha^{-1}, +79%) at the watershed outlet (Figure 4.6). These findings are comparable to those obtained by Merchán *et al.* (2013), who reported an increase of streamflow, nitrate load, and nitrate concentration by 23%, 27%, and 8%, respectively, in the Lerma catchment within the Ebro basin in Spain after irrigation implementation. However, the variation in exported nitrate load and concentration was slightly higher in this study than in Merchán *et al.* (2013) because the Lerma catchment had higher nitrogen concentration levels before irrigation implementation than the Cidacos River watershed due to different fertilization management practices. Similar annual nitrate exportation rates after irrigation implementation have been reported in Monegros within the Ebro basin at 49 kg ha^{-1} (Cavero *et al.*, 2003) and in La Violada irrigation district in north-east Spain at 66 kg ha^{-1} (Barros *et al.*, 2012). Likewise, the reported increases in nitrate concentration values after irrigation of 0.7 to 0.8 mg L^{-1} ha^{-1} in the middle Ebro River basin (Causapé *et al.*,

2004) and 0.91 mg L^{-1} ha^{-1} in the Arba River basin (CHE, 2006) are in close agreement with our findings.

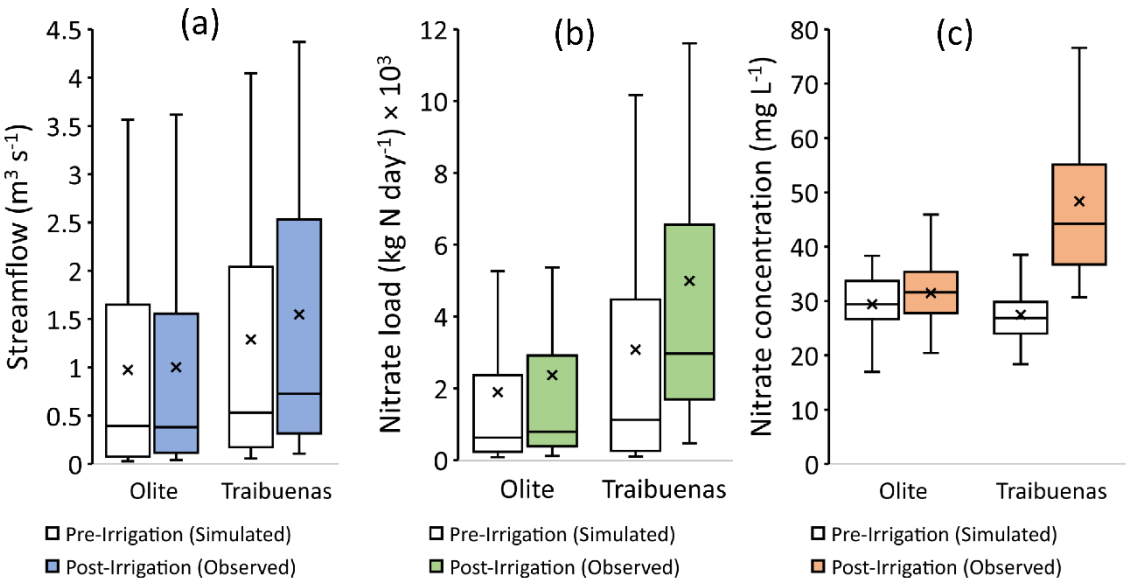

Figure 4.6: Comparison of average annual changes in (a) streamflow, (b) nitrate load, and (c) nitrate concentration before and after irrigation at Olite and Traibuenas stations from mid-2017 to 2020

The increased streamflow in the post-irrigation period was consistent with the addition of irrigation water from outside the watershed via the Navarre canal. The irrigation impact on streamflow was more pronounced in the summer and autumn compared to winter and spring, resulting in changes in the watershed's hydrological behavior (Figure 4.7). More research into the effects of these changes on flora and fauna is needed in the future to understand their impacts.

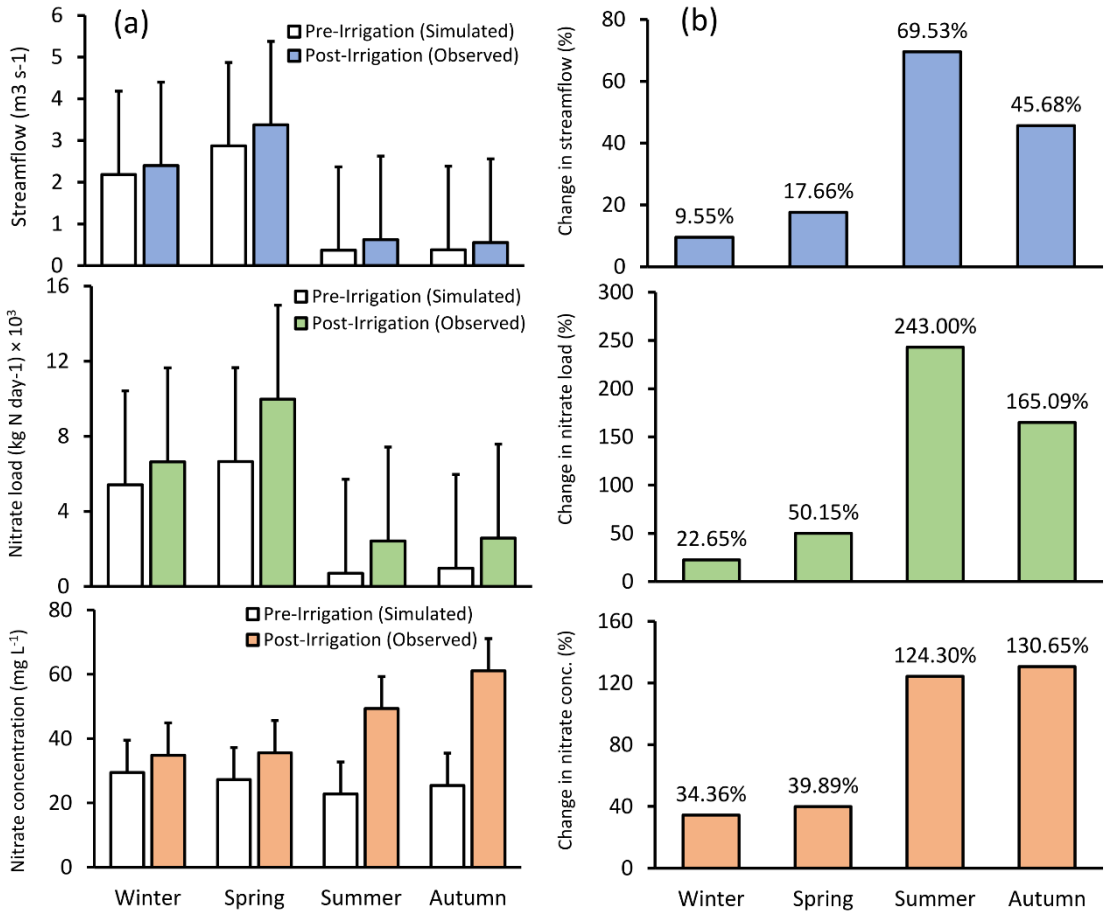

Figure 4.7: Seasonal comparison of (a) pre-irrigation and post-irrigation results and (b) the percentage changes after irrigation implementation for streamflow, nitrate load, and concentration at the Traibuenas gauging stations from mid-2017 to 2020

The changes in nitrate (load and concentration) in the post-irrigation period were attributed to increased nitrogen fertilizer application resulting from cultivating high-value crops (with high nitrogen fertilizer demand) to boost productivity due to irrigation. Furthermore, the introduction of irrigation has resulted in a shift in cropping cycles because crops can now receive water throughout the year, with rainfall primarily supporting agriculture in the winter and spring and irrigation in the summer and autumn. The concentration and exported nitrate were comparatively higher in the summer and autumn (from May to October) due to nitrate mobilization resulting from irrigation, increased fertilizer application during that period, and low streamflow despite the irrigation water contributions. The highest nitrate concentration in the post-irrigation period was observed from August to October, which could be influenced by the top-dressing fertilization (Causapé *et al*., 2004; Merchán *et al*., 2013, 2015).

The increase in exported nitrate load during the summer was very high (243%) due to increases in both streamflow (70%) and nitrate concentration (124%) in the same period (Figure 4.7). The exported nitrate load is directly influenced by streamflow and nitrate concentration, whereby a slight increase in streamflow produces a greater change in the exported nitrate load than a slight increase in the nitrate concentration. This effect of increased flow on the exported nitrate loads has been reported in other studies in irrigated areas (Barros *et al.*, 2012; Merchán *et al.*, 2013). Given the importance of nitrate exportation, some studies (Arauzo *et al*., 2011; Causapé *et al*., 2004; Merchán *et al*., 2013, 2015) have proposed its adoption in agricultural management decisions for nitrogen impact assessment rather than relying solely on the Nitrate Directive's nitrate concentration thresholds.

4.4 Conclusion

The main findings and conclusions of this chapter are provided in Chapter 7, sections 7.1 and 7.2.

Chapter 5:

5 Effects of Climate Change on Streamflow and Nitrate Pollution in the Cidacos River Watershed

This Chapter is based on: **Oduor, B. O**., Campo-Bescós, M. Á., Lana-Renault, N., and Casalí, J. (2023). Effects of climate change on streamflow and nitrate pollution in an agricultural Mediterranean watershed in Northern Spain. *Agricultural Water Management*, *285*, 108378. https://doi.org/10.1016/j.agwat.2023.108378

(Publisher: **Elsevier**; JCI: **Q1** in Agronomy, IF: **6.7**)

5.1 Introduction

Agriculture is one of the most important sectors of any regional or national economy globally. It is the primary source of livelihood and the backbone of most nations' economic systems, with more than 60% of the world population directly dependent on it (FAO, 2017a). However, agricultural intensification puts great pressure on available water resources and the environment, potentially causing damage. These damages could range from soil erosion, which is much more common in agricultural environments than in other soil uses (García-Ruiz *et al.*, 2015; Almagro *et al.*, 2016; Boardman and Poesen, 2006), to water quality degradation caused by non-point source pollution (Chahor *et al.*, 2014; Giménez *et al.*, 2012; Merchán *et al.*, 2018; Sutton *et al.*, 2011). Studies conducted within the Navarra region of northern Spain have identified considerable nitrate and phosphate concentrations in streams in cereal crop areas, where the recommended thresholds are often exceeded, albeit with seasonal and annual variability (Casalí *et al.*, 2008; Hernández-García *et al.*, 2020; Merchán *et al.*, 2019).

The Cidacos River watershed in the Navarre region has diverse land uses, with rainfed agriculture predominating. The watershed holds decades' worth of nitrate concentration, discharge, and meteorological data collected by the Government of Navarra at various stations, hence making it ideal for conducting investigations on agricultural activities' impact on the quality and quantity of water resources in the area. Some of the challenges associated with agricultural practices in the study area are nitrate pollution in surface waters, as evidenced by high nitrate concentration levels in the Cidacos River (Merchán *et al.*, 2020), and anticipated climate change effects due to projected changes in temperature and precipitation affecting the cropping system (Funes *et al.*, 2016; Trnka *et al.*, 2011).

Climate change impacts on water resources can be quantified by using various Global or Regional Climate Models (GCMs or RCMs) and future radiative forcing scenarios, known as Representative Concentration Pathways (RCPs), to establish appropriate adaptation measures and policy interventions (Krysanova *et al.*, 2017). The Mediterranean region, particularly Spain, is considered to be highly vulnerable to the effects of climate change due to its geographical location and the imbalance between the available water resources and the current demands (Vargas-Amelin and Pindado, 2014). Furthermore, most climate change model projections for Spain indicate an increase in temperature and a decrease in precipitation by the end of the 21st Century (Candela *et al.*,

2012; Chirivella Osma *et al.*, 2015; Estrela *et al.*, 2012; Majone *et al.*, 2012; Somot *et al.*, 2008). Climate change is expected to affect all aspects of the environment, compounding agricultural effects on streamflow and nitrate exportation (Arora, 2019). For instance, a change in streamflow due to projected temperature and precipitation changes would result in extreme events such as droughts or floods. These events would, in turn, influence the nitrate dynamics in the watershed by changing the exported nitrates loads and concentration accumulated in the soils and water. Therefore, it is important to investigate the potential effects of climate change on streamflow and nitrate dynamics, as they would impair the current hydrological conditions and hinder the achievement of nitrate standards as stipulated by the European Water Framework Directive (European Communities, 2000).

Nitrate pollution is a global concern that affects water quality by making it unsafe for human consumption (WHO, 2017) and increasing eutrophication (Sutton *et al.*, 2011). Nitrate pollution contributors in a watershed could include agriculture, livestock, and aquaculture (Casalí *et al.*, 2008; Mateo-Sagasta *et al.*, 2018; Menció *et al.*, 2016). Whilst some level of nitrate exportation is inevitable in agricultural areas, improved management practices could limit its effect on streams (Beaudoin *et al.*, 2005; Boithias *et al.*, 2014; Cameron *et al.*, 2013). To address the nitrate pollution challenge, the European Commission has established policy legislations such as the Nitrate Directive (ND, Directive 91/676/EEC) and the European Water Framework Directive (WFD, Directive 2000/60/EEC) to protect water bodies from agricultural nitrate pollution, with a nitrate concentration threshold of 50 mg L^{-1} for European rivers (European Communities, 1991). However, more research is needed to understand the spatial and temporal interactions of water quality variables and quantify the loads to assess their climate change impacts.

Mathematical models are fundamental tools for hydrological and environmental planning, with their greatest potential being the ability to generate scenarios in the face of voluntary or imposed changes in land use or management. The Soil Water Assessment Tool (SWAT) model is one of the best available tools for simulating the response of agricultural (or non-agricultural) watersheds to water quality. The SWAT model has been widely used by water resources experts to understand the characteristics of a watershed and predict its hydrological response to external (climate) and internal (water management, land management, etc.) drivers and their impacts. The SWAT model has been applied in the Mediterranean region and particularly Spain for streamflow analysis (Harraki *et al.*, 2021;

Jimeno-Sáez *et al.*, 2018; Meaurio *et al.*, 2015) and water quality assessment of nitrogen and nitrates (Epelde *et al.*, 2015; Zabaleta *et al.*, 2014; Zettam *et al.*, 2020). The majority of nitrate studies conducted by the SWAT model focus on how to reduce nitrate pollution through land use changes (Ferrant *et al.*, 2011; Wang *et al.*, 2008), as well as regulating fertilizer application rates and other management practices like tillage (Boithias *et al.*, 2014; Cerro *et al.*, 2014; Ferrant *et al.*, 2011; R. Liu *et al.*, 2013). Despite several studies on streamflow and hydrological response to climate change, there has been very little research on the effects of climate change on water quality (Ficklin *et al.*, 2010; Luz Rodríguez-Blanco *et al.*, 2019; Martínková *et al.*, 2011; Molina-Navarro *et al.*, 2014). Moreover, there are no long-term climate change assessments of the effects of agricultural activities on streamflow and water quality in the Navarre region.

This study aimed to evaluate the SWAT model's applicability for climate change prediction of streamflow and nitrate load in a rainfed agricultural Mediterranean watershed in northern Spain. The model was first evaluated for its capacity to simulate streamflow and nitrate export under rainfed agricultural conditions in the upper reaches of the Cidacos River watershed and then used to assess the climate change impacts by comparing future projections to the historical baseline under two emission scenarios (RCP4.5 and RCP8.5). The findings from this study could provide valuable information on climate change adaptation and mitigation measures in the future and deepen the knowledge of nitrate exportation and pollution in the study area.

5.2 Materials and methods

5.2.1 Study area description

The study was carried out in the Cidacos River watershed in Navarre, located in northern Spain. Refer to Chapter 3, section 3.1. for the detailed description of the study area.

5.2.2 Data acquisition

Refer to Chapter 3, section 3.3. for the Cidacos River watershed's data collection and processing information.

5.2.3 Model description

Refer to Chapter 2 for a detailed overview of the SWAT model, including hydrology and nitrate load simulation, and model evaluation criteria.

5.2.4 The model set-up and run

Refer to Chapter 4, section 4.2.4, where the model setup for this study has been discussed. Figure 5.1 illustrates the SWAT model climate change simulation flow diagram for the Cidacos River Watershed.

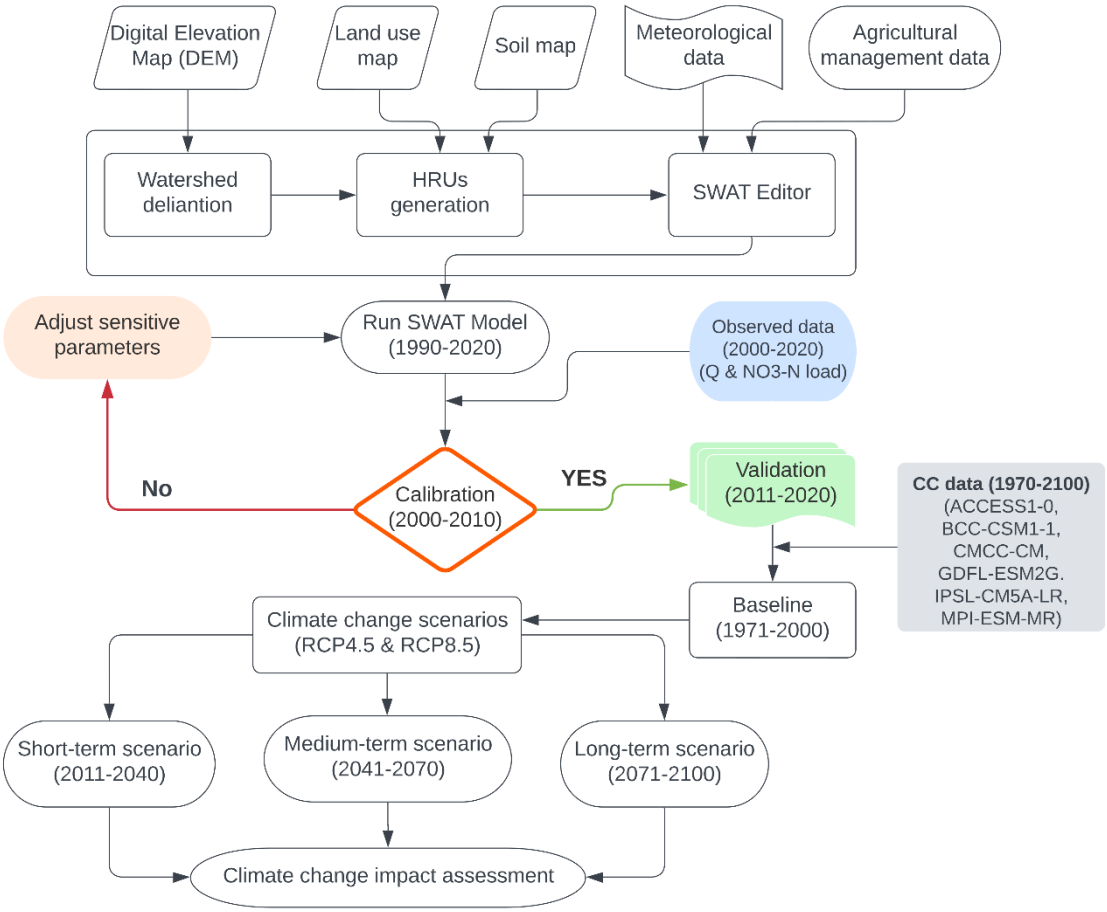

Figure 5.1: Flow diagram of the SWAT model simulation of climate change in the Cidacos River watershed

5.2.5 Sensitivity analysis, calibration, and validation

Refer to Chapter 4, section 4.2.5, where the sensitivity analysis, calibration, and validation of this study have been discussed.

5.2.6 Climate change scenario development

The climate change impact in the study area was analyzed using an ensemble of six Global Climate Models (ACCESS1-0, BCC-CSM1-1, CMCC-CM, GDFL-ESM2G, IPSL-CM5A-LR, and MPI-ESM-MR) from bias-corrected Coupled Model Intercomparison Project (CMIP) climate forcing data statistically downscaled on a 5 km grid for the

Navarre region for historical and future data of RCP4.5 and RCP8.5 emission scenarios. This data was developed by the Spanish National Agency for Meteorology (AEMET) and was downloaded from the Platform on Adaptation to Climate Change in Spain (AdapteCCa) portal (AdapteCCa, 2021). These two projected radiative forcing scenarios represent the potential moderate (RCP4.5) and more aggressive (RCP8.5) climate change impact scenarios, with RCP4.5 assuming that greenhouse gas emissions will be gradually reduced in the coming years to achieve stability by 2100 and RCP8.5 assuming that greenhouse gas (GHG) emissions will continue to rise at current levels throughout the 21st century (IPCC 2014). Only the precipitation and temperature (maximum and minimum) datasets were used for the climate change simulation.

The calibrated SWAT model was used to simulate projected streamflow and nitrate load trends using climate change data (precipitation and temperature) as inputs while assuming all other variables to be constant. Crop heat units were used in the simulation to assign agricultural management operations such as planting, harvesting, and fertilization periods automatically. The simulation was run for each GCM from 1971-2000 for historical reference and 2011-2100 for the RCP4.5 and RCP8.5 future projection scenarios. In total, 18 simulations with six historical and 12 future projections were run (6 for each emission scenario). The future projection scenarios of streamflow and nitrate export were analyzed for three distinct periods categorized into short-term (2011-2040), medium-term (2041-2070), and long-term (2071-2100) by comparing each model to its historical period (1971-2000). Finally, the models' results were combined and averaged to obtain an ensemble for the climate change analysis.

5.3 Results and discussions

5.3.1 Model evaluation

Refer to Chapter 4, section 4.3, where the model evaluation for this study has been exhaustively discussed, including parameterization and sensitivity analysis results, as well as calibration and validation results of streamflow and nitrate load.

5.3.2 Climate change impact analysis

5.3.2.1 Projected precipitation and temperature

Analysis of the future climate projection compared to the historical reference depicts a general decrease in precipitation and an increase in temperature. Figure 5.2 illustrates the

percent decrease in mean annual precipitation and increase in average temperature for all six climate models under RCP4.5 and RCP8.5 emission scenarios over the three projected periods relative to the historical period. The average decline in precipitation in the short-, medium-, and long-term projections were -3.5%, -6.9%, and -7.6% for RCP4.5, and -3.1%, -7.9%, and -14.8% for RCP8.5, respectively. The average temperature projections, on the other hand, increased progressively over the three periods, by 1.2 ºC, 1.9 ºC, and 2.2 ºC for RCP4.5, and 1.4 ºC, 2.0 ºC, and 4.3 ºC for RCP8.5. The projected precipitation data varied more among the selected models than the projected temperature, which was closely comparable across the models. These projections are similar to those reported by the European Environment Agency (EEA) (2017) for the Mediterranean region, indicating a significant increase in warming of 2 ºC to 5ºC from the 2050s to the end of the 21st century, while the mean annual precipitation could decrease by -5% to -15%, and in the worst case scenario, up to -25%, with an acceleration expected at the end of the century. Furthermore, winter and autumn project a higher decrease in precipitation than summer and spring, while summer temperature increases are greater than winter. Projected precipitation decline and temperature increase over the three time periods of 2040, 2070, and 2100 have also been reported for other studies within the Mediterranean region (Abd-Elmabod *et al*., 2020; Al-Mukhtar and Qasim, 2019; Fonseca and Santos, 2019). These projected climate changes are expected to alter the watershed's hydrological cycle by increasing the air temperature and, thus, evapotranspiration. A warmer atmosphere is expected to hold more water vapor, causing precipitation concentrations to rise, resulting in more frequent and intense extreme events (Abd-Elmabod *et al*., 2020; Navarra and Tubiana, 2013). However, greater losses in open surface waters and soils are also expected with the projected high evapotranspiration rates.

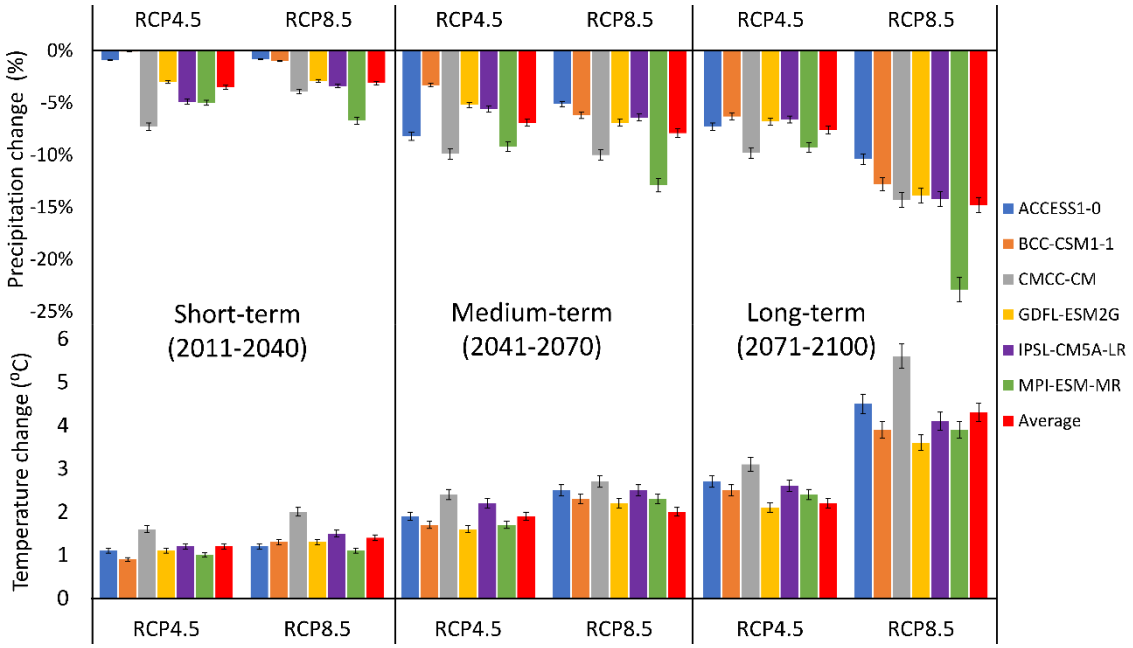

Figure 5.2: Variation in average precipitation (%) and temperature changes (ºC) for the six climate change models under RCP4.5 and RCP8.5 for short-, medium-, and long-term projections relative to historical reference

5.3.2.2 Effects of climate change on streamflow

The simulated climate change projections showed a declining effect on streamflow for both emission scenarios over all the projected periods analyzed with high interannual fluctuations (Figure 5.3). The average annual streamflow decreased by -11.5%, -27.4%, and -28.5% for RCP4.5 and -8.5%, -27.5%, and -52.4% for RCP8.5 during the short-, medium-, and long-term future climate projections, respectively, compared to the historical reference period. This decline was mainly attributed to the projected decrease in precipitation and increasing temperatures for all the climate models used in the study (Figure 5.2), leading to a rise in the watershed's evapotranspiration. Higher evapotranspiration rates and lower precipitation would result in declining discharge unless there is a significant shift in the seasonal pattern with more precipitation occurring during colder seasons (Anand and Oinam, 2019; Molina-Navarro *et al*., 2014, 2016).

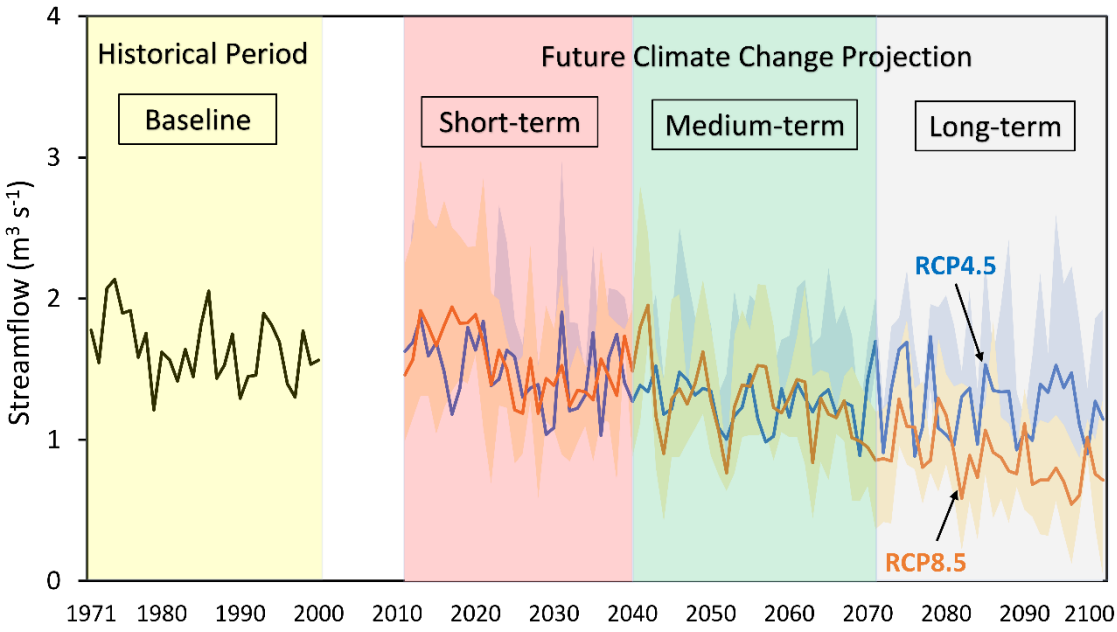

Figure 5.3: Average annual streamflow evolution over historical (1971-2000), short-term (2011-2040), medium-term (2041-2070), and long-term (2071-2100) periods under RCP4.5 and RCP8.5 climate change projections

The long-term climate projection had the highest streamflow reductions for RCP4.5 (-28.5%) and RCP8.5 (-52.4%). The considerable streamflow reduction in RCP8.5 long-term projection compared to RCP4.5 was due to the continuous increase in temperature and decreasing precipitation caused by the lack of climate change mitigation measures to reduce the GHG emissions for this scenario. However, for RCP4.5, some mitigation measures to reduce GHG emissions are expected to be implemented gradually from the mid-term projection onwards. The RCP4.5 long-term projection showed greater extreme streamflow occurrences than the RCP8.5, which could be attributed to variations in precipitation and temperature intensity, timing, and frequency. This could potentially result in more frequent and severe floods and streamflow under RCP4.5, as well as drought and drier conditions under the RCP8.5 scenario, lowering the streamflow.

The projected long-term streamflow reductions were slightly higher in summer and autumn than in winter and spring for both emission scenarios (Figure 5.4a). The long-term projection showed the greatest decrease, with a -66.4% (RCP8.5) and -42.0% (RCP4.5) reduction in streamflow during autumn. The declining patterns of the seasonal projections correspond to changes in precipitation and temperature. These findings are consistent with other studies in the Mediterranean climate that have found that annual streamflow in a watershed or on a regional scale is extremely sensitive to changes in

precipitation, such that a slight decrease in precipitation in regions with high temperatures and consequently higher evapotranspiration rates would likely result in a significant reduction in runoff (Ficklin *et al*., 2013; Molina-Navarro *et al*., 2014, 2016). The results, especially the RCP8.5 long-term projection, have very strong implications for the water available in the river by the end of the century if the current global warming trends continue. A decline of more than 50% of the currently available streamflow would seriously affect the available water resources for the aquatic ecosystem, domestic consumption, and agricultural use.

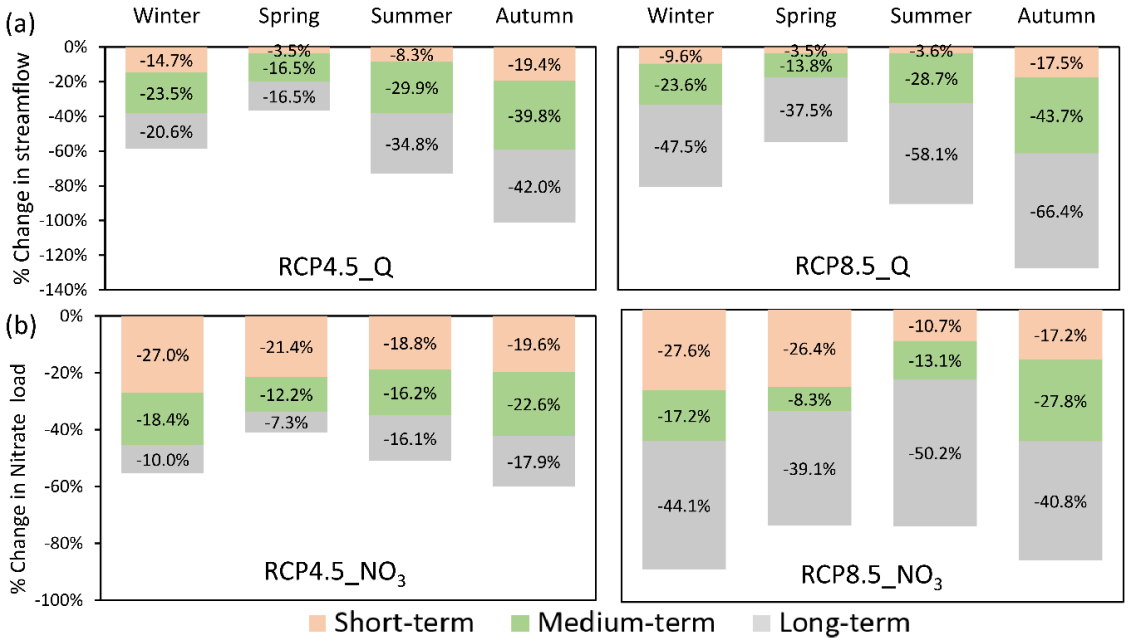

Figure 5.4: Seasonal percent changes in projected future (a) streamflow and (b) nitrate load over the short-, medium-, and long-term periods under RCP4.5 and RCP8.5 emission scenarios relative to the historical reference

5.3.2.3 Effects of climate change on nitrate load

The simulated future annual nitrate load decreased by -21.7%, -17.7%, and -12.8% for RCP4.5 and -20.5%, -16.6%, and -43.6% for RCP 8.5 in the short-, medium-, and long-projections, respectively, compared to the historical reference period with very high interannual variability (Figure 5.5). The short-term and medium-term nitrate load projections under RCP4.5 and RCP8.5 were quite similar. However, there was a considerable difference in the long-term projection, with RCP8.5 experiencing the greatest decline of -43.6% compared to -12.8 for RCP4.5. The decrease in projected nitrate load was primarily due to the reduction in projected streamflow. The statistical

relationship between streamflow and nitrate load showed a good correlation (p-value < 0.05) for RCP4.5 and RCP8.5 over the entire future projection period. This relationship indicates that streamflow, mainly driven by precipitation and temperature, would play an essential and critical role in determining the future nitrate export since it is the primary driving mechanism. However, the relationship between streamflow and nitrate load is not always linear despite streamflow having the greatest influence. Other factors that could play a critical role in determining the sources, amounts, mobilization, and transport pathways of nitrate in an agricultural watershed include precipitation amount and intensity, land cover type and practices, fertilization quantity and type, as well as cropping pattern and schedule (Boithias *et al.*, 2014; Cameron *et al.*, 2013; Parajuli and Risal, 2021). Additionally, the presence of buffer zones and riparian vegetation could help minimize nitrate mobilization and transport to surface waterways (Beaudoin *et al.*, 2005). These results are consistent with other studies within the Mediterranean region (Molina-Navarro *et al.*, 2014) and the Iberian Peninsula (Carvalho-Santos *et al.*, 2016) that have reported a decrease in nitrogen exportation due to the reduced streamflow. Mander *et al.* (2000) also found that reducing surface water runoff considerably reduced nitrate load exportation in cultivated areas.

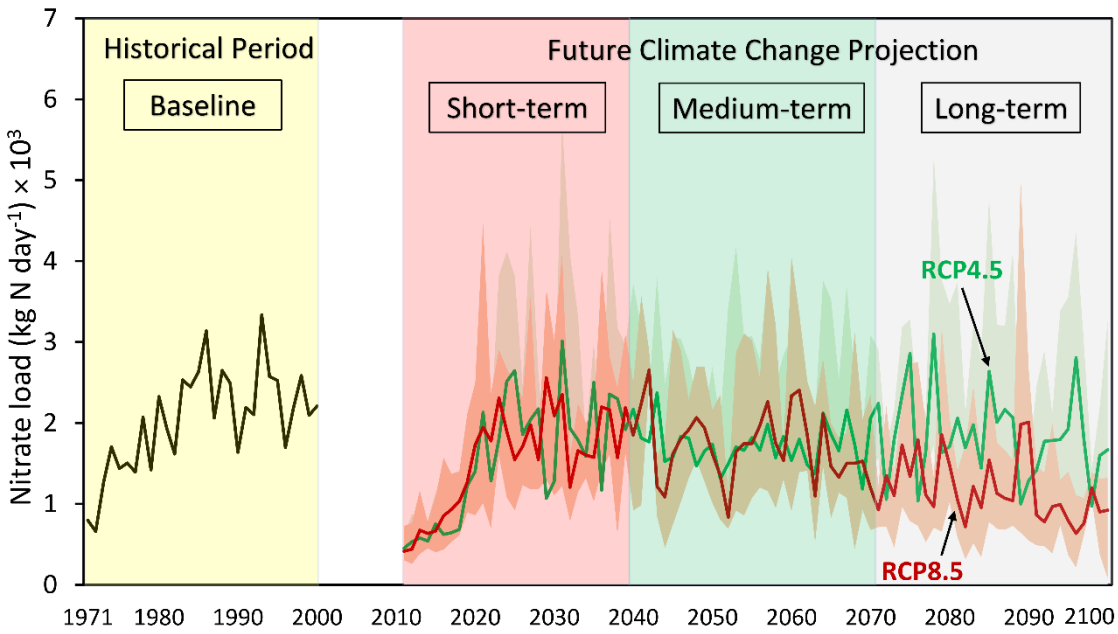

Figure 5.5: Average annual nitrate load evolution over historical (1971-2000), short-term (2011-2040), medium-term (2041-2070), and long-term (2071-2100) periods under RCP4.5 and RCP8.5 climate change projections

The magnitude and frequency of nitrate load occurrence were greater in the long-term projection scenario of RCP4.5 than in RCP8.5, similar to the streamflow results. This pattern could be due to the timing of agricultural management operations, such as fertilization, which could have coincided with heavy rainfall as well as more available water to transport the nitrates. The increase in frequency and severity of extreme precipitation events under RCP4.5 after the 2070s in the Mediterranean region have been reported to result in increased streamflow and nitrate export (Almeida *et al*., 2022; Barredo *et al*., 2017; Giorgi and Lionello, 2008; Todaro *et al*., 2022).

Nitrate load decreased in all seasons and projected periods for both emission scenarios, with the greatest decrease occurring in summer for the RCP8.5 long-term projection (-50.2%) and autumn for the RCP4.5 medium-term projection (-22.6%) (Figure 5.4b). This could be due to higher streamflow reduction and the aforementioned factors during the same period. However, the nitrate concentration is projected to rise by 4.1%, 34.8%, and 45.1% for RCP4.5 and 5.2%, 36.8%, 54.1% for RCP 8.5 in the short-, medium-, and long-term projections, respectively due to the faster streamflow decline than the nitrate exportation rate (Figure 5.6). This would result in the accumulation of more nitrates in the riverbed and soil, resulting in soil and groundwater pollution. Carvalho-Santos *et al.* (2016) observed an increasing trend in future nitrate concentration despite the declining nitrate loads attributed to declining streamflow. The projected increase in nitrate concentration at the end of the century will be of great concern as the current figures within the watershed already indicate a higher nitrate concentration. Findings by Merchán *et al.* (2020) have categorized the watershed as a "Nitrate Vulnerable Zone"; hence, any increase in concentration is likely to exacerbate the problem further. Furthermore, increased nitrate concentration would increase eutrophication in the river, thus enhancing algae bloom and consequently degrading the water quality and resulting in higher water treatment costs (Tong *et al.*, 2012).

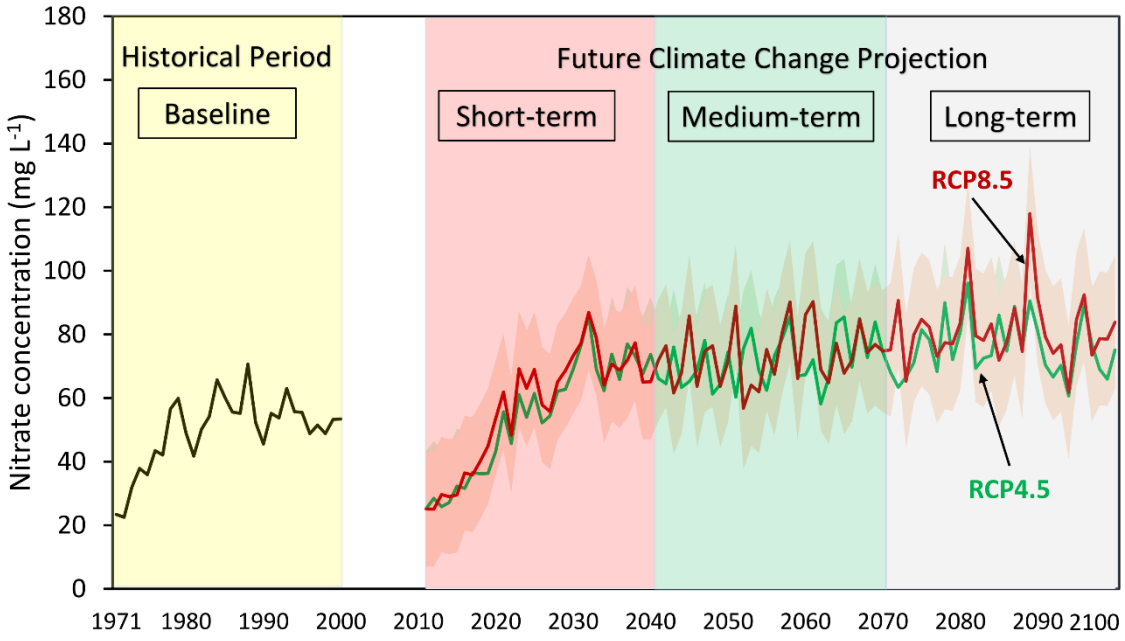

Figure 5.6: Projected evolution of the average annual nitrate concentration in the Cidacos River watershed over historical (1971-2000), short-term (2011-2040), medium-term (2041-2070), and long-term (2071-2100) periods under RCP4.5 and RCP8.5 climate change scenarios

5.3.2.4 Effect of climate change on agriculture

Projected climate change is expected to heavily impact agricultural activities through changes in phenology and cropping cycle (Funes *et al.*, 2016; Trnka *et al.*, 2011), as well as higher water demands due to increased evapotranspiration (Saadi *et al.*, 2015; Valverde *et al.*, 2015). Consequently, crop yields are expected to decline, especially under the RCP8.5 long-term projection with no adaptation measures (Feyen *et al.*, 2020), in addition to higher inter-annual variability and decreased production resilience (Zampieri *et al.*, 2020). Reduced streamflow would greatly affect irrigation, particularly for corn and tomatoes grown in the study area, which relies heavily on irrigation. Extreme warming, as projected in the medium and long term, will shorten the growing seasons for most crops. According to Mougou *et al.* (2011), a temperature increase of 2.5 ºC to 4 ºC would shorten the growing period of wheat in the Mediterranean region by 16 to 30 days. Recurrent drought events could result in heavy agricultural losses of more than -50% in irrigated areas and -15% in rain-fed cereal production (Mougou *et al.*, 2011). Other negative climate change impacts on agriculture in the region include the emergence of new and re-emerging crop pests and diseases, which would increase production losses, as well as increased wildfire incidences caused by the projected extreme weather. These

factors would result in food insecurity and increased economic losses in the region and should thus be mitigated to limit the potential negative consequences.

5.3.2.5 Climate change adaptation and mitigation measures

Based on this study's findings, it's evident that climate change would negatively affect the agricultural areas in northern Spain and the Mediterranean region since water resources will be under great pressure and nitrate pollution of surface and groundwater will increase. As a result, robust agricultural policies, regulatory frameworks, and legislation aimed at climate change adaptation and mitigation would be required to minimize the potential negative impacts. The projected water scarcity and increased drought events would limit irrigation-based adaptation actions. However, agricultural management practices such as crop distribution, schedules, diversification, and rotation would be central to the adaptation strategy at the farm scale. Land use change by introducing drought-resistant crops could also improve climate change resilience. An effective adaptation and mitigation strategy would prioritize the following actions: (i) farming practices, which would include crop diversification, changing crop type and land use, and adjusting rotation patterns; (ii) water management practices, which would emphasize the need for technological development and innovation for crops and agricultural practices such as precision agriculture and modifying irrigation; (iii) farm management practices that focus on diversifying income sources, such as the government establishing programs to ensure agricultural subsidies, the provision of insurance to farmers to stabilize their income, and agricultural financial assistance; (iv) agricultural management practices that focus on optimal nitrogen fertilization, the use of organic fertilizers, and soil health improvement. Nitrogen surplus in the soil can be reduced through efficient application according to the soil nitrogen availability and potential crop yield. Combining these adaptation and mitigation strategies would improve the potential for increasing or at least maintaining crop yield.

5.4 Conclusion

The main findings and conclusions of this chapter are provided in Chapter 7, section 7.3.

Chapter 6:

6 Quantification of Agricultural Best Management Practices Impacts on Sediment and Phosphorous Export in a Small Catchment in Southeastern Sweden

This Chapter is based on: **Oduor, B. O**., Campo-Bescós, M. Á., Lana-Renault, N., Kyllmar, K., Mårtensson, K. and Casalí, J. (2023). Quantification of agricultural best management practices impacts on sediment and phosphorous export in a small catchment in southeastern Sweden. *Agricultural Water Management*, 290, 108595. https://doi.org/10.1016/j.agwat.2023.108595

(Publisher: **Elsevier**; JCI: **Q1** in Agronomy, IF: **6.7**)

6.1 Introduction

Agricultural nutrient pollution is one of the leading sources of nonpoint source pollution in freshwater systems, especially in regions where the intensification of agriculture has led to increased nutrient inputs, affecting more than half of the global freshwater systems (Grizzetti *et al.*, 2021; Mateo-Sagasta *et al.*, 2018; Xia *et al.*, 2020). The runoff from agricultural areas transports suspended sediments and excess nutrients from fertilizers and manure into water bodies. These pollutants endanger the quality of water resources and could have far-reaching consequences for aquatic ecosystems and human health (Oduor *et al.*, 2023; Sutton *et al.*, 2011). Almost 40% of the European Union region's water bodies, such as lakes, rivers, and coastal areas, have been affected by pollution from agricultural areas (Mateo-Sagasta *et al.*, 2017; UN Water, 2015). Most European countries have enacted regulations to reduce nutrient pollution to address this issue, such as limiting nutrient discharges from point sources and implementing best management practices (BMPs) in agricultural areas. Efforts to improve water quality monitoring and data collection have also increased in the past few years to enhance informed decision-making (European Environment Agency (EEA), 2022).

The over-application of fertilizers, manure, and other agricultural inputs can result in the excess accumulation of nutrients in soils, which can then be transported to freshwater systems through runoff and leaching. Excessive phosphorous loading in freshwater systems can lead to eutrophication, which can have severe ecological and economic impacts (Carpenter *et al*., 1998; Sánchez-Colón and Schaffner, 2021). Similarly, intensive cultivation practices like tillage and plowing have contributed to soil erosion, which increases sediment export. Sediments can affect freshwater ecosystems by reducing light penetration through increased turbidity, burying benthic habitats, and transporting pollutants adhered to soil particles (Meyer *et al.*, 2015).

The concentration of nutrients in runoff and drainage water from cultivated areas depends on numerous complex, interrelated factors, including previous agricultural management practices, land use and cover, soil type and characteristics, amount and intensity of precipitation, drainage system, topography, and many others (Ulén and Fölster, 2007). To mitigate the negative impacts of nutrient exportation from agricultural areas, Sweden has put in place various measures, such as regulating fertilizer by setting limits on the amounts of nitrogen and phosphorous fertilization based on soil type and crop needs, managing livestock farming to reduce nutrient runoff from manure, encouraging the growth of cover

crops, establishing buffer zones (filter strips), and restoring wetland to reduce nutrient and sediment runoff into waterways (Kyllmar *et al.*, 2023; Mårtensson *et al.*, 2023). Despite implementing some of these measures, their effectiveness is not well known. Therefore, there is still a need to evaluate and identify the BMPs that could help reduce sediment and phosphorous exports from cultivated areas.

BMPs are land management practices designed to reduce nutrient inputs to soils, prevent soil erosion, and improve water quality. BMPs have been identified to minimize sediment and nutrient pollution from agricultural activities. Previous studies have shown that BMPs, such as reduced tillage, buffer strips, regulated fertilization, etc., can effectively reduce sediment and phosphorous export from agricultural systems (Arabi *et al*., 2006; Sharpley *et al*., 2006; Sharpley *et al*., 2015). However, the effectiveness of these BMPs varies depending on soil type, climate, land use, and the specific BMP implemented. The effectiveness of BMPs can also be influenced by changes in management practices over time, such that if a farmer stops implementing a particular BMP, sediment and phosphorous export may increase again. In spite of these challenges, studies have shown that BMPs can effectively reduce sediment and phosphorous export if properly implemented and managed (Bracmort *et al*., 2006; Gitau *et al*., 2008; Liu *et al*., 2017).

Modeling approaches have been widely used to evaluate the impact of BMPs on nutrient export from agricultural systems. Models enable the examination of scenarios that are not easily studied through direct experimentation, saving time and resources (Moges *et al.*, 2021; Yu, 2015). One widely used model for this purpose is the Soil and Water Assessment Tool (SWAT) model, which has been extensively applied on catchment and regional scales to understand the dynamics of land use and management practices on water quality (Arnold *et al.,* 2012). The SWAT model provides a comprehensive framework for understanding and quantifying the impact of various factors on sediment and nutrient transport, including phosphorus, by modeling the complex interactions between land use, climate, soil, and surface and groundwater (Neitsch *et al.*, 2011). Its applicability and reliability have been demonstrated in numerous studies worldwide, making it an ideal choice for adoption in this study.

In Sweden, most SWAT modeling applications are focused on climate change (e.g., Grusson *et al.*, 2021; Jiménez-Navarro *et al.*, 2023, 2021, etc.), hydrology and water quality (e.g., Bekarias *et al.*, 2005; Exbrayat *et al.*, 2010, etc.), and land use management (e.g., Ekstrand *et al.*, 2010; Thodsen *et al.*, 2017, etc.), however, its application for BMPs

analyses are limited or absent. Nevertheless, other models have been adopted to estimate the potential nutrient reduction of selected BMPs. For instance, Arheimer *et al.* (2005) used the HBV-NP model to assess the cost-effectiveness of implementing different cover crop scenarios, constructed wetlands, and buffer strips in the Ronnea catchment in southern Sweden. Similarly, Mårtensson *et al.* (2023) employed the Nutrient Leaching Coefficient Calculation System (NLeCCS) and the Average Nutrient Leaching Calculator (ANLeC) models to estimate nutrient leakage in the current study area and its entire leaching region by considering different crop combinations, variations in cultivation practices, cover crops, and buffer zones.

The main objective of this study was to use the SWAT model to quantify the effectiveness of selected agricultural BMPs (filter strips, sedimentation ponds, grassed waterways, and no-tillage) in reducing sediment and phosphorus export from a small agricultural catchment in southeastern Sweden. This objective was accomplished by carrying out the following two specific objectives: (i) calibrating and validating the SWAT model for streamflow, sediment, and phosphorous load in the study area and then (ii) using the calibrated model to simulate different BMP scenarios and assessing their effectiveness in reducing sediment and phosphorous export relative to the baseline scenario.

6.2 Materials and Methods

6.2.1 Study area description

The study was carried out in Catchment C6, located in southeastern Sweden. Refer to Chapter 3, section 3.2, for the detailed study area description.

6.2.2 Data acquisition

Refer to Chapter 3, section 3.4. for Catchment C6's data collection and processing information.

6.2.3 Model description

Refer to Chapter 2 for a detailed overview of the SWAT model, including hydrology, sediment load, and phosphorous load simulation and model evaluation criteria.

6.2.4 The model set-up, calibration, and validation

The model was set up using QSWAT3 (version 1.1.1) within the QGIS 3.16 interphase. The catchment was delineated into 34 subbasins using the digital elevation model (DEM)

and the stream shapefile, with the catchment outlet point assigned. The catchment elevation ranged from 10 – 58 m above sea level (a.s.l) with a mean elevation of 27 m a.s.l. (standard deviation ±8.54 m). The DEM was overlaid with land use and soil data to generate 349 HRUs, which served as the model's primary simulation units. The meteorological data and agricultural management information were updated in the SWAT editor before running the model on a daily time-step from 1990 to 2020. The first ten years of the model run were used as a warm-up period for the model initialization. The model outputs for hydrology, sediment transport, and phosphorous export were extracted monthly from 2005 to 2020. These outputs were compared to observations for calibration (2005 – 2012) and validation (2013 – 2020) using the SWAT Calibration and Uncertainty Programs (SWAT-CUP) software. Figure 6.1 illustrates the flow diagram of the SWAT model simulation of agricultural BMPs in the study area.

The model calibration was done using the Sequential Uncertainty Fitting, version 2 (SUFI-2) algorithm of the SWAT-CUP (Abbaspour, 2015). The details of the SWAT-CUP parameterization, sensitivity and uncertainty analyses, calibration, validation, and performance evaluation are already discussed in Chapter 2, sections 2.5 and 2.6. The parameters controlling hydrology processes, sediment, and phosphorous export were selected by reviewing the existing literature on the SWAT model's application in similar catchments. The initial parameter uncertainty ranges were assigned based on the absolute SWAT parameter limits provided in SWAT-CUP. A global sensitivity analysis was conducted through an initial 500 model runs to determine the most sensitive parameters. The most sensitive parameters for each variable are discussed further in section 6.3.1 of the results.

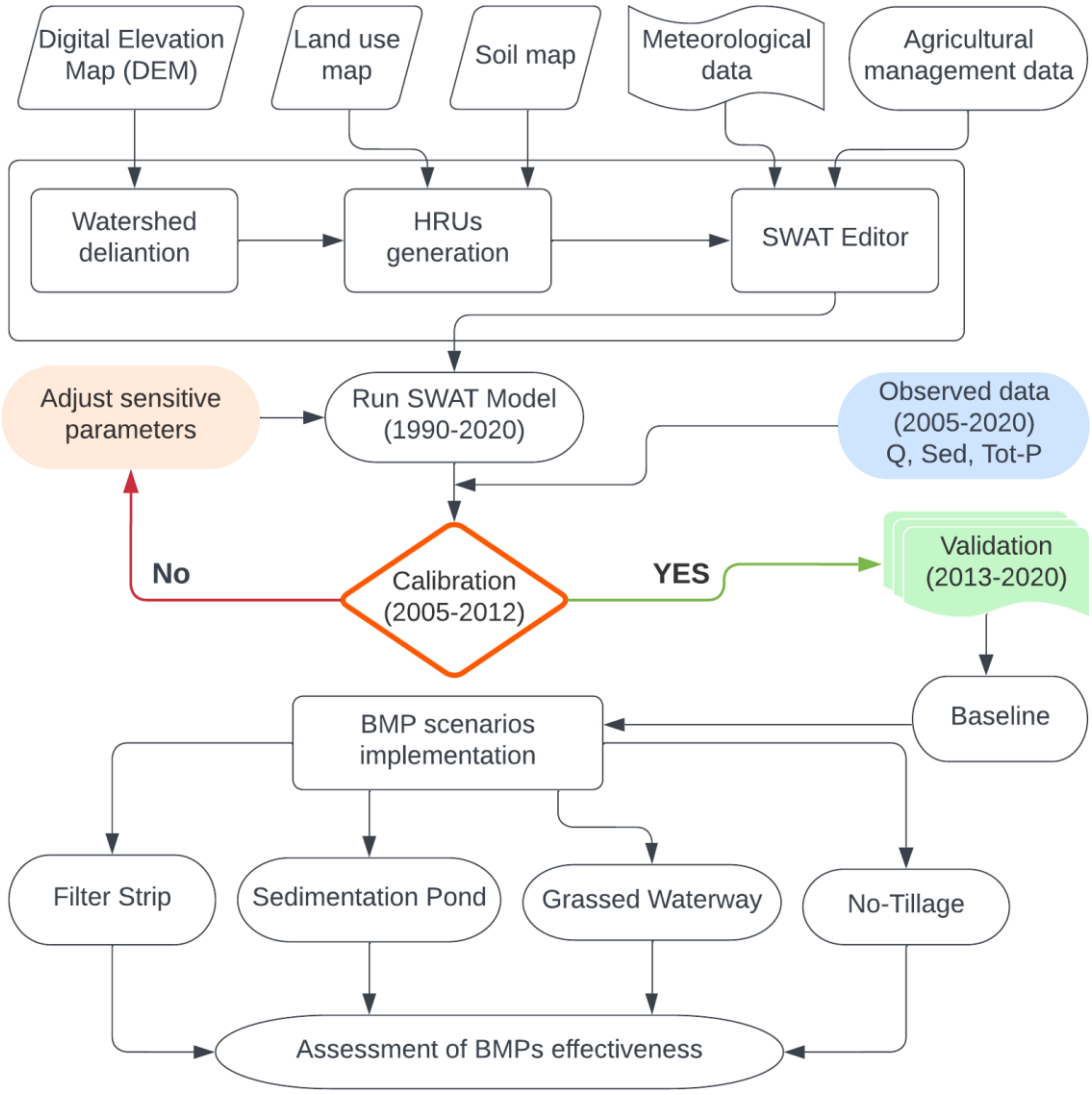

Figure 6.1: Flow diagram for the SWAT model simulation of agricultural BMPs in Catchment C6

6.2.5 Agricultural BMPs scenario representation

The calibrated SWAT model was used to quantify the sediment and phosphorous export for the various BMP scenarios. The BMPs were selected based on the available literature (Arabi *et al*., 2006, 2008; Bracmort *et al*., 2006) and local agricultural management information (Mårtensson *et al.*, 2023). The choice of the BMPs was based on factors such as practicality, ease of adoption and acceptance by the farmers, the viability of implementation, and potential effectiveness in reducing sediment and phosphorous. The calibrated model representing the existing land use and management practices in the catchment was used as the baseline scenario (no BMP implementation). The analyzed scenarios included the implementation of filter strips, sedimentation ponds, grassed

waterways, and conservation tillage practices. The modified SWAT model parameters for each BMP scenario implementation are shown in Table 6.1. The statistical significance of the average annual values of each BMP scenario was assessed using the Wilcoxon–Mann–Whitney Rank-Sum test (Helsel *et al.*, 2020). A BMP scenario was considered statistically significant when the p-value was less than 5% (p-value < 0.05). The efficacy of the BMPs in minimizing sediment and phosphorous export from the catchment was determined by comparing the averages of each implemented BMP scenario to the baseline scenario.

Table 6.1: Modified SWAT model parameters for the BMPs scenarios implementation.

BMP scenario	Modified SWAT parameter		
	Parameter*	Baseline value (No BMP)	Adjustment value (With BMP)
Filter strip	FILTERW.mgt	0	7.5 (m)
Sedimentation ponds	PND_FR.pnd	0	0.5
	PND_PSA.pnd	5	500 (ha)
	PND_PVOL.pnd	25	50 (10^4 m^3 H_2O)
	PND_K.pnd	0	0.05 (mm hr^{-1})
Grassed waterway	CH_COV1.rte	0.25	0.001
	CH_COV2.rte	0.2	0.001
	CH_N2.rte	0.25	0.40
No-tillage (Zero till)	CN2.mgt	Varies**	-10%
	EFFMIX.till.dat	0.95	0.05
	DEPTIL.till.dat	150	25 (mm)

* The parameter descriptions are in the text.

**The CN2 parameter value varies for each HRU depending on land use, soil permeability, and antecedent soil moisture conditions. These values ranged from 55 to 72 in the catchment.

Filter strips, also known as buffer zones, are vegetation (such as trees, shrubs, and grass) planted along the edges of fields to trap sediment and nutrient pollutants that might be carried into nearby waterways. Filter strips are particularly effective in areas where cultivated fields are adjacent to streams or other water bodies. According to Mårtensson *et al.* (2023), filter strips are assumed to be installed along the edges of all fields and that all the fields in the catchment were connected to a watercourse. The primary purpose of filter strips is to reduce the amount of suspended sediments and dissolved contaminants in runoff water (Tuppad *et al.*, 2010). The effectiveness of filter strips in contaminant removal, also known as trapping efficiency ($Trap_{eff}$) is dependent on the filter strip width (FILTERW) and is determined using Equation (2) (Arabi *et al.*, 2008).

$$\mathrm{Trap_{eff}} = 0.367 \times \mathrm{FILTERW}^{0.2967} \quad (6.1)$$

According to Dosskey *et al.* (2008), a properly installed filter strip can effectively retain up to 90% of nutrients and sediment. In the SWAT model, the sediment and nutrient reduction rate across the filter strip is quantified as a function of the average filter strip width and the volume of water from the reach. Filter strip was implemented in the model by modifying the filter strip width (FILTERW) parameters by varying its value from 5 to 10 meters compared to the default without a filter. This range was based on the recommended buffer zone size of between 6 meters and 18 meters for all soil types permitted under the current Swedish regulations (Mårtensson *et al.*, 2023). The sediment and phosphorus reduction rates were then determined for each filter width over the entire range, and the width with the highest reduction was considered the most effective.

Sedimentation ponds, also known as detention ponds or constructed wetlands, are shallow basins with a large surface area typically lined with vegetation designed to trap and reduce or remove sediments and agricultural pollutants from runoff by allowing them to deposit and settle at the bottom of the pond. The settled sediments can then be periodically removed from the pond by dredging or excavation and disposed of properly. Sedimentation and biological processes help to remove and reduce suspended sediments and nutrients in the pond. Nutrient retention occurs in the pond via sorption, precipitation, and incorporation (Waidler *et al.*, 2009). The ponds can also help reduce floods by temporarily storing excess water during heavy rain. Sedimentation ponds were implemented in the SWAT model by adding pond parameters which included the fraction of subbasin area that drains into the ponds (PND_FR), the total surface area of the ponds when filled to the principal spillway (PND_PSA), volume of water needed to fill the ponds (PND_PVOL), and the hydraulic conductivity through the bottom of the pond (PND_K). The selected parameter ranges were based on the absolute SWAT parameter value range in SWAT-CUP (Abbaspour, 2015).

Grassed waterways are typically broad, shallow watercourses vegetated (with grass) to reduce the flow velocity and trap sediments and pollutants. Unlike filter strips, grassed waterways are usually installed in the drainage pathway (Evrard *et al.*, 2007). Grassed waterways can withstand higher in-channel velocities than bare channels since vegetation retards the flow velocity and protects the soil. Grassed waterways were implemented in the SWAT model by modifying the channel parameters such as the channel's Manning's

coefficient of roughness (CH_N2), channel erodibility factor (CH_COV1), and channel cover factor (CH_COV2) as recommended by Bracmort *et al.* (2006) and Kaini *et al.* (2012). The default values for CH_COV1 and CH_COV2 were adjusted to 0.001, while the CH_N2 value was increased by 50% of its original value to represent a fully protected vegetative cover (Arabi *et al.*, 2008; Kaini *et al.*, 2012). It's worth noting that the 0.001 value chosen was an arbitrary, very small number close to zero to prevent the model from using the default values when set to 0. Other grass waterway design parameters found in the management operations file included depth (GWATD), width (GWATW), length (GWATL), and slope (GWATS), which all remained set to the model's default values as provided in the SWAT documentation (Arnold *et al.,* 2012).

No-tillage (zero tillage) was only applied to arable land comprising about 60% of the total catchment area. The no-tillage practice involves leaving the soil undisturbed, and crop residue is maintained on the soil after harvest. No-tillage is one of the conservation tillage practices. Melero *et al.* (2009) describe conservation tillage as any tillage and planting practice that maintains at least 30% of the soil surface covered by residues after planting. In the SWAT model, tillage operations differ based on their mixing efficiencies (EFFMIX), which indicate the fraction of materials (such as residue, nutrients, pesticides, bacteria, etc.) distributed within the mixed soil depth (DEPTIL) of each soil layer. The SWAT model's tillage database provides information on mixing efficiencies and tillage depths for over 100 tillage practices, which maybe be specified in the model using their unique tillage identifiers (TILL_ID). The no-tillage scenario was implemented in the model using TILL_ID = 4. The parameter values for EFFMIX and DEPTIL are set at 0.05 and 25 mm, respectively. It is also recommended to reduce the curve number (CN2) parameter value by 2–3 units up to a maximum of 10% from the calibrated value when implementing tillage BMPs (Tuppad *et al.*, 2010). CN was thus reduced by -10% to achieve the most optimal results.

6.3 Results and discussion

6.3.1 Model evaluation

6.3.1.1 Parameterization and sensitivity analysis

The sensitivity analysis was performed through a global sensitivity test of various selected initial parameters for streamflow, sediment, and phosphorous load. Streamflow parameters were analyzed and calibrated first, then sediments load parameters, and

finally, phosphorous parameters. Several studies (e.g., Abbaspour, 2015; Abbaspour *et al.*, 2018, 2015; Arnold *et al.*, 2012b; Yuan and Koropeckyj-Cox, 2022) have recommended the sequential calibration of streamflow, followed by sediments, and finally nutrients due to the interdependencies between the constituent variables as well as shared transportation processes. Table 6.2 presents the five most sensitive parameters for each variable. All other parameters used for the model simulation in this study area are listed in Table A 2 in Appendix II.

Table 6.2: Selected most sensitive SWAT parameters and adjusted values for streamflow, sediment load, and phosphorous load simulation in Catchment C6.

SWAT input parameter*	Parameter description	Units	Parameter adjustment value			
			Default	Min	Max	Fitted
	Hydrology parameters					
v__SFTMP.bsn	Snowfall temperature	ºC	1	-5	5	-2.5
v__SMTMP.bsn	Snowmelt base temperature	ºC	0.5	0	5	4.5
V__GW_DELAY.gw	Groundwater delay	days	31	0	17.5	3.5
r__SOL_AWC.sol	Available water capacity of the soil layer	mm H_2O/ mm soil	-	-80%	10%	-40%
r__CN2.mgt	Initial SCS runoff curve number for moisture condition II	-	35-98	-20%	-5%	-12%
	Sediment load parameters					
v__CH_N2.rte	Manning's "n" value for the main channel	-	-	0.01	0.3	0.25
v__CH_K2.rte	Effective hydraulic conductivity in the main channel	mm hr^{-1}	-	40	110	65
v__LAT_SED.hru	Sediment concentration in lateral and groundwater flow	mg L^{-1}	0	0	50	27.65
v__SPCON.bsn	Linear parameter for calculating the maximum amount of sediment that can be re-entrained during channel sediment routing	-	0.001	0.001	0.01	0.005
v__PRF_BSN.bsn	Peak rate adjustment of sediment routing in the main channel	-	1	0	2	1.122
	Phosphorous load parameters					
v__PSP.bsn	Phosphorous availability index	-	0.40	0.1	0.7	0.5
v__P_UPDIS.bsn	Phosphorous uptake distribution parameter	-	20	0	100	53.3
v__PHOSKD.bsn	Phosphorous soil partitioning coefficient	m^3 Mg^{-1}	175	100	200	146.3
v__PPERCO.bsn	Phosphorous percolation coefficient	10 m^3 Mg^{-1}	10	10	17.5	17.45
v__RS5.swq	Organic P settling rate in the reach at 20 ºC	day^{-1}	0.05	0.001	0.5	0.095

*" v" represents a parameter change by replacing the existing value with the fitted value, whereas "r" represents a relative change by varying the existing value with the fitted value. Generally, the replacement method is used for basin-wide parameters, whereas the relative change method is adopted for variations in HRU-specific parameters.

Parameters influencing snow, baseflow (or groundwater), soil properties, and land use management were highly sensitive to streamflow (Table 6.2). This region experiences heavy snowfall and accumulation during winter; thus, their dynamics (snowfall and melt) play a pivotal role in the catchment's hydrological processes. The timing, magnitude, and rate of snowfall and snowmelt strongly influence runoff and, consequently, streamflow. The catchment water balance indicated a prevalent baseflow of approximately 90% of the surface runoff in the catchment, thus the sensitivity of groundwater parameters. This was attributed to tile drainage, simulated in the model as lateral flow (Neitsch *et al.*, 2011), and the drainage of surface runoff into baseflow. Variations in the catchment's soil characteristics and land use patterns were captured using the soil and land management parameters such as the available water, soil water capacity, and curve number. The most sensitive sediment parameters included those that influence channel transportation and re-entrainment capacity (CH_N2, CH_K2, SPCON, PRF) and sediment concentration in the baseflow (LAT_SED). These results are comparable to those obtained by Abbaspour *et al.* (2007) and Arabi *et al.* (2008), highlighting the relevance of these parameters in sediment computations.

The phosphorus load simulation in the model used various default parameters. The most sensitive phosphorous load parameters are presented in Table 6.2. The phosphorous availability index (PSP) of 0.5, which is close to the default value of 0.4, indicated that 50% of the phosphorous in the soil was available for plant uptake. Yuan and Koropeckyj-Cox (2022) reported a wide range of PSP parameter values, with higher values observed in agricultural areas with intensive inorganic phosphorous fertilizer application and substantial pools of legacy phosphorous from prior management practices. The phosphorous uptake distribution factor (P-UDIS) has consistently emerged as a sensitive parameter in most SWAT phosphorous load simulation studies (Abbaspour *et al.*, 2007; Y. Liu *et al.*, 2019; Yuan and Koropeckyj-Cox, 2022). This parameter controls the amount of phosphorous taken up by plants across different soil layers. A higher value implies that most phosphorous is taken up from the upper or surface soil layers (top 10 mm), whereas a lower value indicates that phosphorous is mostly taken up from the deeper soil layers.

The PHOSKD and PPERCO parameters govern the soluble P movement through the soil, while the RS5 parameter is responsible for the organic P settling.

6.3.1.2 Model calibration and validation

The magnitude and temporal dynamics of the SWAT model simulations at monthly time-step replicated most of the streamflow, sediment load, and total P load observations during calibration and validation periods (Figure 6.2). The model accurately captured the catchment's hydrological behavior well at low and peak flows. The sediment and total P loads were also reasonably simulated despite the slight underestimation of a few peaks, which may be attributed to process simplifications in the SWAT model, such as the simplification of the soil loss equation adopted by the model (Abbaspour *et al*., 2007; Pandey *et al*., 2021; Tolson and Shoemaker, 2007). However, the 95PPU was used to quantify all these uncertainties associated with the simulations. Notably, the 95PPU band bracketed 79% of streamflow observations, 63% of sediment load observations, and 53% of the total P load observations on average, indicating satisfactory model performance given the inherent uncertainties. These results could be attributed to the detailed, high-resolution input data and the model's ability to capture the dominant processes in the catchment very well.

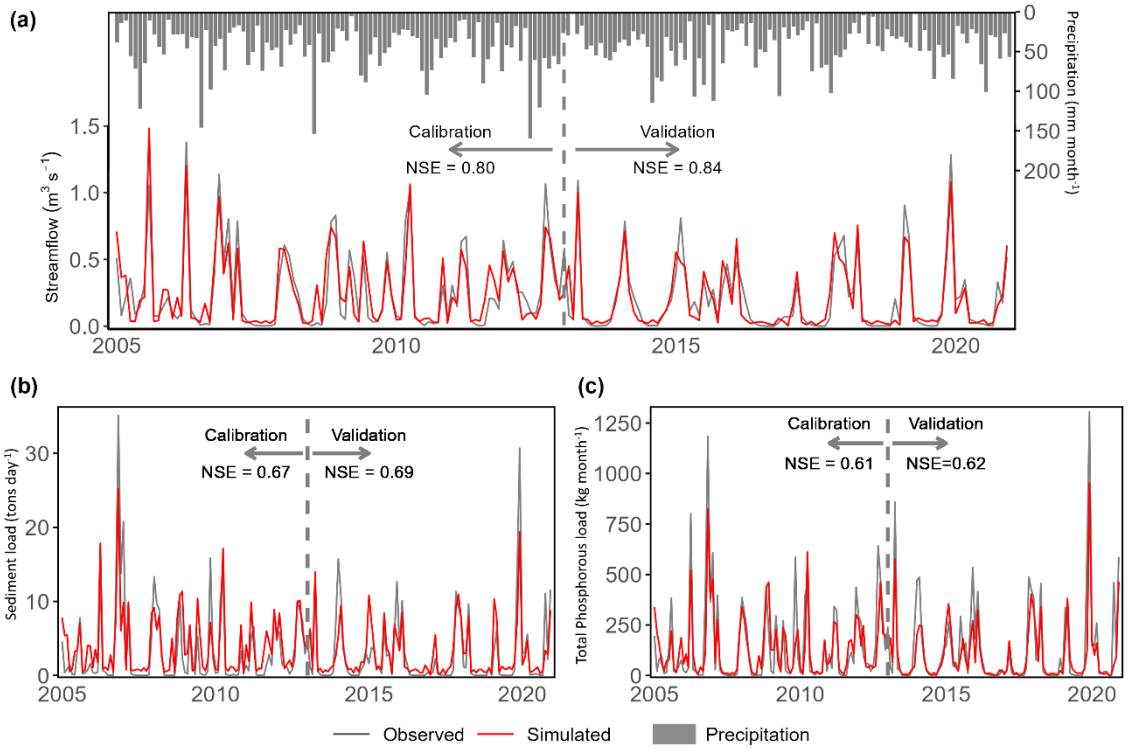

Figure 6.2: Comparison of average monthly simulated (red lines) and observed (grey lines) (a) streamflow, (b) sediment load, and (c) phosphorous load at the catchment outlet

during the calibration and validation period. Observed total monthly precipitation (grey bars) is displayed alongside the streamflow hydrograph.

The statistical performance indicators for the best simulations yielded satisfactory results during calibration and validation periods (Table 6.3). Streamflow simulation exhibited "very good" model performance during calibration/validation periods (NSE = 0.80/0.84). Similarly, sediment load (NSE = 0.67/0.69) and total P load (NSE = 0.61/0.62) demonstrated reasonably good performance. Moriasi *et al.* (2015) recommended that "very good or excellent" model variation performance is achieved when PBIAS is less than ±5% for streamflow, ±10% for sediment load, and ±15% for nutrients. A comparison of average monthly streamflow observation and simulation showed relatively minimal variation (PBIAS < ±5%), indicating excellent performance. A positive PBIAS value indicates that the observations were greater than the simulations, implying that the model underestimated the observations, whereas a negative PBIAS indicates that the observations were less than the simulations, implying that the model overestimated the observations. The performance of sediment load and total P load were also reasonably good despite some slight underestimation but still within the recommended threshold. Based on these findings, the model can be considered good and capable of replicating the catchment dynamics with reasonable certainty, making it suitable for adoption in other applications.

Table 6.3: SWAT model performance statistical indicator metrics for catchment C6.

Variable	Performance indicator	Threshold	Calibration	Validation	Model performance
Streamflow	NSE	> 0.5	0.80	0.84	Very good
	R^2	> 0.5	0.82	0.85	Very good
	PBIAS	±25%	-2.5%	+4.9%	Very good
Sediment load	NSE	> 0.5	0.67	0.69	Good
	R^2	> 0.5	0.72	0.64	Good
	PBIAS	±55%	+14.5%	+21.8%	Good
Total phosphorous load	NSE	> 0.5	0.61	0.62	Good
	R^2	> 0.5	0.64	0.71	Good
	PBIAS	±70%	+26.3%	+18%	Good

*These thresholds are the minimum performance requirement beyond which the model would be deemed unsuitable.

6.3.2 Effect of BMP implementation

The catchment's BMP scenarios had varying effects on streamflow, sediment load, and phosphorous (soluble P and total P) load. The impact of BMP implementation on streamflow was negligible (Table 6.4, Figure 6.3), with no change, except for a −10.8% reduction in streamflow when the sedimentation pond was implemented. Sedimentation ponds are designed to capture and temporarily retain sediment-laden runoff, resulting in a reduced volume of water flowing into the stream and subsequently decreasing the streamflow. Additionally, the extended runoff flow path through sedimentation ponds allows for infiltration and evaporation, thus further contributing to streamflow reduction. However, this retention is temporary, hence the slight decline. Other studies have also reported insignificant to no impact on streamflow due to the implementation of structural BMPs such as filter strips, wetlands, reduced tillage (Motsinger *et al.*, 2016), as well as grassed waterways and filter strips (Bracmort *et al.*, 2006). For sediment, soluble P, and total P loads, only filter strip and sedimentation pond scenarios were statistically significant ($p < 0.05$) relative to the baseline scenario (Table 6.4, Figure 6.3).

Table 6.4: P-values from the Wilcoxon–Mann–Whitney Rank-Sum statistical significance test of average annual values for the BMP scenarios relative to the baseline. A P-value < 0.05 is considered statistically significant.

BMP Scenario	Streamflow	Sediment load	Soluble P load	Total P load
Filter strip (7.5 m)	1	0.003	< 0.001	< 0.001
Sedimentation pond	0.202	0.002	0.021	< 0.001
Grassed waterway	0.980	0.161	0.654	0.601
No-Tillage	1	0.723	0.211	0.921

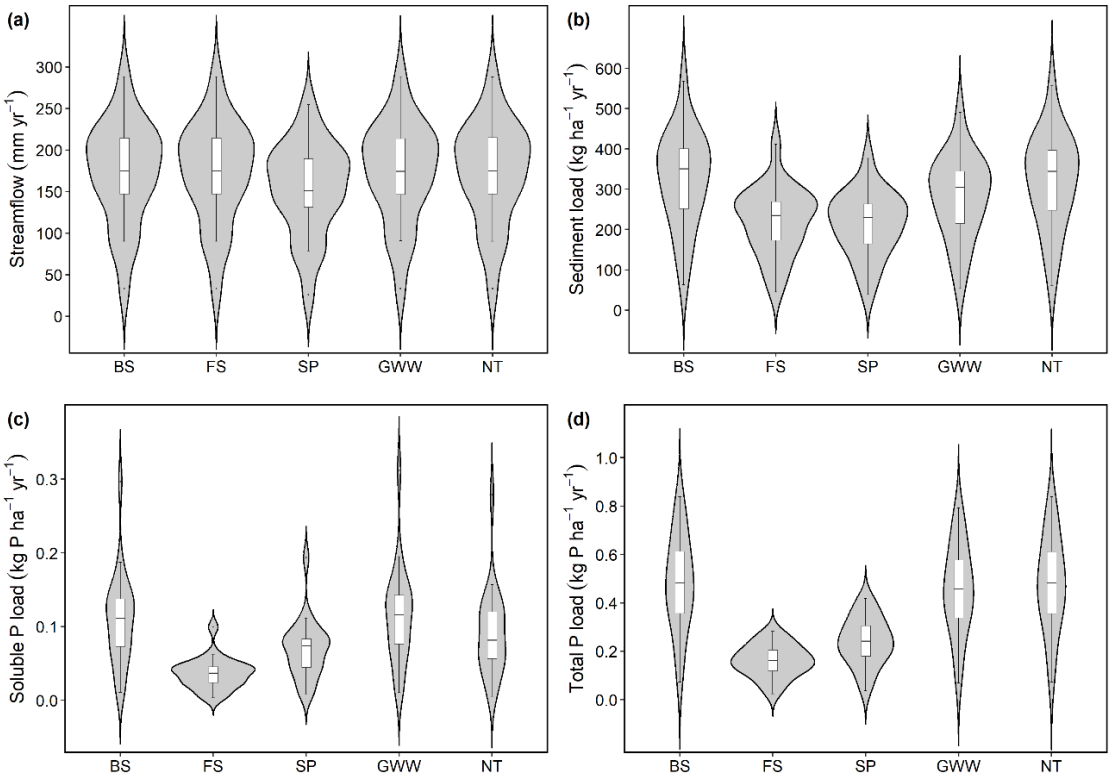

Figure 6.3: Comparative boxplots for annual average (a) streamflow, (b) sediment load, (c) soluble phosphorus load, and (d) total phosphorus load for the baseline scenario (BS) and the various BMPs (filter strip (FS), sedimentation ponds (SP), grassed waterways (GWW), and no-tillage (NT)) implemented on the study area.

The implemented agricultural BMPs reduced sediment and phosphorous loads in the catchment, with varying degrees of reduction for each BMP compared to the baseline, as illustrated in Figure 6.4. Specifically, the average annual sediment load was reduced by 103 kg ha^{-1} year^{-1} (–32%) in the filter strip scenario, 111 kg ha^{-1} year^{-1} (–35%) in the sedimentation pond scenario, 44 kg ha^{-1} year^{-1} (–14%) in the grassed waterways scenario, and 4 kg ha^{-1} year^{-1} (–1.3%) in the no-tillage scenario. Figure 6.4 shows variations in the reductions for soluble P and total P loads across different scenarios, except for the filter strip scenario, where they were relatively equal. Soluble P load reduced by 0.073 kg P ha^{-1} year^{-1} (–67%) in filter strip scenario, 0.040 kg P ha^{-1} year^{-1} (–36%) in the sedimentation pond scenario, and 0.018 kg P ha^{-1} year^{-1} (–17%) in the no-tillage scenario. However, the implementation of grassed waterways resulted in a slight increase in soluble P by 0.005 kg P ha^{-1} year^{-1} (+4%). The total P load followed a similar pattern to the sediment load, with reductions of 0.320 kg P ha^{-1} year^{-1} (–67%) in the filter strip scenario, 0.241 kg P ha^{-1} year^{-1} (–50%) in the sedimentation pond scenario, 0.026 kg P ha^{-1} year^{-1}

(–5%) in grassed waterway scenario, and slight reduction of 0.001 kg P ha^{-1} $year^{-1}$ (–0.2%) in no-tillage scenario.

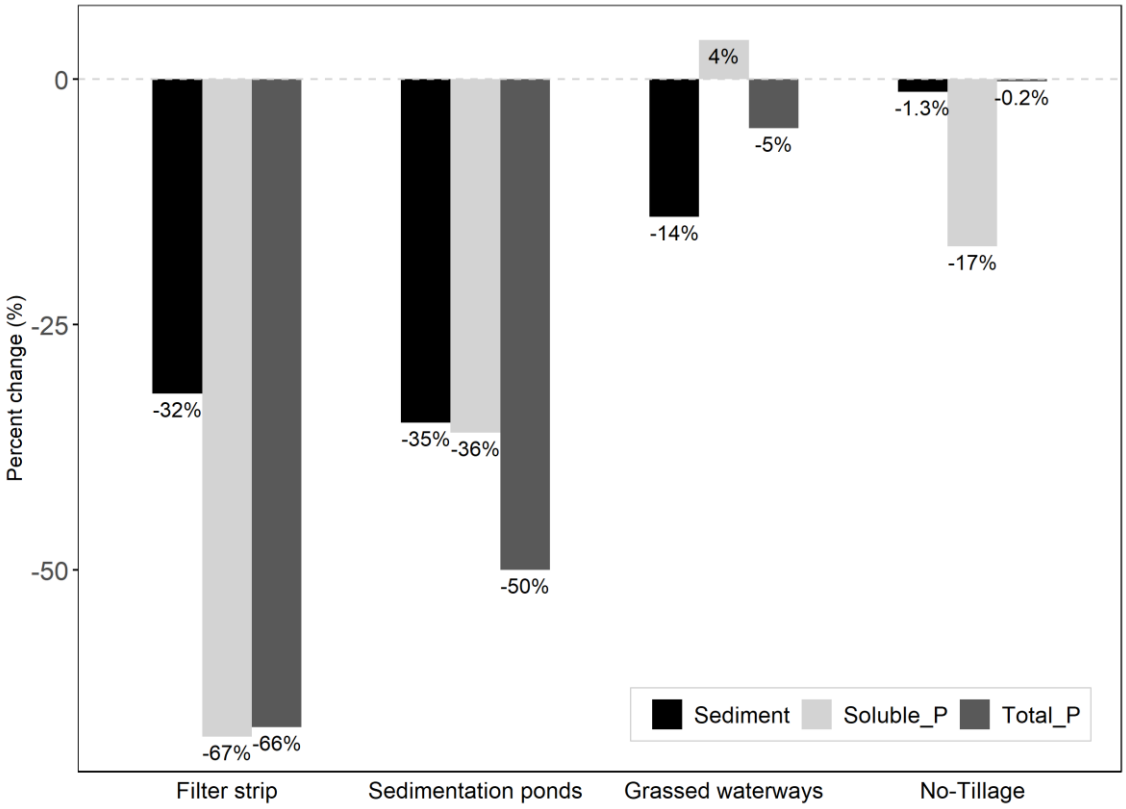

Figure 6.4: Summary of the variation in average annual sediment, soluble phosphorus, and total phosphorus export in the catchment for each BMP scenario relative to the baseline.

The findings indicate that filter strips and sedimentation ponds effectively reduce sediment and phosphorous loads at the catchment outlet, with filter strips being the most effective for reducing phosphorous load and sedimentation ponds effectively reducing sediment load. The catchment's phosphorus (total P and soluble P) load reduction is consistent with the sediment load reduction, though the phosphorous load reduction rate is slightly higher. This could be attributed to the strong relationship between sediment and total phosphorous loads, with R^2 values of 0.96 for observed monthly loads and 0.92 for observed annual loads, explaining the effectiveness of sediment control measures such as filter strips and sedimentation ponds in reducing nutrient losses. Venishetty and Parajuli (2022) observed a similar sediment-phosphorous load relationship for simulation in two agriculture-dominated catchments, where a slight reduction in sediment load by –8% and –15% as a result of filter strip BMP implementation resulted in –33% and –66% reduction

in total P load. Based on these findings, sediment transport could be regarded as the catchment's primary driver of phosphorous export.

The effectiveness of filter strips in reducing sediment and phosphorous export increased with increasing filter strip width, as illustrated in Figure 6.5. The sediment and phosphorous loads were reduced by approximately –25% and –55%, respectively, for the 5 m filter strip width and –30% and –75% for the 10 m filter strip width. The reduction in soluble P and total P was virtually the same, with a mere 1–3% difference that may be considered negligible. Optimal performance was observed with an 8 m filter width, resulting in nearly –40% and –70% reduction in sediment and phosphorus loads, respectively. The effectiveness of filter strips in reducing sediment and nutrient export has been reported in various studies. For instance, Mekonnen *et al.* (2017) reported –15% and –39% reductions in sediment load when 5 m and 30 m filter strip widths were implemented in the snow-dominated Assiniboine River watershed in Canada. The study also found total P reductions of –27% and –60% for the same filter strip widths. Similarly, Syversen (2005) observed a –60% to –89% reduction in total P load for 5 m and 10 m buffer zones on slopes greater than 10% in a study of the effects of buffer zones in the Nordic climate. These findings are consistent with our results, reaffirming the vital role of filter strips in mitigating sediment and nutrient loss in cold regions. Sediment load reduction by filter strips can be attributed to reduced runoff transportation capacity, which facilitates deposition, and dense vegetation, which facilitates sediment entrapment (Akan and Atabay, 2017).

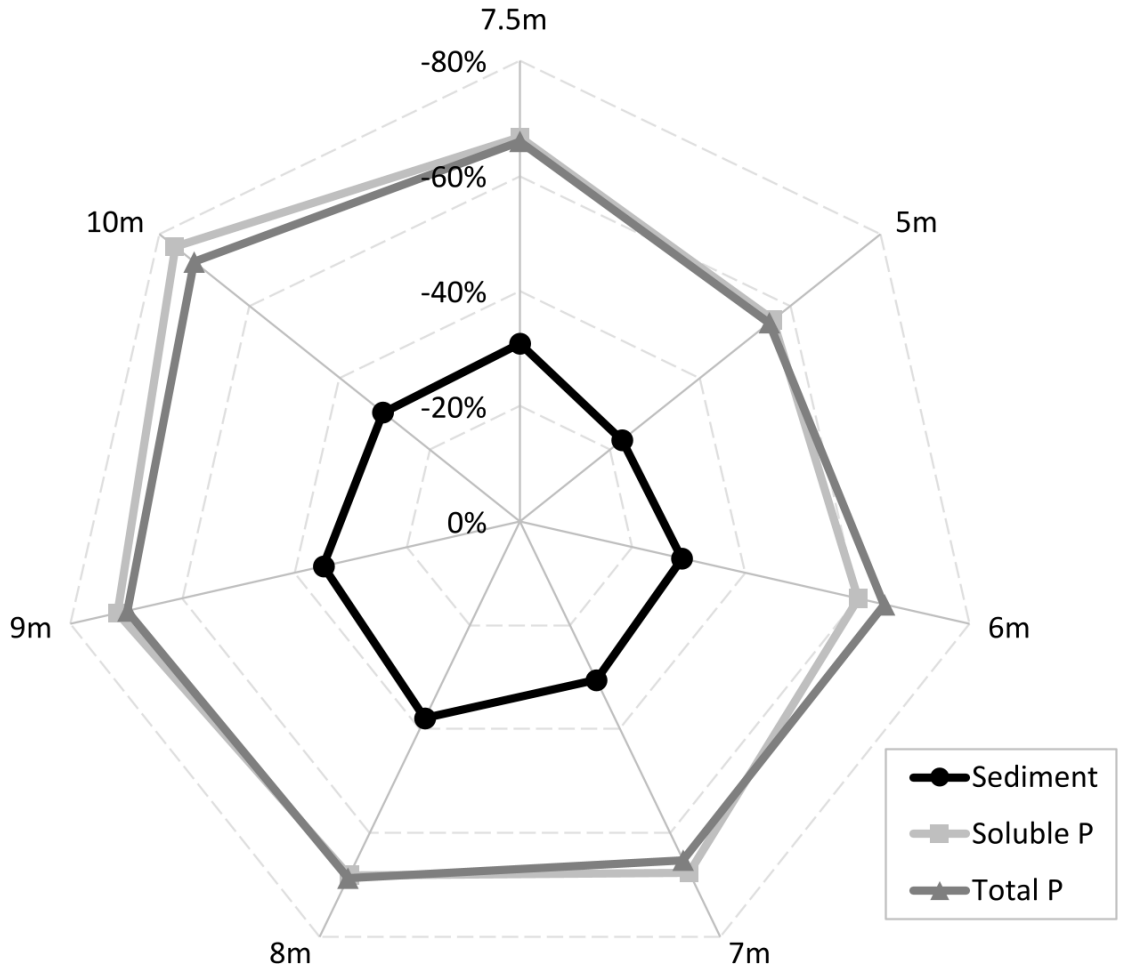

Figure 6.5: Effect of filter strip width variation (from 5 m to 10 m) on the average annual sediment, soluble phosphorus, and total phosphorus reduction.

Sedimentation ponds reduced sediment, soluble P, and total P loads by –35%, –36%, and –50%, respectively. However, these reduction rates were lower compared to some previous findings of –58% (Zhang and Zhang, 2011), –54% (Fiener *et al.*, 2005), and –80% (Markle *et al.*, 2011). The observed different reduction rates could be attributed to various factors, including the size and location of the ponds within the catchment, soil type, and agricultural management practices in the specific catchments, among many others. The flow retention time in the sedimentation pond also plays a crucial role in sediment and nutrient reduction, with shorter durations hindering the adsorption of dissolved and fine particles (Budd *et al.*, 2009; Fiener *et al.*, 2005). It's important to note that if sedimentation ponds are not well maintained and emptied of the settled material, they could become a potential source of legacy phosphorous (Engebretsen *et al.*, 2019).

The effectiveness of grassed waterways and no-tillage in sediment and nutrient removal was not statistically significant (Table 6.4). Grassed waterways reduced sediment and total P loads by −14% and −5%, respectively, but increased soluble P by +4%. Grassed waterways are designed to slow flow velocity and retain sediment-laden runoff, allowing sediments to settle and reducing load. They primarily target sediment and nutrients from surface runoff and may not effectively capture the subsurface pathways such as tile drains, which are common in the study area, hence the observed limited effectiveness. The decrease in sediment load subsequently reduced the total P load since the sediment-bound particulate P (organic P) load was settled with the sediment. However, the total P reduction was minimal due to the concurrent increase in soluble P load, although the particulate P is much greater than soluble P. The slight increase in soluble P could be attributed to potential phosphorus release via desorption since grasses may uptake nutrients and release them into the water as they decompose (Fiener and Auerswald, 2009). According to Jarvie *et al.* (2017), the increase in soluble P despite declining total P resulting from grassed waterways could be due to the gradual accumulation of legacy phosphorous that can be readily mobilized as well as the presence of tile drainage, facilitating rapid and direct runoff transmission into the stream network.

No-tillage, on the other hand, reduced soluble P by −17% but had a minimal effect on sediment and total P loads, reducing them by only −1.3% and −0.2%, respectively. The negligible effect of no-tillage on sediment and total phosphorous could be attributed to the prevalent subsurface flow in the catchment. No-tillage has been shown to be generally more effective in reducing sediment and nutrient transport in surface runoff but less effective in subsurface flows (Koskiaho *et al.*, 2002; Sun *et al.*, 2015; Tiessen *et al.*, 2010). A review of no-tillage practice on phosphorous loss control in the Scandinavian region by Ulén *et al.* (2010) showed greater soluble P losses than total P resulting from shallow tillage, which was attributed to phosphorous accumulation in the non-inverted topsoil. Furthermore, no-tillage has been reported to promote the stratification of soil phosphorous, resulting in differential effects on soluble P and total P (Jarvie *et al.*, 2017; Sharpley *et al.*, 2015; Smith *et al.*, 2015). It preserves the soil's natural structure and reduces soil disturbance during planting while retaining crop residue, which enhances nutrient retention in the soil, thereby reducing soluble P export (Bogunovic *et al.*, 2018).

6.4 Conclusion

The main findings and conclusions of this chapter are provided in Chapter 7, sections 7.1 and 7.4.

Chapter 7:

7 General Conclusion and Recommendations

This chapter summarizes the key findings and conclusions from this dissertation and suggests some future research prospects.

7.1 Conclusion on the SWAT model application in northern Spain and southeastern Sweden

The application of the SWAT model in this research demonstrated its robust capabilities in analyzing the effects of agricultural activities and climate change on water quality at the catchment scale in cultivated lands of northern Spain and southeastern Sweden, with diverse hydrological, climatic, and geographical contexts. In the Cidacos River watershed of northern Spain, the SWAT model's statistical evaluation results during calibration (2000-2010) and validation (2011-2020) periods exhibited good performances with high NSE values of 0.82 and 0.83 for streamflow and 0.71 and 0.68 for nitrate load, indicating its suitability for adoption in the area. The statistical evaluation results during calibration (2005-2012) and validation (2013-2020) periods in the C6 catchment were deemed satisfactory with NSE values of 0.80 and 0.84 for streamflow, 0.67 and 0.69 for sediment load, and 0.61 and 0.62 for total phosphorous load.

These findings highlight the SWAT model's potential as a valuable decision-support tool for watershed management and policy development. The model's ability to reproduce the magnitude and temporal dynamics of the observed data despite the inherent uncertainties demonstrates its capacity to comprehend the complex dynamics between agricultural activities and water quality. These findings demonstrate the SWAT model's potential in guiding sustainable land use practices, optimizing fertilizer application strategies, and designing effective land and water conservation measures. Furthermore, the results emphasize the importance of employing modeling approaches to support evidence-based water resource management and environmental protection strategies in cultivated regions, ultimately enhancing agricultural sustainability.

7.2 Conclusion on the evaluation of the impact of changing from rainfed to irrigated agriculture in the Cidacos River watershed in northern Spain

This study examined the impact of changing from rainfed to irrigated agriculture on streamflow, nitrate load, and nitrate concentration in a Mediterranean watershed in northern Spain by simulating the rainfed conditions using the SWAT model and compared them to the current post-irrigation period. The results indicate a significant increase in the annual streamflow, nitrate load, and concentration at the watershed outlet in the post-

irrigation period. Higher irrigation impact was observed during summer and autumn when irrigation peaked than in winter and spring. The increase in streamflow was explained by additional water from irrigation, whereas the increase in nitrate export and concentration was attributed to increased fertilization from the cultivation of high nitrogen-consuming crops and more available water to mobilize nitrates. The implementation of irrigation and subsequent agricultural intensification resulted in changing cropping patterns and doubling nitrate concentrations at the outlet, exceeding the Nitrate Directive thresholds recommended by the European Commission. Therefore, nitrate minimization practices such as efficient nitrogen fertilizer application and creating nitrogen buffer zones along the river's riparian zone should be considered to control nitrate exportation and pollution from cultivated lands into the river. Despite this study's valuable and significant findings, more data are needed to further analyze and assess the impact of irrigation, especially during summer and autumn, which was modified following irrigation. The methodology and findings from this study can be applied to other areas with similar conditions, allowing a more comprehensive assessment of the effect of changing from rainfed to irrigated agriculture on streamflow and nitrate pollution. These findings could assist farmers, water experts, and policy/decision makers in improving water resources management at the watershed level and be useful in guiding the development of new irrigation systems, thereby improving sustainable agriculture.

7.3 Conclusion on the effects of climate change on streamflow and nitrate pollution in the Cidacos River watershed in northern Spain

The effect of climate change on water resources and nitrate export is of major concern in the Mediterranean region and northern Spain due to its arid and semi-arid climatic conditions. This study evaluated the adoption of the SWAT model for simulating current and future streamflow and nitrate loads under rainfed conditions in a Mediterranean agricultural area in northern Spain. The projected decline in precipitation and rise in temperature negatively impact both the streamflow and nitrate export on spatial and temporal scales. Reduced streamflow would reduce available water resources for agricultural and domestic use, resulting in lower agricultural yield, limited productivity, and conflicts over scarce water resources. Although the projected nitrate load would also decrease due to declining streamflow, the nitrate concentration levels are expected to rise due to the faster streamflow reduction rate than the nitrate load exportation rate, resulting

in nitrate pollution by accumulation in the soil and riverbed as well as groundwater pollution through percolation.

This study's findings could help understand the scope of the climate change problem in northern Spain and develop appropriate adaptation and mitigation measures to help minimize the expected adverse effects. These measures could include more sustainable water resource management and better land management policies such as efficient nitrogen fertilization. These initiatives would be critical to adhere to the European Union's nitrate policies and legislation, as outlined in the Water Framework Directive and the Nitrate Directive. Despite this study's valuable findings, further research using various climate models, ensembles, and other emission scenarios is needed to evaluate these impacts fully. More research could be done to help understand the scope and magnitude of the uncertainties by combining future climate, projected land uses, and population changes.

7.4 Conclusion on quantifying agricultural best management practices impacts on sediment and phosphorous export in Catchment C6 in southeastern Sweden.

This study used the SWAT model to analyze the effectiveness of four BMPs (filter strip, sedimentation ponds, grassed waterways, and no-tillage) in reducing sediment and phosphorous export in a small agricultural intensive catchment in Sweden. Filter strips and sedimentation ponds effectively reduced sediment and phosphorous export. Filter strips were more effective in minimizing phosphorous losses, whereas sedimentation ponds were quite effective in minimizing sediment losses. Grassed waterways and no-tillage were less effective in pollutant reduction, with a slight increment in soluble P observed for grassed waterways. These results provide valuable insights for agricultural water management not only in the study area but also in Sweden and other regions globally facing similar water quality issues from agricultural activities.

The findings from this study contribute to the ongoing efforts to mitigate sediment and nutrient pollution in Swedish agricultural areas, thereby supporting the conservation and restoration of aquatic ecosystems. These results are instrumental in attaining the Swedish Environmental Protection Agency's targets of lowering sediment and nutrient levels in watercourses and contributing to achieving the European Water Framework Directives' goal of "good ecological status" by 2027 and ultimately zero eutrophication someday. However, further research is necessary using field experiments and other water quality

models in the catchment to corroborate these findings and enhance the efficacy of BMPs in water quality management and pollution reduction. Researchers around the world could adopt this study's methodology and results as a reference for similar studies in different regions. By sharing results and experiences, countries facing similar environmental challenges can work together to develop best practices and solutions. This research contributes to the knowledge base and guides decision-making processes for sustainable agriculture and water resource management at the local, national, regional, and international levels.

7.5 Final remarks

This research has contributed to the body of knowledge on sustainable agricultural practices and water resource management by demonstrating the SWAT model's applicability in diverse geographical and climatic conditions. The findings have the potential to inform evidence-based decision-making, policy formulation, and agricultural practices not only in the studied regions but also in other similar areas globally facing similar challenges.

The research has emphasized the necessity for effective nutrient management practices, particularly in irrigated areas of northern Spain and the Mediterranean region at large, to help reduce nitrate pollution and adhere to the recommended water quality standards. There is an urgent need to address the looming climate change-related concerns by implementing adaptative strategies, such as optimized water resource management and efficient nitrogen fertilization, to mitigate the potential negative climate change effects on water availability and quality. This research has reaffirmed the importance of agricultural conservation measures in minimizing sediment and nutrient export to enhance agricultural sustainability.

The application of the SWAT model in the case studies has produced valuable insights into the complex interactions between agricultural activities and water quality, thereby offering practical guidance for sustainable land and water resources management. The research findings could be useful to farmers, decision- and policy-makers, as well as researchers aiming to enhance agricultural sustainability and protect water resources.

Furthermore, this research recommends the continued exploration into other BMPs and their combinations besides those examined in this study to further understand their effectiveness. Future research is also recommended into the scenarios of water use or

demand and the integration of holistic strategies to ensure a harmonious balance between agricultural productivity and environmental management.

References

Abbaspour, K. C., Johnson, C. A., & van Genuchten, M. T. (2004). Estimating uncertain flow and transport parameters using a Sequential Uncertainty Fitting procedure. *Vadose Zone Journal*, *3*(4). https://doi.org/10.2136/vzj2004.1340

Abbaspour, Karim C., Yang, J., Maximov, I., Siber, R., Bogner, K., Mieleitner, J., Zobrist, J., & Srinivasan, R. (2007). Modelling hydrology and water quality in the pre-alpine/alpine Thur watershed using SWAT. *Journal of Hydrology*, *333*, 413–430. https://doi.org/10.1016/j.jhydrol.2006.09.014

Abbaspour, Karim C. (2015). SWAT-CUP: SWAT-Calibration and Uncertainty Programs (CUP) - A user manual. In *EAWAG Aquatic Research*. EAWAG Swiss Federal Institute of Aquatic Science and Technology. https://swat.tamu.edu/media/114860/usermanual_swatcup.pdf

Abbaspour, Karim C, Rouholahnejad, E., Vaghefi, S., Srinivasan, R., Yang, H., & Kløve, B. (2015). A continental-scale hydrology and water quality model for Europe: Calibration and uncertainty of a high-resolution large-scale SWAT model. *Journal of Hydrology*, *524*, 733–752. https://doi.org/10.1016/j.jhydrol.2015.03.027

Abbaspour, Karim C, Vaghefi, S. A., & Srinivasan, R. (2018). A guideline for successful calibration and uncertainty analysis for soil and water assessment: A review of papers from the 2016 international SWAT conference. *Water*, *10*(6), 1–18. https://doi.org/10.3390/w10010006

Abd-Elmabod, S. K., Muñoz-Rojas, M., Jordán, A., Anaya-Romero, M., Phillips, J. D., Laurence, J., Zhang, Z., Pereira, P., Fleskens, L., van der Ploeg, M., & de la Rosa, D. (2020). Climate change impacts on agricultural suitability and yield reduction in a Mediterranean region. *Geoderma*, *374*(114453), 1–14. https://doi.org/10.1016/j.geoderma.2020.114453

AdapteCCa. (2021). *Platform on Adaptation to Climate Change in Spain*. Spanish Climate Change Office (OECC) and the Biodiversity Foundation (FB). https://escenarios.adaptecca.es/

Akan, A. O., & Atabay, S. (2017). Grass filter strip residence time-trap efficiency relationship. *Water and Environment Journal*, *31*, 277–283. https://doi.org/10.1111/wej.12240

Al-Mukhtar, M., & Qasim, M. (2019). Future predictions of precipitation and temperature

in Iraq using the statistical downscaling model. *Arabian Journal of Geosciences*, *12*(2). https://doi.org/10.1007/s12517-018-4187-x

Allen, R. (2005). Penman – Monteith equation. *Encyclopedia of Soils in the Environment*, 180–188. https://doi.org/10.1016/B0-12-348530-4/00399-4

Almagro, M., de Vente, J., Boix-Fayos, C., García-Franco, N., Melgares de Aguilar, J., González, D., Solé-Benet, A., & Martínez-Mena, M. (2016). Sustainable land management practices as providers of several ecosystem services under rainfed Mediterranean agroecosystems. *Mitigation and Adaptation Strategies for Global Change*, *21*(7). https://doi.org/10.1007/s11027-013-9535-2

Almeida, A. M., Martins, M. J., Campagnolo, M. L., Fernandez, P., Albuquerque, T., Gerassis, S., Gonçalves, J. C., & Ribeiro, M. M. (2022). Prediction scenarios of past, present, and future environmental suitability for the Mediterranean species Arbutus unedo L. *Scientific Reports*, *12*(84), 1–15. https://doi.org/10.1038/s41598-021-03996-0

Anand, V., & Oinam, B. (2019). Future climate change impact on hydrological regime of river basin using SWAT model. *Global Journal of Environmental Science and Management*, *5*(4), 471–484. https://doi.org/10.22034/gjesm.2019.04.07

Andrés, R., & Cuchí, J. A. (2014a). Salt and nitrate exports from the sprinkler-irrigated Malfarás creek watershed (Ebro River Valley, Spain) during 2010. *Environmental Earth Sciences*, *72*(7), 2667–2682. https://doi.org/10.1007/s12665-014-3174-0

Andrés, R., & Cuchí, J. A. (2014b). Analysis of sprinkler irrigation management in the LASESA District, Monegros (Spain). *Agricultural Water Management*, *131*, 95–107. https://doi.org/10.1016/J.AGWAT.2013.09.016

Arabi, M., Frankenberger, J. R., Engel, B. A., & Arnold, J. G. (2008). Representation of agricultural conservation practices with SWAT. *Hydrological Processes*, *22*, 3042–3055. https://doi.org/10.1002/hyp.6890

Arabi, M., Govindaraju, R. S., Hantush, M. M., & Engel, B. A. (2006). Role of watershed subdivision on modeling the effectiveness of best management practices with SWAT. *Journal of the American Water Resources Association*, *42*(2), 513–528. https://doi.org/10.1111/J.1752-1688.2006.TB03854.X

Arauzo, M., Valladolid, M., & Martínez-Bastida, J. J. (2011). Spatio-temporal dynamics of nitrogen in river-alluvial aquifer systems affected by diffuse pollution from agricultural sources: Implications for the implementation of the Nitrate Directive. *Journal of Hydrology*, *411*, 155–168. https://doi.org/10.1016/j.jhydrol.2011.10.004

Arheimer, B., Löwgren, M., Pers, B. C., & Rosberg, J. (2005). Integrated catchment modeling for nutrient reduction: Scenarios showing impacts, potential, and cost of measures. *Ambio*, *34*(7), 513–520. https://doi.org/10.1579/0044-7447-34.7.513

Arnold, J. G., Kiniry, J. R., Srinivasan, R., Williams, J. R., Haney, E. B., & Neitsch, S. L. (2012). *Input/Output documentation Soil & Water Assessment Tool, version 2012*. Texas Water Resources Insitute, TR-439. https://swat.tamu.edu/media/69296/swat-io-documentation-2012.pdf

Arnold, J. G., Moriasi, D. N., Gassman, P. W., Abbaspour, K. C., White, M. J., Srinivasan, R., Santhi, C., Harmel, R. D., Van Griensven, A., Van Liew, M. W., Kannan, N., & Jha, M. K. (2012). SWAT: Model use, calibration, and validation. *Transactions of the ASABE*, *55*(4), 1491–1508. https://doi.org/10.13031/2013.42256

Arora, N. K. (2019). Impact of climate change on agriculture production and its sustainable solutions. *Environmental Sustainability*, *2*, 95–96. https://doi.org/10.1007/s42398-019-00078-w

Barredo, J. I., Caudullo, J. I., & Mauri, G. (2017). Mediterranean habitat loss under RCP4.5 and RCP8.5 climate change projections. In *European Commision; JRC Technical Reports*. https://doi.org/10.2760/622174

Barros, R., Isidoro, D., & Aragüés, R. (2012). Irrigation management, nitrogen fertilization, and nitrogen losses in the return flows of La Violada irrigation district (Spain). *Agriculture, Ecosystems and Environment*, *155*, 161–171. https://doi.org/10.1016/j.agee.2012.04.004

Beaudoin, N., Saad, J. K., Van Laethem, C., Machet, J. M., Maucorps, J., & Mary, B. (2005). Nitrate leaching in intensive agriculture in Northern France: Effect of farming practices, soils, and crop rotations. *Agriculture, Ecosystems & Environment*, *111*, 292–310. https://doi.org/10.1016/j.agee.2005.06.006

Bekarias, I. G., Panagopoulos, I. N., & Mimikou, M. A. (2005). Application of the SWAT (Soil and Water Assessment Tool) model in the Ronnea catchment of Sweden.

Global NEST Journal, *7*(3), 252–257. https://doi.org/10.30955/gnj.000343

Boardman, J., & Poesen, J. (2006). Soil erosion in Europe. In *John Wiley & Sons, Ltd*. British Library. https://doi.org/10.1002/0470859202

Boezeman, D., Wiering, M., & Crabbé, A. (2020). Agricultural diffuse pollution and the EU water framework directive: Problems and progress in governance. *Water*, *12*(9), 1–7. https://doi.org/10.3390/W12092590

Bogunovic, I., Pereira, P., Kisic, I., Sajko, K., & Sraka, M. (2018). Tillage management impacts on soil compaction, erosion and crop yield in Stagnosols (Croatia). *Catena*, *160*, 376–384. https://doi.org/10.1016/j.catena.2017.10.009

Boithias, L., Srinivasan, R., Sauvage, S., Macary, F., & Sánchez-Pérez, J. M. (2014). Daily nitrate losses: Implication on long-term river quality in an intensive agricultural catchment of Southwestern France. *Journal of Environmental Quality*, *43*, 1–10. https://doi.org/10.2134/jeq2011.0367

Bracmort, K. S., Arabi, M., Frankenberger, J. R., Engel, B. A., & Arnold, J. G. (2006). Modeling long-term water quality impact of structural BMPs. *Transactions of the ASABE*, *49*(2), 367–374. https://doi.org/10.13031/2013.20411

Budd, R., O'Geen, A., Goh, K. S., Bondarenko, S., & Gan, J. (2009). Efficacy of constructed wetlands in pesticide removal from tailwaters in the central valley, California. *Environmental Science and Technology*, *43*(8), 2925–2930. https://doi.org/10.1021/es802958q

Cameron, K. C., Di, H. J., & Moir, J. L. (2013). Nitrogen losses from the soil/plant system: A review. In *Annals of Applied Biology* (Vol. 162, pp. 145–173). https://doi.org/10.1111/aab.12014

Candela, L., Tamoh, K., Olivares, G., & Gomez, M. (2012). Modelling impacts of climate change on water resources in ungauged and data-scarce watersheds. Application to the Siurana catchment (NE Spain). *Science of The Total Environment*, *440*, 253–260. https://doi.org/10.1016/j.scitotenv.2012.06.062

Carpenter, S. R., Caraco, N. F., Correll, D. L., Howarth, R. W., Sharpley, A. N., & Smith, V. H. (1998). Nonpoint pollution of surface waters with phosphorus and nitrogen. *Ecological Applications*, *8*(3), 559–568. https://doi.org/10.1890/1051-

0761(1998)008[0559:NPOSWW]2.0.CO;2

Carvalho-Santos, C., Nunes, J. P., Monteiro, A. T., Hein, L., & Honrado, J. P. (2016). Assessing the effects of land cover and future climate conditions on the provision of hydrological services in a medium-sized watershed of Portugal. *Hydrological Processes*, *30*(5), 720–738. https://doi.org/10.1002/hyp.10621

Casalí, J., Gastesi, R., Álvarez-Mozos, J., De Santisteban, L. M., Lersundi, J. D. V. de, Giménez, R., Larrañaga, A., Goñi, M., Agirre, U., Campo, M. A., López, J. J., & Donézar, M. (2008). Runoff, erosion, and water quality of agricultural watersheds in central Navarre (Spain). *Agricultural Water Management*, *95*(10), 1111–1128. https://doi.org/10.1016/j.agwat.2008.06.013

Causapé, J., Quílez, D., & Aragüés, R. (2004). Assessment of irrigation and environmental quality at the hydrological basin level II. Salt and nitrate loads in irrigation return flows. *Agricultural Water Management*, *70*(3), 211–228. https://doi.org/10.1016/j.agwat.2004.06.006

Cavero, J., Beltrán, A., & Aragüés, R. (2003). Nitrate exported in drainage waters of two sprinkler-irrigated watersheds. *Journal of Environmental Quality*, *32*, 916–926. https://doi.org/10.2134/jeq2003.9160

Cerro, I., Antigüedad, I., Srinivasan, R., Sauvage, S., Volk, M., & Sanchez-Perez, J. M. (2014). Simulating land management options to reduce nitrate pollution in an agricultural watershed dominated by an alluvial aquifer. *Journal of Environmental Quality*, *43*, 67–74. https://doi.org/10.2134/jeq2011.0393

Chahor, Y., Casalí, J., Giménez, R., Bingner, R. L., Campo, M. A., & Goñi, M. (2014). Evaluation of the AnnAGNPS model for predicting runoff and sediment yield in a small Mediterranean agricultural watershed in Navarre (Spain). *Agricultural Water Management*, *134*, 24–37. https://doi.org/10.1016/j.agwat.2013.11.014

Chaubey, I., Migliaccio, K. W., Green, C. H., Arnold, J. G., & Srinivasan, R. (2006). Phosphorus modeling in soil and water assessment tool (SWAT) model. In *Modeling Phosphorus in the Environment* (pp. 163–187). USDA-ARS. https://doi.org/10.1201/9781420005417.sec2

CHE (Confederación Hidrográfica del Ebro). (2006). *Control de los retornos de las actividades agrarias de la cuenca del Ebro: Evaluación de tendencias en la calidad*

del agua, control experimental de los retornos y propuesta de red de control (in Spanish). www.chebro.es

Chirivella Osma, V., Capilla Romá, J. E., & Pérez Martín, M. A. (2015). Modelling regional impacts of climate change on water resources: The Júcar Basin, Spain. *Hydrological Sciences Journal*, *60*(1), 30–49. https://doi.org/10.1080/02626667.2013.866711

Cho, J., Lowrance, R. R., Bosch, D. D., Strickland, T. C., Her, Y., & Vellidis, G. (2010). Effect of watershed subdivision and filter width on SWAT simulation of a coastal plain watershed. *Journal of the American Water Resources Association*, *46*(3), 586–602. https://doi.org/10.1111/j.1752-1688.2010.00436.x

Conley, D. J., Carstensen, J., Aigars, J., Axe, P., Bonsdorff, E., Eremina, T., Haahti, B. M., Humborg, C., Jonsson, P., Kotta, J., Lännegren, C., Larsson, U., Maximov, A., Medina, M. R., Lysiak-Pastuszak, E., Remeikaitè-Nikienè, N., Walve, J., Wilhelms, S., & Zillén, L. (2011). Hypoxia is increasing in the coastal zone of the baltic sea. *Environmental Science and Technology*, *45*, 6777–6783. https://doi.org/10.1021/es201212r

Crovella, T., Paiano, A., & Lagioia, G. (2022). A meso-level water use assessment in the Mediterranean agriculture. Multiple applications of water footprint for some traditional crops. *Journal of Cleaner Production*, *330*, 1–14. https://doi.org/10.1016/j.jclepro.2021.129886

DDRMAAL. (2021). *Estadísticas agrícolas. Negociado de Estadística*. Departamento de Desarrollo Rural, Medio Ambiente y Administración Local–Gobierno de Navarra. http://www.navarra.es/home_es/Temas/Ambito+rural/Indicadores/agricultura.htm

Dodds, W. K., & Smith, V. H. (2016). Nitrogen, phosphorus, and eutrophication in streams. *Inland Waters*, *6*(2), 155–162. https://doi.org/10.5268/IW-6.2.909

Donmez, C., Sari, O., Berberoglu, S., Cilek, A., Satir, O., & Volk, M. (2020). Improving the applicability of the SWAT model to simulate flow and nitrate dynamics in a flat data-scarce agricultural region in the Mediterranean. *Water*, *12*(3479), 1–24. https://doi.org/10.3390/w12123479

Dosskey, M. G., Helmers, M. J., & Eisenhauer, D. E. (2008). A design aid for determining width of filter strips. *Journal of Soil and Water Conservation*, *63*(4), 232–241.

https://doi.org/10.2489/jswc.63.4.232

Duarte, R., Pinilla, V., & Serrano, A. (2021). The globalization of Mediterranean agriculture: A long-term view of the impact on water consumption. *Ecological Economics*, *183*, 1–12. https://doi.org/10.1016/j.ecolecon.2021.106964

Dubrovsky, N. M., Burow, K. R., Clark, G. M., Gronberg, J. A. M., Hamilton, P. A., Hitt, K. J., Mueller, D. K., Munn, M. D., Nolan, B. T., Puckett, L. J., Rupert, M. G., Short, T. M., Spahr, N. E., Sprague, L. A., & Wilber, W. G. (2010). The quality of our Nation's waters-nutrients in the Nation 's streams and groundwater, 1992 – 2004. In *U.S. Geological Survey Circular 1350*.

Duncan, R. A., Bethune, M. G., Thayalakumaran, T., Christen, E. W., & McMahon, T. A. (2008). Management of salt mobilisation in the irrigated landscape - A review of selected irrigation regions. In *Journal of Hydrology* (Vol. 351, Issues 1–2). https://doi.org/10.1016/j.jhydrol.2007.12.002

Ekstrand, S., Wallenberg, P., & Djodjic, F. (2010). Process based modelling of phosphorus losses from arable land. *Ambio*, *39*(2), 100–115. https://doi.org/10.1007/s13280-010-0016-5

Engebretsen, A., Vogt, R. D., & Bechmann, M. (2019). SWAT model uncertainties and cumulative probability for decreased phosphorus loading by agricultural Best Management Practices. *Catena*, *175*, 154–166. https://doi.org/10.1016/j.catena.2018.12.004

Epelde, A. M., Cerro, I., Sánchez-Pérez, J. M., Sauvage, S., Srinivasan, R., & Antigüedad, I. (2015). Application of the SWAT model to assess the impact of changes in agricultural management practices on water quality. *Hydrological Sciences Journal*, *60*(5), 825–843. https://doi.org/10.1080/02626667.2014.967692

Estrela, T., Perez-Martin, M. a, & Vargas, E. (2012). Impacts of climate change on water resources in Spain. *Hydrological Sciences Journal-Journal Des Sciences Hydrologiques*, *57*(6), 1154–1167. https://doi.org/10.1080/02626667.2012.702213

European Communities. (1991). Council Directive of 12 December 1991 concerning the protection of waters against pollution caused by nitrate from agricultural sources (91/676/EEC). In *Official Journal of the European Communities* (91/676/EEC; Vol. 375). https://ec.europa.eu/environment/water/water-nitrates/index_en.html

European Communities. (2000). Directive 2000/60/EC of the European Parliament and the Council of 23 October 2000 establishing a framework for community action in the field of water policy. In *Official Journal of the European Commission* (2000/60/EC; Vol. 327). https://eur-lex.europa.eu/resource.html?uri=cellar:5c835afb-2ec6-4577-bdf8-756d3d694eeb.0004.02/DOC_1&format=PDF

European Environment Agency (EEA). (2005). Source apportionment of nitrogen and phosphorus inputs into the aquatic environment. In *European Environment Agency* (Issue EEA Report No7/2005). http://www.eea.europa.eu/publications/eea_report_2005_7

European Environment Agency (EEA). (2017). *Climate Change, impacts and vulnerability in Europe 2016. An indicator-based report. EEA Report No1/2017*. https://doi.org/10.2800/534806

European Environment Agency (EEA). (2020). Is Europe living within the limits of our planet? An assessment of Europe's environmental footprints in relation to planetary boundaries. In *EEA Report No. 01/2020* (Issue 01). https://doi.org/10.2800/890673

European Environment Agency (EEA). (2021). Water and agriculture: towards sustainable solutions. In *EEA Report No. 17/2020* (Issue 17). https://doi.org/10.2800/73735

European Environment Agency (EEA). (2022). *Zero pollution monitoring assessment 2022. Cross-cutting story 4: Nutrients*. EEA Web Report No. 03/2022. https://doi.org/10.2800/515047

European Parliamentary Research Service (EPRS). (2019). Irrigation in EU agriculture. In *Think Tank European Parliament* (Issue December). https://www.europarl.europa.eu/RegData/etudes/BRIE/2019/644216/EPRS_BRI(2019)644216_EN.pdf

Evrard, O., Persoons, E., Vandaele, K., & van Wesemael, B. (2007). Effectiveness of erosion mitigation measures to prevent muddy floods: A case study in the Belgian loam belt. *Agriculture, Ecosystems & Environment*, *118*(1–4), 149–158. https://doi.org/10.1016/j.agee.2006.02.019

Exbrayat, J. F., Viney, N. R., Seibert, J., Wrede, S., Frede, H. G., & Breuer, L. (2010).

Ensemble modelling of nitrogen fluxes: Data fusion for a Swedish meso-scale catchment. *Hydrology and Earth System Sciences*, *14*(12), 238.3-2397. https://doi.org/10.5194/hess-14-2383-2010

FAO. (2017a). *The future of food and agriculture - Trends and challenges* (Vol. 1). FAO. http://www.fao.org/3/i6583e/i6583e.pdf

FAO. (2017b). Water for sustainable food and agriculture: A report produced for the G20 Presidency of Germany. In *Food and Agriculture Organization of the United Nations*. https://www.fao.org/3/i7959e/i7959e.pdf

FAO. (2022). The State of the World's Land and Water Resources for Food and Agriculture 2021 – Systems at breaking point. In *Main Report*. Food and Agriculture Organization (FAO) of the United Nations. https://doi.org/10.4060/cb9910en

Faramarzi, M., Abbaspour, K. C., Schulin, R., & Yang, H. (2009). Modelling blue and green water resources availability in Iran. *Hydrological Processes*, *23*(3), 486–501. https://doi.org/10.1002/hyp.7160

Farzin, H., & Grogan, K. (2008). California water quality: The role of agriculture. In *Agricultural and Resource Economics Update* (Vol. 11, Issue 6, pp. 8–11). University of California Giannini Foundation of Agricultural Economics.

Ferrant, S., Oehler, F., Durand, P., Ruiz, L., Salmon-Monviola, J., Justes, E., Dugast, P., Probst, A., Probst, J. L., & Sanchez-Perez, J. M. (2011). Understanding nitrogen transfer dynamics in a small agricultural catchment: Comparison of a distributed (TNT2) and a semi distributed (SWAT) modeling approaches. *Journal of Hydrology*, *406*, 1–15. https://doi.org/10.1016/j.jhydrol.2011.05.026

Feyen, L., Ciascar, J., Gosling, S., Ibarreta, D., Soria, A., Dosio, A., Naumann, G., Russo, S., Formetta, G., Forzieri, G., Girardello, M., Spinoni, J., Mentaschi, L., Bisselink, B., Bernhard, J., Gelati, E., Adamovic, M., Guenther, S., de Roo, A., … Olariaga, M. (2020). Climate change impacts and adaptation in Europe: JRC Science for policy report. JRC PESETA IV final report. In *Publications Office of the European Union*. https://doi.org/10.2760/171121

Ficklin, D. L., Luo, Y., Luedeling, E., Gatzke, S. E., & Zhang, M. (2010). Sensitivity of agricultural runoff loads to rising levels of CO2 and climate change in the San Joaquin Valley watershed of California. *Environmental Pollution*, *158*(1), 223–234.

https://doi.org/10.1016/j.envpol.2009.07.016

Ficklin, D. L., Luo, Y., & Zhang, M. (2012). Watershed modelling of hydrology and water quality in the Sacramento River watershed, California. *Hydrological Processes*, *27*, 1–15. https://doi.org/10.1002/hyp.9222

Ficklin, D. L., Stewart, I. T., & Maurer, E. P. (2013). Effects of projected climate change on the hydrology in the Mono Lake Basin, California. *Climatic Change*, *116*(1), 1–21. https://doi.org/10.1007/s10584-012-0566-6

Fiener, P., & Auerswald, K. (2009). Effects of hydrodynamically rough grassed waterways on dissolved reactive phosphorus loads coming from agricultural watersheds. *Journal of Environmental Quality*, *38*(2), 548–559. https://doi.org/10.2134/jeq2007.0525

Fiener, P., Auerswald, K., & Weigand, S. (2005). Managing erosion and water quality in agricultural watersheds by small detention ponds. *Agriculture, Ecosystems & Environment*, *110*, 132–142. https://doi.org/10.1016/j.agee.2005.03.012

Fonseca, A. R., & Santos, J. A. (2019). Predicting hydrologic flows under climate change: The Tâmega Basin as an analog for the Mediterranean region. *Science of The Total Environment*, *668*, 1013–1024. https://doi.org/10.1016/j.scitotenv.2019.01.435

Funes, I., Aranda, X., Biel, C., Carbó, J., Camps, F., Molina, A. J., de Herralde, F., Grau, B., & Savé, R. (2016). Future climate change impacts on apple flowering date in a Mediterranean subbasin. *Agricultural Water Management*, *164*, 19–27. https://doi.org/10.1016/j.agwat.2015.06.013

Galloway, J. N., Townsend, A. R., Erisman, J. W., Bekunda, M., Cai, Z., Freney, J. R., Martinelli, L. A., Seitzinger, S. P., & Sutton, M. A. (2008). Transformation of the nitrogen cycle: Recent trends, questions, and potential solutions. *Science*, *320*(5878), 889–892. https://doi.org/10.1126/science.1136674

García-Garizábal, I., Causapé, J., & Abrahao, R. (2011). Application of the irrigation land environmental evaluation tool for flood irrigation management and evaluation of water use. *CATENA*, *87*(2), 260–267. https://doi.org/10.1016/J.CATENA.2011.06.010

García-Garizábal, I., Causapé, J., & Abrahao, R. (2012). Nitrate contamination and its

relationship with flood irrigation management. *Journal of Hydrology*, *442–443*, 15–22. https://doi.org/10.1016/j.jhydrol.2012.03.017

García-Garizábal, I., Causapé, J., & Merchán, D. (2017). Evaluation of alternatives for flood irrigation and water usage in Spain under Mediterranean climate. *CATENA*, *155*, 127–134. https://doi.org/10.1016/J.CATENA.2017.02.019

Gill, M. A. (1978). Flood routing by the Muskingum method. *Journal of Hydrology*, *36*(3–4), 353–363. https://doi.org/10.1016/0022-1694(78)90153-1

Giménez, R., Casalí, J., Grande, I., Díez, J., Campo-Bescós, M. A., Álvarez-Mozos, J., & Goñi, M. (2012). Factors controlling sediment export in a small agricultural watershed in Navarre (Spain). *Agricultural Water Management*, *110*, 1–8. https://doi.org/10.1016/j.agwat.2012.03.007

Giorgi, F., & Lionello, P. (2008). Climate change projections for the Mediterranean region. *Global and Planetary Change*, *63*, 90–104. https://doi.org/10.1016/J.GLOPLACHA.2007.09.005

Gitau, M. W., Gburek, W. J., & Bishop, P. L. (2008). Use of the SWAT model to quantify water quality effects of agricultural BMPs at the farm-scale level. *Transactions of the ASABE*, *51*(6), 1925–1936. https://doi.org/10.13031/2013.25398

Government of Navarre. (2022). *Description of the Navarre Canal*. Canal de Navarra, SA (CANASA). https://www.canasa.es/proyecto/descripcion-canal-de-navarra

Green, C. H., & van Griensven, A. (2008). Autocalibration in hydrologic modeling: Using SWAT2005 in small-scale watersheds. *Environmental Modelling and Software*, *23*(4), 422–434. https://doi.org/10.1016/j.envsoft.2007.06.002

Green, W. H., & Ampt, G. A. (1911). Studies on soil physics: Part 1 - The flow of air and water through soils. *Journal of Agricultural Science*, *4*(1), 1–24. https://doi.org/https://doi.org/10.1017/S0021859600001441

Grizzetti, B., Vigiak, O., Udias, A., Aloe, A., Zanni, M., Bouraoui, F., Pistocchi, A., Dorati, C., Friedland, R., De Roo, A., Benitez Sanz, C., Leip, A., & Bielza, M. (2021). How EU policies could reduce nutrient pollution in European inland and coastal waters. *Global Environmental Change*, *69*, 1–13. https://doi.org/10.1016/j.gloenvcha.2021.102281

Grusson, Y., Wesström, I., Svedberg, E., & Joel, A. (2021). Influence of climate change on water partitioning in agricultural watersheds: Examples from Sweden. *Agricultural Water Management*, *249*, 1–18. https://doi.org/10.1016/j.agwat.2021.106766

Harraki, W. El, Ouazar, D., Bouziane, A., & Harraki, I. El. (2021). Streamflow prediction upstream of a dam using SWAT and assessment of the impact of land use spatial resolution on model performance. *Environmental Processes*, *8*, 1165–1186. https://doi.org/10.1007/s40710-021-00532-0

Heinrich Böll Foundation. (2019). *Agriculture Atlas: Facts and Figures on EU Farming Policy* (1st ed.). The European Commission's LIFE Programme. https://www.arc2020.eu/wp-content/uploads/2019/05/agricultureatlas2019_web_190508-compressed.pdf#page=32

Helsel, D. R., Hirsch, R. M., Ryberg, K. R., Archfield, S. A., & Gilroy, E. J. (2020). Statistical methods in water resources: Chapter 3 of section A, statistical analysis. Book 4, Hydrologic analysis and interpretation. In U.S Department of the Interior (Ed.), *USGS science for a changing world* (version 1., pp. 1–458). US Geological Survey. https://doi.org/https://doi.org/10.3133/tm4a3

Helsinki Commission (HELCOM). (2009). Eutrophication in the Baltic Sea: An integrated thematic assessment of the effects of nutrient enrichment in the Baltic Sea region: Executive Summary. In *Baltic Sea Environment Proceedings No. 115A* (Issue 115 A).

Hernández-García, I., Merchán, D., Aranguren, I., Casalí, J., Giménez, R., Campo-Bescós, M. A., & Del Valle de Lersundi, J. (2020). Assessment of the main factors affecting the dynamics of nutrients in two rainfed cereal watersheds. *Science of the Total Environment*, *733*(3), 1–14. https://doi.org/10.1016/j.scitotenv.2020.139177

Iital, A., Klõga, M., Pihlak, M., Pachel, K., Zahharov, A., & Loigu, E. (2014). Nitrogen content and trends in agricultural catchments in Estonia. *Agriculture, Ecosystems and Environment*, *198*, 44–53. https://doi.org/10.1016/j.agee.2014.03.010

Intergovernmental Panel on Climate Change (IPCC). (2014). *Climate change impacts, adaptation, and vulnerability. Part A: Global and sectoral aspects. Working Group*

II contribution to the Fifth Assessment Report of the Intergovernmental Panel on Climate Change (C. B. Field, V. R. Barros, D. J. Dokken, K. J. Mach, M. D. Mastrandrea, T. E. Bilir, M. Chatterjee, K. L. Ebi, Y. O. Estrada, R. C. Genova, B. Girma, E. S. Kissel, A. N. Levy, S. MacCracken, P. R. Mastrandrea, & L. L. White (eds.)). Cambridge University Press. https://www.ipcc.ch/assessment-report/ar5/

INTIA. (2019). *Informe corregido del seguimiento de la zona regable del canal de Navarra durante la campaña 2018: Balance hídrico, calidad del riego y contaminación por sales y nitratos*. https://www.intiasa.es/

INTIA. (2020). *Informe del seguimiento de la zona regable del canal de Navarra durante la campaña 2019: Balance hídrico, calidad del riego y contaminación por sales y nitratos*. https://www.intiasa.es/

INTIA. (2021). *Informe del Seguimiento de la Zona Regable del Canal de Navarra durante la Campaña 2020: Balance Hídrico, Calidad del Riego y Contaminación por Sales y Nitratos*. https://www.intiasa.es/

Isidoro, D., & Aragüés, R. (2007). River water quality and irrigated agriculture in the ebro basin: An overview. In *International Journal of Water Resources Development* (Vol. 23, Issue 1). https://doi.org/10.1080/07900620601159743

IUSS Working Group WRB. (2015). World reference base for soil resources 2014: International soil classification system for naming soils and creating legends for soil maps, update 2015. In *World Soil Resources Reports No. 106* (Vol. 106). Food and Agriculture Organization (FAO) of the United Nations. https://doi.org/10.1017/S0014479706394902

Jain, C. K., & Singh, S. (2019). Best management practices for agricultural nonpoint source pollution: Policy interventions and way forward. *World Water Policy*, *5*(2), 207–228. https://doi.org/10.1002/wwp2.12015

Jarvie, H. P., Johnson, L. T., Sharpley, A. N., Smith, D. R., Baker, D. B., Bruulsema, T. W., & Confesor, R. (2017). Increased soluble phosphorus loads to Lake Erie: Unintended consequences of conservation practices? *Journal of Environmental Quality*, *46*(1), 123–132. https://doi.org/10.2134/jeq2016.07.0248

Jégo, G., Martínez, M., Antigüedad, I., Launay, M., Sanchez-Pérez, J. M., & Justes, E. (2008). Evaluation of the impact of various agricultural practices on nitrate leaching

under the root zone of potato and sugar beet using the STICS soil-crop model. *Science of the Total Environment*, *394*(2–3), 207–221. https://doi.org/10.1016/j.scitotenv.2008.01.021

Jiménez-Navarro, I. C., Jimeno-Sáez, P., López-Ballesteros, A., Pérez-Sánchez, J., & Senent-Aparicio, J. (2021). Impact of climate change on the hydrology of the forested watershed that drains to Lake Erken in Sweden: An analysis using SWAT+ and CMIP6 scenarios. *Forests*, *12*(1803), 1–21. https://doi.org/10.3390/f12121803

Jiménez-Navarro, I. C., Mesman, J. P., Pierson, D., Trolle, D., Nielsen, A., & Senent-Aparicio, J. (2023). Application of an integrated catchment-lake model approach for simulating effects of climate change on lake inputs and biogeochemistry. *Science of the Total Environment*, *885*, 1–16. https://doi.org/10.1016/j.scitotenv.2023.163946

Jimeno-Sáez, P., Senent-Aparicio, J., Pérez-Sánchez, J., & Pulido-Velazquez, D. (2018). A comparison of SWAT and ANN Models for daily runoff simulation in different climatic zones of Peninsular Spain. *Water*, *10*(192), 1–19. https://doi.org/10.3390/w10020192

Kaini, P., Artita, K., & Nicklow, J. W. (2012). Optimizing structural best management practices using SWAT and genetic algorithm to improve water quality goals. *Water Resources Management*, *26*(7), 1827–1845. https://doi.org/10.1007/S11269-012-9989-0

Kamali, B., Abbaspour, K. C., & Yang, H. (2017). Assessing the uncertainty of multiple input datasets in the prediction of water resource components. *Water*, *9*(709), 1–16. https://doi.org/10.3390/w9090709

Koskiaho, J., Kivisaari, S., Vermeulen, S., Kauppila, R., Kallio, K., & Puustinen, M. (2002). Reduced tillage: Influence on erosion and nutrient losses in a clayey field in southern Finland. *Agricultural and Food Science in Finland*, *11*(1), 37–50. https://doi.org/10.23986/afsci.5711

Kouchi, D. H., Esmaili, K., Faridhosseini, A., Sanaeinejad, S. H., Khalili, D., & Abbaspour, K. C. (2017). Sensitivity of calibrated parameters and water resource estimates on different objective functions and optimization algorithms. *Water*, *9*(6). https://doi.org/10.3390/w9060384

Krause, P., Boyle, D. P., & Bäse, F. (2005). Comparison of different efficiency criteria

for hydrological model assessment. *Advances in Geosciences*, *5*, 89–97. https://doi.org/10.5194/adgeo-5-89-2005

Krysanova, V., Vetter, T., Eisner, S., Huang, S., Pechlivanidis, I., Strauch, M., Gelfan, A., Kumar, R., Aich, V., Arheimer, B., Chamorro, A., Van Griensven, A., Kundu, D., Lobanova, A., Mishra, V., Plötner, S., Reinhardt, J., Seidou, O., Wang, X., … Hattermann, F. F. (2017). Intercomparison of regional-scale hydrological models and climate change impacts projected for 12 large river basins worldwide - a synthesis. *Environmental Research Letters*, *12*, 1–12. https://doi.org/10.1088/1748-9326/aa8359

Kyllmar, K., Bechmann, M., Blicher-Mathiesen, G., Fischer, F. K., Fölster, J., Iital, A., Lagzdiņš, A., Povilaitis, A., & Rankinen, K. (2023). Nitrogen and phosphorus losses in Nordic and Baltic agricultural monitoring catchments – Spatial and temporal variations in relation to natural conditions and mitigation programmes. *Catena*, *230*. https://doi.org/10.1016/j.catena.2023.107205

Kyllmar, K., Carlsson, C., Gustafson, A., Ulén, B., & Johnsson, H. (2006). Nutrient discharge from small agricultural catchments in Sweden: Characterisation and trends. *Agriculture, Ecosystems & Environment*, *115*(1–4), 15–26. https://doi.org/10.1016/j.agee.2005.12.004

Kyllmar, K., Forsberg, L. S., Andersson, S., & Mårtensson, K. (2014). Small agricultural monitoring catchments in Sweden representing environmental impact. *Agriculture, Ecosystems and Environment*, *198*, 25–35. https://doi.org/10.1016/j.agee.2014.05.016

Ladrera, R., Belmar, O., Tomás, R., Prat, N., & Cañedo-Argüelles, M. (2019). Agricultural impacts on streams near Nitrate Vulnerable Zones: A case study in the Ebro basin, Northern Spain. *PLoS ONE*, *14*(11), 1–17. https://doi.org/10.1371/JOURNAL.PONE.0218582

Lam, Q. D., Schmalz, B., & Fohrer, N. (2009). Ecohydrological modelling of water discharge and nitrate loads in a mesoscale lowland catchment, Germany. *Advances in Geosciences*, *21*, 45–55. https://doi.org/10.5194/adgeo-21-49-2009

Lassaletta, L., García-Gómez, H., Gimeno, B. S., & Rovira, J. V. (2010). Headwater Streams: Neglected Ecosystems in the EU Water Framework Directive. Implications

for Nitrogen Pollution Control. *Environmental Science and Policy*, *13*, 423–433. https://doi.org/10.1016/j.envsci.2010.04.005

Le Moal, M., Gascuel-Odoux, C., Ménesguen, A., Souchon, Y., Étrillard, C., Levain, A., Moatar, F., Pannard, A., Souchu, P., Lefebvre, A., & Pinay, G. (2019). Eutrophication: A new wine in an old bottle? *Science of the Total Environment*, *651*(1), 1–11. https://doi.org/10.1016/j.scitotenv.2018.09.139

Legates, D. R., & McCabe, G. J. (1999). Evaluating the use of "goodness-of-fit" measures in hydrologic and hydroclimatic model validation. *Water Resources Research*, *35*(1), 233–241. https://doi.org/10.1029/1998WR900018

Leip, A., Britz, W., Weiss, F., & De Vries, W. (2011). Farm, land, and soil nitrogen budgets for agriculture in Europe calculated with CAPRI. *Environmental Pollution*, *159*(11), 3243–3253. https://doi.org/10.1016/J.ENVPOL.2011.01.040

Lévesque, É., Anctil, F., van Griensven, A., & Beauchamp, N. (2008). Evaluation of streamflow simulation by SWAT model for two small watersheds under snowmelt and rainfall. *Hydrological Sciences Journal*, *53*(5), 961–976. https://doi.org/10.1623/hysj.53.5.961

Linefur, H., Norberg, L., Kyllmar, K., Andersson, S., & Blomberg, M. (2022). Plant nutrient losses in small agriculturally dominated catchments 2020/2021. In *Ecohydrology* (Issue 175). http://pub.epsilon.slu.se

Liu, R., Zhang, P., Wang, X., Chen, Y., & Shen, Z. (2013). Assessment of effects of best management practices on agricultural non-point source pollution in Xiangxi River watershed. *Agricultural Water Management*, *117*, 9–18. https://doi.org/10.1016/j.agwat.2012.10.018

Liu, Y., Engel, B. A., Flanagan, D. C., Gitau, M. W., McMillan, S. K., & Chaubey, I. (2017). A review on effectiveness of best management practices in improving hydrology and water quality: Needs and opportunities. In *Science of the Total Environment* (Vols. 601–602, pp. 580–593). https://doi.org/10.1016/j.scitotenv.2017.05.212

Liu, Y., Wang, R., Guo, T., Engel, B. A., Flanagan, D. C., Lee, J. G., Li, S., Pijanowski, B. C., Collingsworth, P. D., & Wallace, C. W. (2019). Evaluating efficiencies and cost-effectiveness of best management practices in improving agricultural water

quality using integrated SWAT and cost evaluation tool. *Journal of Hydrology*, *577*, 1–16. https://doi.org/10.1016/j.jhydrol.2019.123965

Lu, C. M., & Chiang, L. C. (2019). Assessment of sediment transport functions with the modified SWAT-Twn model for a Taiwanese small mountainous watershed. *Water (Switzerland)*, *11*(9). https://doi.org/10.3390/w11091749

Luz Rodríguez-Blanco, M., Mercedes Taboada-Castro, M., Arias, R., & Teresa Taboada-Castro, M. (2019). Assessing the expected impact of climate change on nitrate load in a small Atlantic agro-forested catchment. In *Climate Change and Global Warming* (pp. 11–24). https://doi.org/10.5772/intechopen.80709

Majone, B., Bovolo, C. I., Bellin, A., Blenkinsop, S., & Fowler, H. J. (2012). Modeling the impacts of future climate change on water resources for the Gallego River basin (Spain). *Water Resources Research*, *48*(1), 1–18. https://doi.org/10.1029/2011WR010985

Malmaeus, J. M., & Karlsson, O. M. (2010). Estimating costs and potentials of different methods to reduce the Swedish phosphorus load from agriculture to surface water. *Science of The Total Environment*, *408*(3), 473–479. https://doi.org/10.1016/J.SCITOTENV.2009.10.021

Mander, Ü., Kull, A., Kuusemets, V., & Tamm, T. (2000). Nutrient runoff dynamics in a rural catchment: Influence of land-use changes, climatic fluctuations and ecotechnological measures. *Ecological Engineering*, *14*, 405–417. https://doi.org/10.1016/S0925-8574(99)00064-6

MAPA. (2021). *Gestión sostenible de regadíos*. Minesterio de Agricultura, Pesca y Alimentatacion. https://www.mapa.gob.es/es/desarrollo-rural/temas/gestion-sostenible-regadios/

Markle, J. C., Watson, T. E., Prichard, T. L., & Klassen, P. (2011). Efficacy of sediment basins for reducing sediment and pyrethroid transport in almond orchards. *ACS Symposium Series*, *1075*, 51–63. https://doi.org/10.1021/bk-2011-1075.ch004

Mårtensson, K., Johnsson, H., & Kyllmar, K. (2023). Estimated nutrient leakage from arable land in different bioeconomy scenarios for two areas in central Sweden, determined using a leaching coefficient method. *Catena*, *226*, 1–10. https://doi.org/10.1016/j.catena.2023.107102

Martínková, M., Hesse, C., Krysanova, V., Vetter, T., & Hanel, M. (2011). Potential impact of climate change on nitrate load from the Jizera catchment (Czech Republic). *Physics and Chemistry of the Earth*, *36*(13), 673–683. https://doi.org/10.1016/j.pce.2011.08.013

Mateo-Sagasta, J., Zadeh, S. M., & Turral, H. (2018). More people, more food, worse water? A global review on water pollution from agriculture. In J. Mateo-Sagasta, S. M. Zadeh, & H. Turral (Eds.), *FAO and IWMI*. http://www.fao.org/3/ca0146en/ca0146en.pdf

Mateo-Sagasta, J., Zadeh, S. M., Turral, H., & Burke, J. (2017). Water pollution from agriculture: A global review, Executive summary. In J. Mateo-Sagasta, S. M. Zadeh, H. Turral, & J. Burke (Eds.), *FAO and IWMI*. https://www.fao.org/3/i7754e/i7754e.pdf

McElroy, A. D., Chiu, S. Y., Nebgen, J. W., Aleti, A., & Bennett, F. W. (1976). Loading functions for assessment of water pollution from nonpoint sources. In *USEPA, Athens, GA*.

Meaurio, M., Zabaleta, A., Uriarte, J. A., Srinivasan, R., & Antigüedad, I. (2015). Evaluation of SWAT model's performance to simulate streamflow spatial origin. The case of a small forested watershed. *Journal of Hydrology*, *525*, 326–334. https://doi.org/10.1016/j.jhydrol.2015.03.050

Mekonnen, B. A., Mazurek, K. A., & Putz, G. (2017). Modeling of nutrient export and effects of management practices in a cold-climate prairie watershed: Assiniboine River watershed, Canada. *Agricultural Water Management*, *180*, 235–251. https://doi.org/10.1016/j.agwat.2016.06.023

Melero, S., López-Garrido, R., Murillo, J. M., & Moreno, F. (2009). Conservation tillage: Short- and long-term effects on soil carbon fractions and enzymatic activities under Mediterranean conditions. *Soil and Tillage Research*, *104*(2), 292–298. https://doi.org/10.1016/j.still.2009.04.001

Menció, A., Mas-Pla, J., Otero, N., Regàs, O., Boy-Roura, M., Puig, R., Bach, J., Domènech, C., Zamorano, M., Brusi, D., & Folch, A. (2016). Nitrate pollution of groundwater; all right..., but nothing else? *Science of the Total Environment*, *539*, 241–251. https://doi.org/10.1016/j.scitotenv.2015.08.151

Merchán, D., Casalí, J., Del Valle de Lersundi, J., Campo-Bescós, M. A., Giménez, R., Preciado, B., & Lafarga, A. (2018). Runoff, nutrients, sediment and salt yields in an irrigated watershed in southern Navarre (Spain). *Agricultural Water Management*, *195*, 120–132. https://doi.org/10.1016/j.agwat.2017.10.004

Merchán, D., Causapé, J., & Abrahão, R. (2013). Impact of irrigation implementation on hydrology and water quality in a small agricultural basin in Spain. *Hydrological Sciences Journal*, *58*(7), 1400–1413. https://doi.org/10.1080/02626667.2013.829576

Merchán, D., Causapé, J., Abrahão, R., & García-Garizábal, I. (2015). Assessment of a newly implemented irrigated area (Lerma Basin, Spain) over a 10-year period. II: Salts and nitrate exported. *Agricultural Water Management*, *158*, 288–296. https://doi.org/10.1016/j.agwat.2015.04.019

Merchán, D., Luquin, E., Hernández-García, I., Campo-Bescós, M. A., Giménez, R., Casalí, J., & Del Valle de Lersundi, J. (2019). Dissolved solids and suspended sediment dynamics from five small agricultural watersheds in Navarre, Spain: A 10-year study. *Catena*, *173*(September 2018), 114–130. https://doi.org/10.1016/j.catena.2018.10.013

Merchán, D., Sanz, L., Alfaro, A., Pérez, I., Goñi, M., Solsona, F., Hernández-García, I., Pérez, C., & Casalí, J. (2020). Irrigation implementation promotes increases in salinity and nitrate concentration in the lower reaches of the Cidacos River (Navarre, Spain). *Science of the Total Environment*, *706*, 1–11. https://doi.org/10.1016/j.scitotenv.2019.135701

Meyer, J. L., Paul, M. J., & Taulbee, W. K. (2015). Stream ecosystem function in urbanizing landscapes Stream ecosystem function in urbanizing landscapes. *Journal of the North American Benthological Society*, *24*(3), 602–612. https://doi.org/10.1899/04-021.1

Moges, E., Demissie, Y., Larsen, L., & Yassin, F. (2021). Review: Sources of hydrological model uncertainties and advances in their analysis. In *Water (Switzerland)* (Vol. 13, Issue 1, p. 1.23). https://doi.org/10.3390/w13010028

Molina-Navarro, E., Hallack-Alegría, M., Martínez-Pérez, S., Ramírez-Hernández, J., Mungaray-Moctezuma, A., & Sastre-Merlín, A. (2016). Hydrological modeling and

climate change impacts in an agricultural semiarid region. Case study: Guadalupe River basin, Mexico. *Agricultural Water Management*, *175*, 29–42. https://doi.org/10.1016/j.agwat.2015.10.029

Molina-Navarro, E., Trolle, D., Martínez-Pérez, S., Sastre-Merlín, A., & Jeppesen, E. (2014). Hydrological and water quality impact assessment of a Mediterranean limno-reservoir under climate change and land use management scenarios. *Journal of Hydrology*, *509*, 354–366. https://doi.org/10.1016/j.jhydrol.2013.11.053

Moriasi, D. N., Arnold, J. G., Van Liew, M. W., Bingner, R. L., Harmel, R. D., & Veith, T. L. (2007). Model evaluation guidelines for systematic quantification of accuracy in watershed simulations. *Transactions of the ASABE*, *50*(3), 885–900. https://doi.org/10.13031/2013.23153

Moriasi, D. N., Gitau, M. W., Pai, N., & Daggupati, P. (2015). Hydrologic and water quality models: Performance measures and evaluation criteria. *Transactions of the ASABE*, *58*(6), 1763–1785. https://doi.org/10.13031/trans.58.10715

Motsinger, J., Kalita, P., & Bhattarai, R. (2016). Analysis of best management practices implementation on water quality using the Soil and Water Assessment Tool. *Water*, *8*(145), 1–17. https://doi.org/10.3390/w8040145

Mougou, R., Mansour, M., Iglesias, A., Chebbi, R. Z., & Battaglini, A. (2011). Climate change and agricultural vulnerability: A case study of rain-fed wheat in Kairouan, Central Tunisia. *Regional Environmental Change*, *11*(1), 137–142. https://doi.org/10.1007/s10113-010-0179-4

Muñoz-Carpena, R., Ritter, A., Socorro, A. R., & Pérez, N. (2002). Nitrogen evolution and fate in a Canary Islands (Spain) sprinkler fertigated banana Plot. *Agricultural Water Management*, *52*, 93–117. https://doi.org/10.1016/S0378-3774(01)00131-7

Nash, J. E., & Sutcliffe, J. V. (1970). River flow forecasting through conceptual models part I - A discussion of principles. *Journal of Hydrology*, *10*, 282–290. https://doi.org/10.1016/0022-1694(70)90255-6

Navarra, A., & Tubiana, L. (2013). Regional assessment of climate change in the Mediterranean. Volume 3: Case studies. In Antonio Navarra & L. Tubiana (Eds.), *Advances in Global Change Research* (1st ed.). Springer Dordrecht. https://doi.org/10.1007/978-94-007-5769-1

Neitsch, S. L., Arnold, J. G., Kiniry, J. R., & Williams, J. R. (2011). Soil & Water Assessment Tool theoretical documentation, version 2009. In *Texas Water Resources Institute*. https://swat.tamu.edu/media/99192/swat2009-theory.pdf

Niraula, R., Meixner, T., & Norman, L. M. (2015). Determining the importance of model calibration for forecasting absolute/relative changes in streamflow from LULC and climate changes. *Journal of Hydrology*, *522*, 439–451. https://doi.org/10.1016/j.jhydrol.2015.01.007

Oduor, B. O., Campo-Bescós, M. Á., Lana-Renault, N., & Casalí, J. (2023). Effects of climate change on streamflow and nitrate pollution in an agricultural Mediterranean watershed in Northern Spain. *Agricultural Water Management*, *285*, 1–12. https://doi.org/10.1016/j.agwat.2023.108378

OECD. (2012). Water quality and agriculture: meeting the policy challenge. Key Messages and Executive Summary. In *OECD studies on water*. https://doi.org/10.1787/9789264168060-en

Oger, A. (2022). *The fertiliser transition: Addressing social and environmental spillovers in the fertiliser sector*. https://ieep.eu/wp-content/uploads/2022/11/The-fertiliser-transition_IEEP-2022.pdf

Orellana-Macías, J. M., Merchán, D., & Causapé, J. (2020). Evolution and assessment of a nitrate vulnerable zone over 20 years: Gallocanta groundwater body (Spain). *Hydrogeology Journal*, *28*(6), 2207–2221. https://doi.org/10.1007/s10040-020-02184-0

Pandey, A., Bishal, K. C., Kalura, P., Chowdary, V. M., Jha, C. S., & Cerdà, A. (2021). A Soil Water Assessment Tool (SWAT) modeling approach to prioritize soil conservation management in river basin critical areas coupled with future climate scenario analysis. *Air, Soil and Water Research*, *14*. https://doi.org/10.1177/11786221211021395

Parajuli, P. B., & Risal, A. (2021). Evaluation of climate change on streamflow, sediment, and nutrient load at watershed scale. *Climate*, *9*(11), 1–14. https://doi.org/10.3390/cli9110165

Pulido-Bosch, A., Rigol-Sanchez, J. P., Vallejos, A., Andreu, J. M., Ceron, J. C., Molina-Sanchez, L., & Sola, F. (2018). Impacts of agricultural irrigation on groundwater

salinity. *Environmental Earth Sciences*, *77*(5). https://doi.org/10.1007/s12665-018-7386-6

Rostamian, R., Jaleh, A., Afyuni, M., Mousavi, S. F., Heidarpour, M., Jalalian, A., & Abbaspour, K. C. (2008). Application of a SWAT model for estimating runoff and sediment in two mountainous basins in central Iran. *Hydrological Sciences Journal*, *53*(5), 977–988. https://doi.org/10.1623/hysj.53.5.977

Rouholahnejad, E., Abbaspour, K. C., Srinivasan, R., Bacu, V., & Lehmann, A. (2014). Water resources of the Black Sea basin at high spatial and temporal resolution. *Water Resources Research*, *50*(7), 5866–5885. https://doi.org/10.1002/2013WR014132

Saadi, S., Todorovic, M., Tanasijevic, L., Pereira, L. S., Pizzigalli, C., & Lionello, P. (2015). Climate change and Mediterranean agriculture: Impacts on winter wheat and tomato crop evapotranspiration, irrigation requirements and yield. *Agricultural Water Management*, *147*, 1–13. https://doi.org/10.1016/j.agwat.2014.05.008

Sánchez-Colón, Y. M., & Schaffner, F. C. (2021). Identifying nonpoint sources of phosphorus and nitrogen: A case study of pollution that enters a freshwater wetland (Laguna Cartagena, Puerto Rico). *Journal of Water Resource and Protection*, *13*(08), 588–604. https://doi.org/10.4236/jwarp.2021.138032

Scott, J., Rosen, M. R., Saito, L., & Decker, D. L. (2011). The influence of irrigation water on the hydrology and lake water budgets of two small arid-climate lakes in Khorezm, Uzbekistan. *Journal of Hydrology*, *410*, 114–125. https://doi.org/10.1016/J.JHYDROL.2011.09.028

Setegn, S. G., Srinivasan, R., & Dargahi, B. (2008). Hydrological modelling in the Lake Tana Basin, Ethiopia using SWAT model. *The Open Hydrology Journal*, *2*(1), 49–62. https://doi.org/10.2174/1874378100802010049

Sharpley, A. N., Daniel, T., Gibson, G., Bundy, L., Cabrera, M., Sims, T., Stevens, R., Lemunyon, J., Kleinman, P., & Parry, R. (2006). Best management practices to minimize agricultural phosphorus impacts on water quality. In *United States Department of Agriculture (USDA) - Agricultural Research Service (ARS)* (Vol. 163). https://www.ars.usda.gov/is/np/bestmgmtpractices/best management practices.pdf

Sharpley, Andrew N., Bergström, L., Aronsson, H., Bechmann, M., Bolster, C. H.,

Börling, K., Djodjic, F., Jarvie, H. P., Schoumans, O. F., Stamm, C., Tonderski, K. S., Ulén, B., Uusitalo, R., & Withers, P. J. A. (2015). Future agriculture with minimized phosphorus losses to waters: Research needs and direction. *Ambio*, *44*(2), 163–179. https://doi.org/10.1007/s13280-014-0612-x

Siebert, S., Burke, J., Faures, J. M., Frenken, K., Hoogeveen, J., Döll, P., & Portmann, F. T. (2010). Groundwater use for irrigation – a global inventory. *Hydrology and Earth System Sciences*, *14*(10), 1863–1880. https://doi.org/10.5194/hess-14-1863-2010

Skhiri, A., & Dechmi, F. (2012). Impact of sprinkler irrigation management on the Del Reguero River (Spain). I: Water balance and irrigation performance. *Agricultural Water Management*, *103*, 120–129. https://doi.org/10.1016/J.AGWAT.2011.11.003

Smith, D. R., Francesconi, W., Livingston, S. J., & Huang, C. (2015). Phosphorus losses from monitored fields with conservation practices in the Lake Erie Basin, USA. *Ambio*, *44*(2), 319–331. https://doi.org/10.1007/s13280-014-0624-6

Somot, S., Sevault, F., Déqué, M., & Crépon, M. (2008). 21st century climate change scenario for the Mediterranean using a coupled atmosphere–ocean regional climate model. *Global and Planetary Change*, *63*(2–3), 112–126. https://doi.org/10.1016/j.gloplacha.2007.10.003

Stamatis, G., Parpodis, K., Filintas, A., & Zagana, E. (2011). Groundwater quality, nitrate pollution and irrigation environmental management in the Neogene sediments of an agricultural region in Central Thessaly (Greece). *Environmental Earth Sciences*, *64*, 1081–1105. https://doi.org/10.1007/s12665-011-0926-y

Sun, Y., Zeng, Y., Shi, Q., Pan, X., & Huang, S. (2015). No-tillage controls on runoff: A meta-analysis. *Soil and Tillage Research*, *153*, 1–6. https://doi.org/10.1016/j.still.2015.04.007

Sutton, M. A., Howard, C. M., & Erisman, J. W. (2011). The European Nitrogen Assessment - Sources, effects and policy perspectives. In *Cambridge University Press*. https://doi.org/10.1017/CBO9780511976988

Swedish Environmental Emissions Data (SMED). (2019). Leakage of nutrients from Swedish farmland. In *Report No. 5*. https://smed.se/vatten/4539

Syversen, N. (2005). Effect and design of buffer zones in the Nordic climate: The

influence of width, amount of surface runoff, seasonal variation and vegetation type on retention efficiency for nutrient and particle runoff. *Ecological Engineering*, *24*, 483–490. https://doi.org/10.1016/j.ecoleng.2005.01.016

Thodsen, H., Farkas, C., Chormanski, J., Trolle, D., Blicher-Mathiesen, G., Grant, R., Engebretsen, A., Kardel, I., & Andersen, H. E. (2017). Modelling nutrient load changes from fertilizer application scenarios in six catchments around the Baltic sea. *Agriculture*, *7*(41), 1–17. https://doi.org/10.3390/agriculture7050041

Tiessen, K. H. D., Elliott, J. A., Yarotski, J., Lobb, D. A., Flaten, D. N., & Glozier, N. E. (2010). Conventional and conservation tillage: Influence on seasonal runoff, sediment, and nutrient losses in the Canadian Prairies. *Journal of Environmental Quality*, *39*(3), 964–980. https://doi.org/10.2134/jeq2009.0219

Todaro, V., D'Oria, M., Secci, D., Zanini, A., & Tanda, M. G. (2022). Climate change over the Mediterranean region: Local temperature and precipitation variations at five pilot sites. *Water (Switzerland)*, *14*, 1–24. https://doi.org/10.3390/w14162499

Tolson, B. A., & Shoemaker, C. A. (2007). Cannonsville Reservoir watershed SWAT2000 model development, calibration and validation. *Journal of Hydrology*, *337*(1–2), 68–86. https://doi.org/10.1016/j.jhydrol.2007.01.017

Tong, S. T. Y., Sun, Y., Ranatunga, T., He, J., & Yang, Y. J. (2012). Predicting plausible impacts of sets of climate land land use change scenarios on water resources. *Applied Geography*, *32*(2), 477–489. https://doi.org/10.1016/j.apgeog.2011.06.014

Trnka, M., Olesen, J. E., Kersebaum, K. C., Skjelvåg, A. O., Eitzinger, J., Seguin, B., Peltonen-Sainio, P., Rötter, R., Iglesias, A., Orlandini, S., Dubrovský, M., Hlavinka, P., Balek, J., Eckersten, H., Cloppet, E., Calanca, P., Gobin, A., Vučetić, V., Nejedlik, P., … Žalud, Z. (2011). Agroclimatic conditions in Europe under climate change. *Global Change Biology*, *17*(7), 2298–2318. https://doi.org/10.1111/j.1365-2486.2011.02396.x

Tuppad, P., Kannan, N., Srinivasan, R., Rossi, C. G., & Arnold, J. G. (2010). Simulation of agricultural management alternatives for watershed protection. *Water Resources Management*, *24*(12), 3115–3144. https://doi.org/10.1007/S11269-010-9598-8

Ulén, B., Aronsson, H., Bechmann, M., Krogstad, T., Øygarden, L., & Stenberg, M. (2010). Soil tillage methods to control phosphorus loss and potential side-effects: A

Scandinavian review. In *Soil Use and Management* (Vol. 26, Issue 2, pp. 94–107). https://doi.org/10.1111/j.1475-2743.2010.00266.x

Ulén, B., & Fölster, J. (2007). Recent trends in nutrient concentrations in Swedish agricultural rivers. *Science of the Total Environment*, *373*, 473–487. https://doi.org/10.1016/j.scitotenv.2006.11.032

UN Water. (2015). Water for a sustainable world. In *World Water Development Report (WWDR) 2015*. UNESCO. https://sustainabledevelopment.un.org/content/documents/1711Water for a Sustainable World.pdf

UNEP. (2019). *Mediterranean Action Plan Barcelona Convention*. Mediterranean Action Plan of the United Nations Environment Programme (UNEP/MAP). https://www.unep.org/unepmap/node/7619

USDA. (2004). Estimation of direct runoff from storm Rainfall. In *Part 630 Hydrology National Engineering Handbook* (210th-VI-NEH ed., pp. 1–51). United States Department of Agriculture Natural Resources Conservation Service. https://directives.sc.egov.usda.gov/OpenNonWebContent.aspx?content=17752.wba

Valverde, P., Serralheiro, R., de Carvalho, M., Maia, R., Oliveira, B., & Ramos, V. (2015). Climate change impacts on irrigated agriculture in the Guadiana river basin (Portugal). *Agricultural Water Management*, *152*, 17–30. https://doi.org/10.1016/j.agwat.2014.12.012

Vargas-Amelin, E., & Pindado, P. (2014). The challenge of climate change in Spain: Water resources, agriculture and land. *Journal of Hydrology*, *518*, 243–249. https://doi.org/10.1016/j.jhydrol.2013.11.035

Venishetty, V., & Parajuli, P. B. (2022). Assessment of BMPs by estimating hydrologic and water quality outputs using SWAT in Yazoo River watershed. *Agriculture*, *12*(4), 1–14. https://doi.org/10.3390/agriculture12040477

Vigiak, O., Udías, A., Grizzetti, B., Zanni, M., Aloe, A., Weiss, F., Hristov, J., Bisselink, B., de Roo, A., & Pistocchi, A. (2023). Recent regional changes in nutrient fluxes of European surface waters. *Science of the Total Environment*, *858*, 1–12. https://doi.org/10.1016/j.scitotenv.2022.160063

Waidler, D., White, M., Steglich, E., Wang, S., Williams, J., Jones, C. A., & Srinivasan, R. (2009). Conservation practice modeling guide for SWAT and APEX. In *Soil Water Assessment Tool*. https://swat.tamu.edu/media/57882/Conservation-Practice-Modeling-Guide.pdf

Wang, S., Kang, S., Zhang, L., & Li, F. (2008). Modelling hydrological response to different land-use and climate change scenarios in the Zamu River basin of Northwest China. *Hydrological Processes*, *22*, 2502–2510. https://doi.org/10.1002/hyp.6846

WHO. (2017). *Guidelines for drinking-water quality: Fourth edition incorporating the first addendum*. World Health Organization. https://www.who.int/publications/i/item/9789241549950

Williams, J. R. (1975). Sediment routing for agricultural watersheds. *Journal of the American Water Resources Association*, *11*(5), 965–974. https://doi.org/10.1111/j.1752-1688.1975.tb01817.x

Williams, J. R., & Hann, R. W. (1978). Optimal operations of large agricultural watersheds with water quality constraints. In *Texas Water Resources Institute*.

Wittmer, I. K., Scheidegger, R., Bader, H. P., Singer, H., & Stamm, C. (2011). Loss rates of urban biocides can exceed those of agricultural pesticides. *Science of The Total Environment*, *409*(5), 920–932. https://doi.org/10.1016/j.scitotenv..2010.11.031

World Bank. (2020). *Water in Agriculture*. The World Bank Group: Understanding Poverty. https://www.worldbank.org/en/topic/water-in-agriculture#1

Xia, Y., Zhang, M., Tsang, D. C. W., Geng, N., Lu, D., Zhu, L., Igalavithana, A. D., Dissanayake, P. D., Rinklebe, J., Yang, X., & Ok, Y. S. (2020). Recent advances in control technologies for non-point source pollution with nitrogen and phosphorous from agricultural runoff: current practices and future prospects. In *Applied Biological Chemistry* (Vol. 63, Issue 8, pp. 1–13). https://doi.org/10.1186/s13765-020-0493-6

Yu, Z. (2015). Hydrology, Floods and Droughts: Modeling and Prediction. In *Encyclopedia of Atmospheric Sciences: Second Edition* (pp. 217–223). https://doi.org/10.1016/B978-0-12-382225-3.00172-9

Yuan, Y., & Koropeckyj-Cox, L. (2022). SWAT model application for evaluating agricultural conservation practice effectiveness in reducing phosphorous loss from the Western Lake Erie basin. *Journal of Environmental Management*, *302*, 114000. https://doi.org/10.1016/j.jenvman.2021.114000

Zabaleta, A., Meaurio, M., Ruiz, E., & Antigüedad, I. (2014). Simulation climate change impact on runoff and sediment yield in a small watershed in the Basque Country, Northern Spain. *Journal of Environmental Quality*, *43*, 235–245. https://doi.org/10.2134/jeq2012.0209

Zampieri, M., Toreti, A., Ceglar, A., Naumann, G., Turco, M., & Tebaldi, C. (2020). Climate resilience of the top ten wheat producers in the Mediterranean and the Middle East. *Regional Environmental Change*, *20*(41), 1–9. https://doi.org/10.1007/s10113-020-01622-9

Zeng, R., & Cai, X. (2014). Analyzing streamflow changes: Irrigation-enhanced interaction between aquifer and streamflow in the Republican River basin. *Hydrology and Earth System Sciences*, *18*(2), 493–502. https://doi.org/10.5194/hess-18-493-2014

Zettam, A., Taleb, A., Sauvage, S., Boithias, L., Belaidi, N., & Sanchez-Perez, J. M. (2020). Applications of a SWAT model to evaluate the contribution of the Tafna catchment (North-West Africa) to the nitrate load entering the Mediterranean sea. *Environmental Monitoring and Assessment*, *192*(510), 1–17. https://doi.org/10.1007/s10661-020-08482-0

Zhang, X., & Zhang, M. (2011). Modeling effectiveness of agricultural BMPs to reduce sediment load and organophosphate pesticides in surface runoff. *Science of the Total Environment*, *409*(10), 1949–1958. https://doi.org/10.1016/j.scitotenv.2011.02.012

Zhao, F., Wu, Y., Qiu, L., Sun, Y., Sun, L., Li, Q., Niu, J., & Wang, G. (2018). Parameter uncertainty analysis of the SWAT model in a mountain-loess transitional watershed on the Chinese Loess Plateau. *Water (Switzerland)*, *10*(690), 1–16. https://doi.org/10.3390/w10060690

Appendices

Appendix I: Publications

Publications in peer-reviewed journals

1. **Oduor, B. O**., Campo-Bescós, M. Á., Echarri, A. A., and Casalí, J. (2023). Evaluation of the impact of changing from rainfed to irrigated agriculture in a Mediterranean watershed in Spain. *Agriculture*, *13*(1), 106. https://doi.org/10.3390/agriculture13010106
2. **Oduor, B. O**., Campo-Bescós, M. Á., Lana-Renault, N., and Casalí, J. (2023). Effects of climate change on streamflow and nitrate pollution in an agricultural Mediterranean watershed in Northern Spain. *Agricultural Water Management*, *285*, 108378. https://doi.org/10.1016/j.agwat.2023.108378
3. **Oduor, B. O**., Campo-Bescós, M. Á., Lana-Renault, N., Kyllmar, K., Mårtensson, K. and Casalí, J. (2023). Quantification of agricultural best management practices impacts on sediment and phosphorous export in a small catchment in southeastern Sweden. *Agricultural Water Management*, *290*, 108595. https://doi.org/10.1016/j.agwat.2023.108595

Presentations at international conferences

1. **Oduor, B. O**., Kyllmar K., Campo-Bescós, M. Á., Lana-Renault, N., and Casalí, J. (**2023**). Assessing the effectiveness of best management practices in reducing sediment and phosphorous export in a small Swedish agricultural catchment. *Conference on Research in the Unsaturated Soil* Zone (*ZNS'23), Seville, 7-9 Nov 2023.* Vol. 16: 264-271. https://zonanosaturada.com/jornadas-zns-2023/
2. **Oduor, B. O.**, Campo-Bescós, M. Á., Lana-Renault, N., and Casalí, J. (**2023**). Impacts of climate change on streamflow and nitrate export in an agricultural watershed in Northern Spain. *Climate Week 2023: Second World Conference on Climate Change and Sustainability*, *Rome, Italy, 16–18 Oct 2023*. https://climateweek.thepeopleevents.com/
3. **Oduor, B. O**., Kyllmar K., Campo-Bescós, M. Á., Lana-Renault, N., and Casalí, J. (**2023**). Assessing the effectiveness of best management practices in reducing sediment and phosphorous export in a small Swedish agricultural catchment. *International Soil and Water Assessment Tool (SWAT) Conference 2023, Aarhus University, Denmark, 26-30 Jun 2023.* https://swat.tamu.edu/conferences/2023-aarhus/

4. **Oduor, B. O.**, Campo-Bescós, M. Á., Lana-Renault, N., and Casalí, J. (**2023**). Modeling the impacts of climate change on streamflow and nitrate export in a Mediterranean agricultural watershed in Spain. *European Geophysical Union (EGU) General Assembly 2023, Vienna, Austria, 24–28 Apr 2023,* EGU23-11247. https://doi.org/10.5194/egusphere-egu23-11247
5. **Oduor, B. O.**, Campo-Bescós, M. Á., Lana-Renault, N., and Casalí, J. (**2022**). Evaluating the impacts of agricultural transformation from rainfed to irrigation on streamflow and nitrates in a Mediterranean agricultural watershed in Spain. *International Interdisciplinary Conference on Land Use and Water Quality Agriculture and the Environment (LuWQ2022), Maastricht, The Netherlands, 12-15 Sep 2022*. Abstract#73. https://www.luwq2022.nl/volume-of-abstracts-pdf/
6. **Oduor, B. O.**, Campo-Bescós, M. Á., Lana-Renault, N., and Casalí, J. (**2022**). Modeling the impacts of climate change on streamflow and nitrate export in a Mediterranean agricultural watershed in Spain. *International Interdisciplinary Conference on Land Use and Water Quality Agriculture and the Environment (LuWQ2022), Maastricht, The Netherlands, 12-15 Sep 2022*. Abstract#72. https://www.luwq2022.nl/volume-of-abstracts-pdf/
7. **Oduor, B. O.**, Campo-Bescós, M. Á., Lana-Renault, N., and Casalí, J. (**2022**). Modeling the impacts of climate change on streamflow and nitrate export in a Mediterranean agricultural watershed in Spain. *International Soil and Water Assessment Tool (SWAT) Conference 2022, Czech University of Life Sciences Prague, Czech Republic, 11-15 Jul 2022*. https://swat.tamu.edu/conferences/2022-prague/
8. **Oduor, B. O.,** Campo-Bescós, M. Á., Lana-Renault, N. S., and Casalí, J. (**2022**). Evaluating the Impacts of Agricultural Transformation from Rainfed to Irrigation on Streamflow and Nitrates in a Mediterranean Agricultural Watershed in Spain, *European Geophysical Union (EGU) General Assembly 2022, Vienna, Austria, 23–27 May 2022*, EGU22-6032. https://doi.org/10.5194/egusphere-egu22-6032
9. **Oduor, B. O.,** Campo-Bescós, M. Á., Lana-Renault, N. S., and Casalí, J. (**2021**). Evaluating SWAT Model's application for estimating streamflow in the Cidacos River Watershed in Navarre, Spain. In F. J. S. Calvete, A. P. González, D. J. Dafonte, and E. V. Vázquez (Eds.) *XV edition of the Conference on Research in the Unsaturated Soil* Zone (*ZNS'21), A Coruña, Spain, 9-11 Nov 2021*, Vol. 15: 211-218. Universidade da Coruña. https://doi.org/10.17979/spudc.9788497498210

Presentations at workshops and seminars

1. **Oduor, B. O.,** Campo-Bescós, M. Á., Lana-Renault, N., and Casalí, J. (**2023**). Modeling impacts of climate change on streamflow and nitrate export in a Mediterranean agricultural watershed in Spain. *IS-FOOD Day 2023, Pamplona, Spain, 19 May 2023*.
2. **Oduor, B. O.,** Campo-Bescós, M. Á., Lana-Renault, N., and Casalí, J. (**2022**). Evaluating the impacts of climate change on streamflow and nitrate export in an agricultural Mediterranean watershed in Spain. *VIII Jornadas Doctorales de Campus Campus Iberus, Jaca, 27-29 Jun 2022*.
3. **Oduor, B. O.,** Campo-Bescós, M. Á., Lana-Renault, N., and Casalí, J. (**2021**). Evaluating SWAT model's application for estimating streamflow and nitrates in the Cidacos River watershed in Navarre, Spain. *VII Jornadas Doctorales de Campus Iberus, Jaca, 4-6 Oct 2021*.
4. **Oduor, B. O.,** Campo-Bescós, M. Á., Lana-Renault, N., and Casalí, J. (**2021**). Evaluation of SWAT model for simulating land use transformation from rainfed agriculture to irrigation in the Cidacos River watershed. *IS-FOOD Day 2021, Pamplona, Spain, 16 Apr 202*.

Appendix II: SWAT Model Input Parameters

Table A 1: The SWAT model input parameters and adjusted values for streamflow and nitrate load simulation in the Cidacos River watershed in Spain

SWAT input parameter	Parameter description	Units	Parameter adjustment value			
			Default	Min	Max	Best fit
		Hydrology parameters				
v__ALPHA_BF.gw	Baseflow alpha factor	day^{-1}	0.048	0.2	1	0.5
v__GW_REVAP.gw	Groundwater "revap" coefficient.	-	0.02	0.11	0.17	0.12
v__GW_DELAY.gw	Groundwater delay	days	31	20	80	53.5
v__REVAPMN.gw	Threshold depth of water in the shallow aquifer for "revap" to occur	mm H_2O	1	0	100	51
v__GWQMN.gw	Threshold depth of water in the shallow aquifer required for return flow to occur	mm H_2O	1000	50	200	150
r__SOL_AWC.sol	Available water capacity of the soil layer	mm H_2O/ mm soil	-	-20%	30%	20%
r__SOL_BD.sol	Moist bulk density	mm H_2O/ mm soil	-	-15%	10%	1.5%
r__SOL_K.sol	Saturated hydraulic conductivity	mm H_2O/ mm soil	-	-30%	0	-8.4%
r__CN2.mgt	Initial SCS runoff curve number for moisture condition II	-	35-98	-20%	20%	-12%
r__ESCO.hru	Soil evaporation compensation factor	-	0.95	-45%	28%	-31%
r__OV_N.hru	Manning's "n" value for overland flow	-	0.14	5%	15%	6.5%

v__EPCO.bsn	Plant uptake compensation factor	-	-	0.1	0.95	0.74
	Nitrate load parameters					
v__LAT_ORGN.gw	Organic N in the baseflow	mg L^{-1}	0	10	31	16
r__SHALLST_N.gw	Concentration of nitrate in groundwater contribution to streamflow from subbasin	mg L^{-1}	0	-28%	45%	-20%
r__ANION_EXCL.sol	Fraction of porosity from which anions are excluded	-	0.5	-15%	53%	-5%
v__ERORGN.hru	Organic N enrichment ratio	-	0	1.05	3.15	1.85
r__SOLN_CON.hru	Soluble nitrogen concentration in runoff	mg L^{-1}	0	-5%	80%	9.5%
v__N_UPDIS.bsn	Nitrogen uptake distribution parameter	-	20	12.3	37.2	34.1
v__RCN.bsn	Concentration of nitrogen in precipitation	mg L^{-1}	1	1.25	3.75	2.85
v__NPERCO.bsn	Nitrogen percolation coefficient	-	0.2	0.01	0.6	0.05
v__CMN.bsn	Rate factor for humus mineralization of active organic nutrients (N and P)	-	0.0003	0.001	0.003	0.002
v__CDN.bsn	Denitrification exponential rate coefficient	-	1.4	0	0.162	0.04
v__SDNCO.bsn	Denitrification threshold water content	-	1.1	0.35	1.1	0.75
v__FIXCO.bsn	Nitrogen fixation coefficient	-	0	0.45	1.4	1.16
v__BC3_BSN.bsn	Rate constant for hydrolosis of organic nitrogen to ammonia	day^{-1}	0.21	0.11	0.31	0.24
r__SOL_NO3.chm	Initial NO3 concentration in the soil layer	mg kg^{-1}	-	-18%	45%	15.1%

Table A 2: The SWAT model input parameters and adjusted values for streamflow, sediment load, and total phosphorous load simulation in the Catchment C6 in southeastern Sweden.

SWAT input parameter	Parameter description	Units	Parameter adjustment value			
			Default	Min	Max	Best fit
		Hydrology parameters				
v__SFTMP.bsn	Snowfall temperature	ºC	1	-5	5	-2.5
v__SMTMP.bsn	Snowmelt base temperature	ºC	0.5	0	5	4.5
v__SMFMX.bsn	Maximum melt rate for snow during the year (on 21 Jun)	mm H_2O/ °C-day	4.5	-5	5	2.5
v__SMFMN.bsn	Minimum melt rate for snow during the year (on 21 Dec)	mm H_2O/ °C-day	4.5	0	5	1.8
v__TIMP.bsn	Snowpack temperature lag factor	-	1	0.01	1	0.5
v__SURLAG.bsn	Surface runoff lag coefficient	-	4	1	10	5.722
v__ALPHA_BF.gw	Baseflow alpha factor	day^{-1}	0.048	0.01	1	0.85
v__GW_REVAP.gw	Groundwater "revap" coefficient.	-	0.02	0.02	0.2	0.075
v__GW_DELAY.gw	Groundwater delay	days	31	0	17.5	3.5
v__REVAPMN.gw	Threshold depth of water in the shallow aquifer for "revap" to occur	mm H_2O	1	17	55	45
v__GWQMN.gw	Threshold depth of water in the shallow aquifer required for return flow to occur	mm H_2O	1000	2.5	10	5.1
v__RCHRG_DP.gw	Deep aquifer percolation fraction	-	0.05	0	1	0.2
Soil parameters						
r__SOL_AWC.sol	Available water capacity of the soil layer	mm H_2O/ mm soil	-	-80%	10%	-40%
r__CN2.mgt	Initial SCS runoff curve number for moisture condition II	-	35-98	-20%	0	-12%

v__ESCO.hru	Soil evaporation compensation factor	-	0.95	0.2	1	0.71
r__OV_N.hru	Manning's "n" value for overland flow	-	0.14	-90%	10%	-40%
r__CANMX.hru	Maximum canopy storage	mm H_2O	-	-30%	50%	+40%
	Sediment load parameters					
v__CH_N2.rte	Manning's "n" value for the main channel	-	-	0.01	0.3	0.25
v__CH_K2.rte	Effective hydraulic conductivity in the main channel	mm hr^{-1}	-	40	110	65
v__ALPHA_BNK.rte	Baseflow alpha factor for bank storage	-	0.1	0.1	0.7	0.5
v__CH_COV1.rte	Channel erodibility factor	-	1	0.05	0.6	0.25
v__CH_COV2.rte	Channel cover factor	-	1	0.01	0.5	0.2
r__USLE_K.sol	USLE equation soil erodibility (K) factor	-	0.013	-50%	50%	+27.5%
v__USLE_P.mgt	USLE equation support practice factor	-	0	0	1	0.778
v__LAT_SED.hru	Sediment concentration in lateral and groundwater flow	mg L^{-1}	0	0	50	27.65
v__SPCON.bsn	Linear parameter for calculating the maximum amount of sediment that can be re-entrained during channel sediment routing	-	0.0001	0.0001	0.01	
v__SPEXP.bsn	Exponent parameter for calculating sediment re-entrained in channel sediment routing	-	1	1	2	1.065
v__ADJ_PKR.bsn	Peak rate adjustment for sediment routing in the subbasin (tributary channels)	-	1	0.5	2	1.729
v__PRF_BSN.bsn	Peak rate adjustment of sediment routing in the main channel	-	1	0	2	1.122
	Phosphorous load parameters					
v__LAT_ORGP.gw	Organic P in baseflow	mg L^{-1}	0	0	10	8.22
v__ANION_EXCL.sol	Fraction of porosity from which anions are excluded	-	0.5	0.01	1.00	0.134
v__ERORGP.hru	Phosphorous enrichment ratio for loading without sediment	-	0	0	5	0.465
v__PSP.bsn	Phosphorous availability index	-	0.40	0.1	0.7	0.466

v__P_UPDIS.bsn	Phosphorous uptake distribution parameter	-	20	0	100	53.3
v__PHOSKD.bsn	Phosphorous soil partitioning coefficient	m^3 Mg^{-1}	175	100	200	146.3
v__PPERCO.bsn	Phosphorous percolation coefficient	10 m^3 Mg^{-1}	10	10	17.5	17.433
v__CMN.bsn	Rate factor for humus mineralization of active organic nutrients (N and P)	-	0.0003	0.001	0.003	0.002
v__BC4_BSN.bsn	The rate constant for the decay of organic P to dissolved P	day^{-1}	0.35	0.01	0.70	0.084
v__RS5.swq	Organic P settling rate in the reach at 20 ºC	day^{-1}	0.05	0.001	0.5	0.095